NTNU – Trondheim
Norwegian University of
Science and Technology

Carbon nanotubes (CNT) for enhanced oil production from shales

Aqeel Hussain

Chemical Engineering
Submission date: July 2014
Supervisor: De Chen, IKP
Co-supervisor: Erling Rytter, Statoil, Norge

Norwegian University of Science and Technology
Department of Chemical Engineering

NORWEGIAN UNIVERSITY OF SCIENCE & TECHNOLOGY)

Abstract

Natural Science & Technology
Department of Chemical Engineering

MSc Chemical Engg

Carbon Nanotubes for Enhanced Shale Gas Production

by Aqeel Hussain

The shale gas production has brought a revolution in US energy market and the global prospect of shale gas production is on continuous increase. The advancements in hydraulic fracturing made it possible to extract very low permeability shale gas through fracturing the shale rock. The once fractured shale rock is kept open with the induction of spherical particles known as proppants. The performance of proppants is crucial for oil & gas production. Therefore, the prospect of application of carbon nanotubes was explored in the present work for the development of proppants particles. The proppants testing was carried out with $N_2 Physiosrption$, xrd, density measurement, treating with the 12:3 HCl:HF solution and Instron strength testing. The proppants testing results showed excellent properties for ceramics proppants but the performance of sand proppants was very poor.

The poor performance of sand proppants attracted motivation for the application of carbon nanotubes to improve the properties of sand proppants. The Chemical Vapor Deposition method was used for the growth of carbon nanotubes around the surface of sand particles. The testing of CNTs grown proppants was carried out for analysis of improvements in the properties of proppants. There ware no observable improvements in sphericity and strength of the sand with the coating of carbon nanotubes. There was decrease in density of CNTs sand particles which was considered to be an improvement. The increase in surface area with CNTs grown sand was motivation for development of multifunctional proppants to be used as vehicle for chemical delivery in the reservoir. The multifunctional prospect of the CNTs sand proppants was explored with the adsorption of phosphonates scale inhibitor on the surface of the CNTs sand particle. The results presented an increase in phosphonates loading with the increase in CNTs yield and reaction time which is considered to be and indication that the application of CNTs can provide breakthrough in the development of multi purpose proppants. So, the carbon nanotubes has potential to find applications for development of proppants.

Acknowledgements

I would like to thank my supervisor Professor De Chen for his invaluable help and guidance through out the research work and also for time he managed every time I need help during his very busy schedule. I would also thank Professor Erling Rytter for kind discussion and guidance during the monthly research results presentations to Statoil.

I would also thank to post doc Navaneethan Muthuswammy for his support and encouragement during the lab work. I am grateful to Karin Wiggen Dragsten to make sure the availability of every equipment needed for lab work. I highly acknowledge the financial support provided by Statoil in form summer job and Chemical Engineering department, NTNU to provide every possible facility for the research work.

Contents

Abstract i

Acknowledgements ii

Contents iii

List of Figures vi

List of Tables viii

Abbreviations ix

Physical Constants x

Symbols xi

1 Introduction 1

2 Theoretical Background 3

2.1 Shale Gas . . . 3

2.1.1 Europe Shale Gas Potential . . . 5

2.1.2 Production of shale gas . . . 7

2.1.3 Environmental Concerns . . . 8

2.1.3.1 Water Contamination . . . 9

2.1.3.2 Seismic Risks . . . 10

2.2 Proppants . . . 11

2.2.1 Types of Proppants . . . 12

2.2.1.1 Sand Proppants . . . 12

2.2.1.2 Ceramics Proppants . . . 13

2.2.2 Properties of Proppants . . . 14

2.2.2.1 Light Weight . . . 14

2.2.2.2 High Mechanical Strength . . . 16

2.2.2.3 Chemical Resistance . . . 17

2.3 Scale Inhibition . . . 18

2.3.1 Phosphonates . . . 19

2.3.2 Mechanism of Scale Inhibition . . . 20

2.3.3 Chemical Scale Inhibitor Placement . . . 22
2.3.4 Development of Multifunctional Proppants . . . 24
2.3.4.1 CNT Developed Multifunctional Proppants . . . 25
2.4 Carbon Nanotubes . . . 27
2.4.1 Types of Carbon Nanotubes . . . 27
2.4.2 Molecular Structure of Carbon Nanotubes . . . 28
2.4.3 Synthesis of CNTs . . . 30
2.4.3.1 Chemical Vapor Deposition (CVD) . . . 30

3 Material & Method 32
3.1 Catalyst Preparation . . . 32
3.2 CNT Synthesis . . . 33
3.2.1 Reduction . . . 34
3.2.2 Synthesis . . . 34
3.3 Characterization . . . 35
3.3.1 N_2 Physisorption . . . 35
3.3.2 X-ray Diffraction XRD . . . 36
3.3.3 Scanning Electron Microscope . . . 36
3.4 Scale Inhibitor Adsorption . . . 36
3.5 Proppants Testing . . . 37
3.5.1 Acid Solubility . . . 37
3.5.2 Density Measurements . . . 38
3.5.3 Sphericity & Roundness . . . 38
3.5.4 Mechanical Testing . . . 39

4 Results & Discussion 40
4.1 Proppants Testing . . . 40
4.1.1 Surface Area of Proppants . . . 40
4.1.2 Mechanical Strength . . . 41
4.1.3 Acid Solubility . . . 42
4.1.3.1 SEM Analysis . . . 44
4.1.3.2 Xrd Analysis . . . 45
4.1.4 Proppants Density Measurement . . . 46
4.2 CNT Proppants Synthesis & Characterization . . . 47
4.2.1 % Yield . . . 47
4.2.2 SEM Characterization . . . 49
4.2.3 CNTs Surface Area Measurement . . . 51
4.2.4 CNT Density Analysis . . . 52
4.2.5 Sphericity & Roundness . . . 53
4.2.6 X-rays Diffraction Analysis . . . 55
4.2.7 Mechanical Strength of CNT Sand . . . 56
4.3 Scale Inhibition . . . 58
4.3.1 Inhibitor Adsorption with CNTs yield . . . 59
4.3.2 Inhibitor Adsorption with PH variation . . . 62
4.3.3 SEM Analysis of Inhibitor Adsorption . . . 63

5 Perspective & Future Work 66

6 Conclusion **68**

Bibliography **69**

A Catalyst Preparation **75**

B SEM Results **76**

C Mechanical Strength Testing **83**

D Surface Area Measurement **86**

E Density & Acid Solubility Measurement **88**

F Scale Inhibition **91**

G X-ray Diffraction **93**
G.1 X-ray Diffraction 93

H Sphericity & Roundness **95**
H.1 X-ray Diffraction 95

List of Figures

2.1 Reservoir Permeability . . . 4
2.2 Estimation of US gas production . . . 5
2.3 Global Spread in Shale gas Resources . . . 6
2.4 Share of EU gas imports . . . 7
2.5 Horizontal Drilling with Hydraulic Fracturing . . . 8
2.6 Composition of Proppants Laden Fracturing Fluid . . . 9
2.7 Propped Fracture . . . 11
2.8 Comparison of proppants settling velocity . . . 15
2.9 Pressure compaction mechanism . . . 17
2.10 Stability constant of 1:1 complex (M+HL) of phosphonates with transition metals . . . 19
2.12 Nucleation & crystal growth process . . . 21
2.13 Comparison of adsorption of 9.8 uM Phoshphonates on goethite . . . 22
2.14 Comparison of Bullhead convention inhibitor injection method with Scale-FRAC system . . . 23
2.15 Encapsulated Scale Inhibitor . . . 24
2.16 Scale Inhibitor Return Profile . . . 25
2.17 Conductivity Comparison of Porous Impregnated Proppants . . . 26
2.18 Scale Inhibitor Impregnated CNT Proppants . . . 27
2.19 Schematic diagram for graphene sheet . . . 27
2.20 Types of carbon nanotubes (A)graphene sheet (B)SWCNTs (C) MWCNTs 28
2.21 Structure of Carbon Nanotubes . . . 29

3.1 Chemical Vapor Deposition method . . . 34

4.1 Load deformation curves of proppants . . . 42
4.2 Acid solubility of proppants . . . 43
4.3 Acid solubility variation with time . . . 43
4.4 SEM analysis of acid treated surfaces . . . 44
4.5 Xrd analysis of acid treated surfaces . . . 45
4.6 Variation of % CNT yield with time for pure sand and Ni supported on sand . . . 48
4.7 Low resolution SEM of CNT sand surface A) 2hr growth time with 0.6 % yield B) 4hr growth time with 2.2 % yield C) 10 hr growth time with 12% yield D) CNT on pure sand for 12 hr . . . 49
4.8 High resolution SEM of CNT on Ni sand surface A) 2hr growth time with 0.6 % yield B) 4hr growth time with 2.2 % yield C) 10 hr growth time with 12% yield D) CNT pure sand for 12 hr . . . 50

4.9 CNTs surface area variation with % yield . . . 51
4.10 CNTs pore volume variation with yield . . . 52
4.11 Density variations with CNT growth . . . 53
4.12 Xrd for sand with CNTs on sand . . . 55
4.13 Xrd analysis for heat treated sand . . . 56
4.14 Load deformation curve for sand & CNT sand . . . 57
4.15 Phosphonates loading with variation of % yield of CNT . . . 60
4.16 Phosphonates loading with variation of time for 0.6 % yield of CNT . . . 61
4.17 Phosphonates loading with variation of time for 4 % yield of CNT . . . 62
4.18 Phosphonates loading with variation of time for 12 % yield of CNT . . . 63
4.19 Phosphonates loading with variation of PH for 13 % cnt yield . . . 64
4.20 Phosphonates inhibitor adsorption: A) & B) 1.14% inhibitor loading, C) & D) without inhibitor loading . . . 65

B.1 SEM images of sand proppants particle . . . 76
B.2 SEM images of alumina proppants particle . . . 77
B.3 SEM images of carbolite proppants particle . . . 78
B.4 SEM images of gravel proppants particle . . . 79
B.5 SEM images of CNT on Ni sand for 2hr grwoth time . . . 80
B.6 SEM images of CNT on Ni sand for 4hr grwoth time . . . 81
B.7 SEM images of CNT on Ni sand for 13hr grwoth time . . . 82

C.1 Load deformation curve for sand & cnt sand . . . 83
C.2 Load deformation curve for ceramics & cnt ceramics . . . 84
C.3 Load deformation curve for carbolite . . . 84
C.4 Load deformation curve for alumina . . . 85

E.1 Bulk density measurement . . . 88
E.2 Apparent or particle density from fluid displacement methoth . . . 89
E.3 Proppants density & porosity data . . . 89
E.4 Acid solubility of proppants . . . 90
E.5 Acid solubility of proppants . . . 90

F.1 Scale Inhibitor adsorption for cnts on pure sand with less than 1 % yield . 91
F.2 Scale Inhibitor adsorption for cnts on pure sand with 4 % yield . . . 91
F.3 Scale Inhibitor adsorption for cnts on pure sand with 12 % yield . . . 92
F.4 Phosphonates adsorption variation on CNTs with the time . . . 92

G.1 Xrd analysis for carbolite . . . 93
G.2 Xrd analysis for ceramics . . . 94
G.3 Xrd analysis for gravel and limgrus . . . 94
G.4 Xrd analysis for alumina . . . 94

H.1 Chemsizer analysis for proppants . . . 95
H.2 Chemsizer analysis for pure sand . . . 96
H.3 Chemsizer analysis for CNTs on pure sand . . . 96
H.4 Chemsizer analysis for CNTs on Ni sand . . . 97

List of Tables

2.1 Shale gas resources distribution 4
2.2 Comparison of estimation of water needed for hydraulic fracturing for different Shale play [51] 10
2.3 Quartz sand proppants permeability data [23] 12
2.4 Sintered Bauxite proppants permeability data 14
2.5 Comparison of proppants density [2] 15

4.1 Surface measurement of proppants 41
4.2 Proppants density measurement data 46
4.3 Spehricity and roundness variation with CNTs coating on sand 54
4.4 Spehricity and roundness variation with CNTs coating on sand 55
4.5 Young modulus of sand and CNT grown sand proppants 58

Abbreviations

CNT	**C**arbon **N**ano **T**ube
IEA	**I**nternational **E**nergy **A**gency
tcf	**t**rillion **c**ubic **f**oot
OECD	**O**rganization of **E**conomic **C**ooperation **D**evelopment
bcma	**b**illion **c**ubic **m**eter
tcm	**t**rillion **c**ubic **m**tere
TDS	**T**otal **D**issolved **S**olid
API	American Petroleum Institute
ISO	International Organization of Standardization
PPE	Personal Protective Equipment
ISP	**I**ntermediate **S**trength **P**roppants
HSP	**H**igh **S**trength **P**roppants
EOR	**E**nhanced **O**il **R**ecovery
EDTA	**e**thylene**d**iamine**t**etra**a**cetic
MP	Methylphosphonic
HEDP	hydroxymethylphosphonic
NTMP	Nitrolotris-methylphosphonic
EDTMP	Ethylenedinitrolotetrakismethylene phosphonic
DTPMP	Diethylenedinitrlopentakismethylene phosphonic
MIC	Minimum Inhibitor Concentration
SWNT	Single Wall Carbon Nanotubes
MWNT	Multi Wall Carbon Nanotubes
SEM	Scanning Electron Microscope
CVD	Chemical Vapor Deposition
XRD	X Ray Diffraction

Physical Constants

Adsorption constant for calcite	K_d	=	$0.27\ L/m^2$
Adsorption constant for barite	K_d	=	$0.22\ L/m^2$

Symbols

HF	Hydro floric acid
HCl	Hydro chloric acid
CO_2	Carbon dioxide
$H2S$	Hydrogen sulfide
Ca^{+2}	Calcium ion
Mg^{+2}	Magnesium ion
Ba^{+2}	Barium ion
Sr^{+2}	Strontium ion
Ni	Nickel
Fe	Iron
Co	Cobalt
$Fe(O)(OH)$	Goethite
$Ni(NO_3)_2$	Nickel nitrate
HNO_3	Nitric Acid
CO	Carbon monoxide
Ar	Argon

The work is dedicated to my parents, brother and sisters ...

Chapter 1

Introduction

The global demand for energy resources is on continuous increase especially from emerging economies like China & India which resulted in high oil pricing and fluctuation in energy market. In high demanding energy market, the development of shale gas resources is a positive sign and the changing the whole scenario of global energy demand. The north America is most benefited with the development of shale gas resources. The shale gas production has been sharply risen in USA and expected to dominate growth in coming decades. The conventional energy resources are mostly concentrated within the middle east and commonwealth states. The nice thing with shale gas resources is that they are evenly distributed all around the world. So, the shale gas resources has potential for development all around the world.The Europe also has potential for the development of shale gas resource along with some challenges.

Shale gas is natural gas which is trapped within different parts of the shale rock with very low permeability. It is very difficult to extract as compared to conventional energy resources. The development of horizontal drilling and hydraulic fracturing techniques are miles stone for the production of shale gas resources. The hydraulic fracturing technique employ very high pressure fracturing fluid which strike shale rock deep subsurface and cause fracture within the rock. The fracture within the rock connect natural gas trapped between different parts of the rock and allow for production. It is important the once created fracture should remain open to keep connect the natural gas for flow through fractures. The spherical particles known as proppant are commonly used to keep open the fractures within the rocks.

The development of proppants particles is main focused area for the present report. The proppants are spherical particles with very high mechanical strength, light weight, cheap and chemical resistance. The carbon nanotubes has the potential to improve the properties of proppants. The carbon nanotubes are nano scale tubes of carbon

form by rolling the graphene sheet in tube form. The carbon nanotube are extremely strong material with the young modulus five time than the modulus of steel [30]. Along with the exceptional properties of carbon nanotubes, they can be investigated for the development of proppants.

The proppants are designed to keep open the fracture as their main purpose. However, they can also be used for additional application which originate the idea of multi-functional proppants. There were previous attempts to use proppants for multi purpose for the placement of chemical in the reservoir and to make the self suspended proppants. Proppants can be use to improve the scale inhibition operation deep in the reservoir. Scaling is phenomena which happen with the precipitation of minerals present in the reservoir due to decrease in their solubilities. The proppants were previously investigated for effective delivery of scale inhibitor in the reservoir. The previous attempts were to make the porous structure proppant with enhance surface area following deposition of scale inhibitor over the proppants [53].

The carbon nanotubes are used in catalysis as support material to carry the catalyst material for the reaction. The same approach originate the idea of application of carbon nanotubes to carry the chemical such as scale inhibitor in the reservoir. The approach can be built with the synthesis of carbon nanotubes around the surface of sand particle following adsorption of phosphonates scale inhibitor on the surface CNTs sand particle as illustrated in figure 2.18. The idea of self suspended proppant is also interesting which can be built by the growth of hydro-gel polymer on the surface of the CNTs sand. The polymer grown proppant can be expanded with the contact of water during the transport of proppants resulting in self suspension. So, there are possibility for carbon nanotubes to find application for the development of proppantshh.

Chapter 2

Theoretical Background

2.1 Shale Gas

Oil and gas originate from the remains of prehistoric living material which were buried over geological time beneath the sediment. Under the increased temperature and pressure, the organic material first transformed into waxy material known as kerogen and with further increased in heat converted into oil and gas. The rock where first kerogen formed and converted into oil and gas is known as source rock. The oil and gas formed in source rock can pass through pores and faults and tend to reach surface of the earth. Alternatively it can be trapped within porous rock known as reservoir by impermeable rock strata above the reservoir. Gas in the reservoir either can be dissolved in oil known as associated gas or can be present separately without oil known as non-associated gas [46].

Oil and gas can be present in conventional and unconventional reservoir. A comparison of permeabilities of conventional & unconventional reservoir is illustrated in figure 2.1. Conventional reservoirs are of very good quality reservoir with high permeability where commercial scale oil and gas can be produced by simply drilling a vertical hole, perforate the productive interval without significant stimulation. The unconventional reservoirs are of low quality with very low permeability. Low permeability reservoirs such as tight gas, tight oil, shale gas, and coal bed methane are classified as unconventional reservoirs. The unconventional reservoirs with very low permeability are required to be stimulated to enhance permeability for the smooth flow and recovery of oil and gas. Unconventional reservoirs required advanced technologies with higher investment for smooth commercial scale production of oil and gas. The success of horizontal drilling and advancement in multistage hydraulic fracturing resulted in development of unconventional oil and gas reservoirs [20].

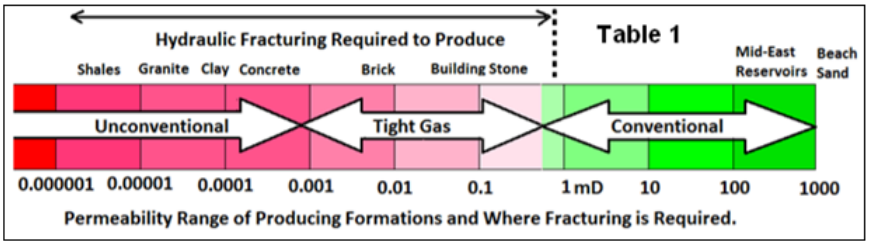

FIGURE 2.1: Reservoir Permeability [25]

Shale gas is natural gas which fails to find path from the source rock due to lack of faults and porous rock. Therefore, the shale gas does not accumulated in a specified reservoir like in conventional reservoir rather it is trapped within the source rock. Shale gas itself has very low permeability and conventional oil and gas production techniques cannot be employed for smooth production of shale gas. Shale gas can be trapped through different mechanisms: within the pores of the rock, within natural occurring fractures or adsorbed on to the shale minerals and organic material within the shale. The shale gas is trapped within the rock and distributed between different portion of the rock. The unavailability of common channel between different shale containing parts of rock, the shale gas cannot find flow path and cannot accumulate at specific parts of rock. So hydraulic fracturing techniques are employed to create fracture within the rock to provide smooth path for flow of oil and gas through the propped fractures [1].

Conventional natural gas resources are concentrated in Russia and Middle East with 25% and 41% of the global proven reserves respectively [46]. However, the shale gas resources are evenly distributed around the globe providing potential for development of shale gas resources throughout the world. The scale of recoverable unconventional resources worldwide is thought to be very large but these resources are poorly mapped and quantified. The table 2.1 gives a simple overview of distribution of recoverable shale gas resources. With some reasonable estimates, the IEA estimates remaining recoverable unconventional resources to some 380 Tcm. This is sufficient for 125 year of present world gas consumption [1].

TABLE 2.1: Shale gas resources distribution [1]

Region	**Shale gas reserve (tcm)**
Middle East & North Africa	72
Sub Saharan Africa	8
Former Soveit Union	18
Asia Pacific	174
Central Asia and China	100
OECD Pacific	65
South Asia	0

Shale gas has brought revolution in US energy market and this revolution is also considered to be main factor in lowering gas prices in the world market. In 2010, total production reached to 5 trillion cubic feet (tcf) and expected to reach this number three times in 2035 [37]. Figure 2.2 shows the natural gas production in the US which show an increase in shale gas shares in US gas consumption and the share of shale gas is expected to increase up to 46 % for the year 2035. Development of shale gas resulted in sharp reduction in US natural gas imports to lead US towards self-dependent oil & gas market [15].

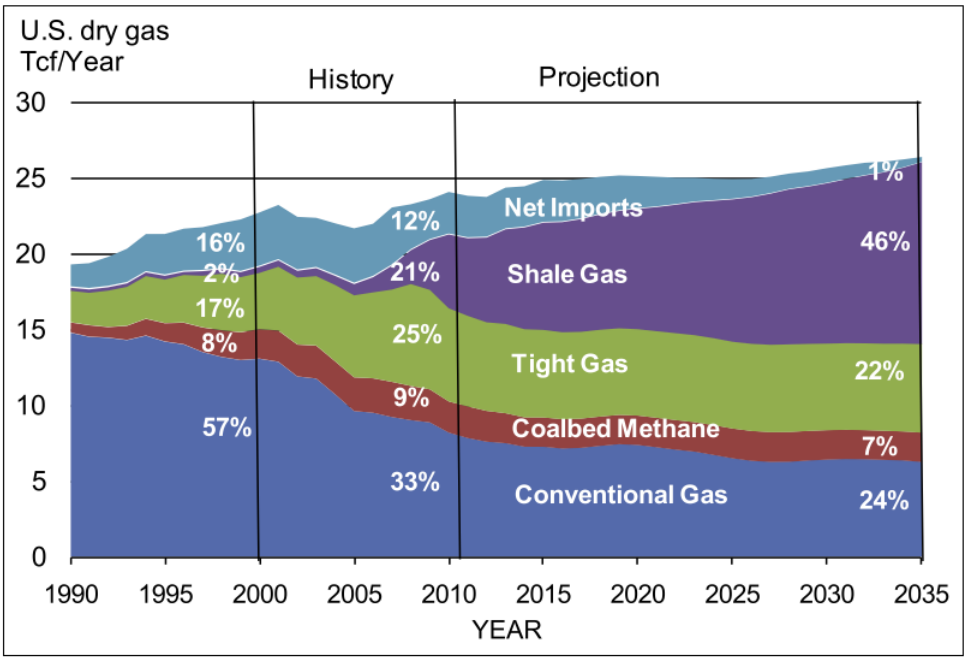

FIGURE 2.2: Estimation of US gas production [15]

2.1.1 Europe Shale Gas Potential

Europe natural gas dependence is on continuous increase and there is increased interest to burn relatively cleaner fuel for thermal power generation. Europe natural gas consumption was 25% as primary energy supply in 2009 according to IEA, however, consumption was 10% in 1973 and 1% in 1960. In addition to domestic production Europe has to depend upon imports to offset the gap. Among 22 Europe OECD member states only Norway, Netherland and Denmark have sufficiently gas reserves to cover domestic demand. The dependence of Europe on natural gas is expected to rise, however, the domestic production of Europe is following falling trend. Europe gas consumption is expected to grow from 600 bcma to 650 bcma in 2020 and 680 bcma by 2030. As

a result the Europe gas imports will increase thereby higher level of dependency with higher security supply risk figure 2.4 [55].

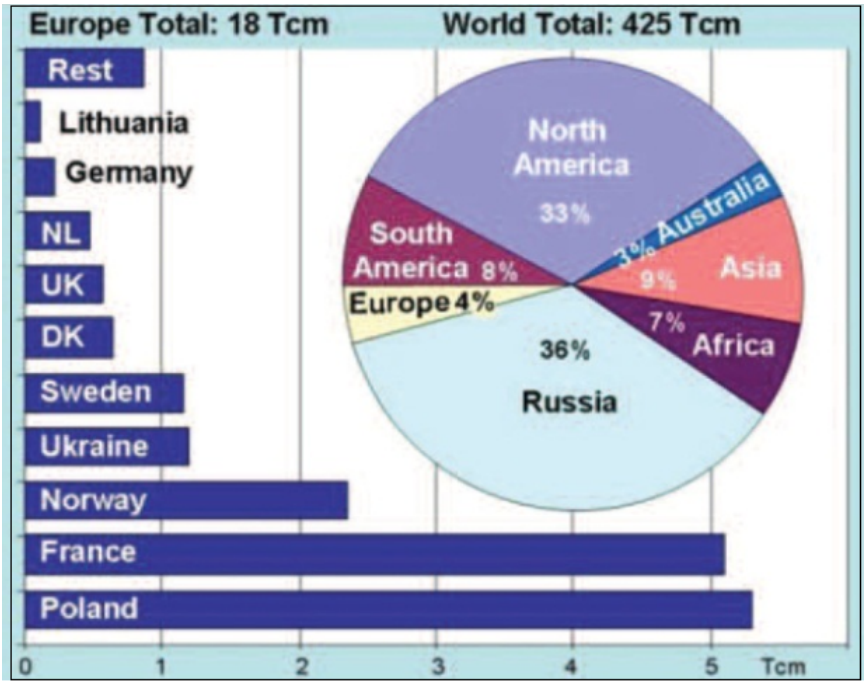

FIGURE 2.3: Global Spread in Shale gas Resources [55]

The development of shale gas in Europe can go long to meet increasing demand, declining production, security of supply and challenges related gas supply interruption. Europe can be benefitted from the US successful experience with development of shale gas resources. Europe has 16 tcm or according to some other sources 18 tcm shale gas potential comprising only 4% of world total reserves which is very less compared to world other regions with Asia 30% and North America 25%. However, if these reserves are fully developed, they have potential to provide Europe gas supply with another 25 year at projected consumption level of 600 to 700 bcma/y [46].

Poland has highest shale gas resources and has high prospect for the development of shale gas resources. The development of shale gas reserve can help Poland to decrease its dependency on Russian gas imports and natural gas will replace coal as cleaner energy source. France has next largest shale gas resources, however, local public opposition act as major hurdle in development of shale gas resources. Norway is major European conventional oil & gas producer and exporter with largely depend upon hydropower for enrgy requirements. Therefore, the prospect for development of shale gas in Norway is very less. Ukraine holds fourth largest shale gas resources in Europe, however, energy policy much influenced by Russian energy strategy. Therefore, the development of shale gas resources in Ukraine is politically much more complex [55].

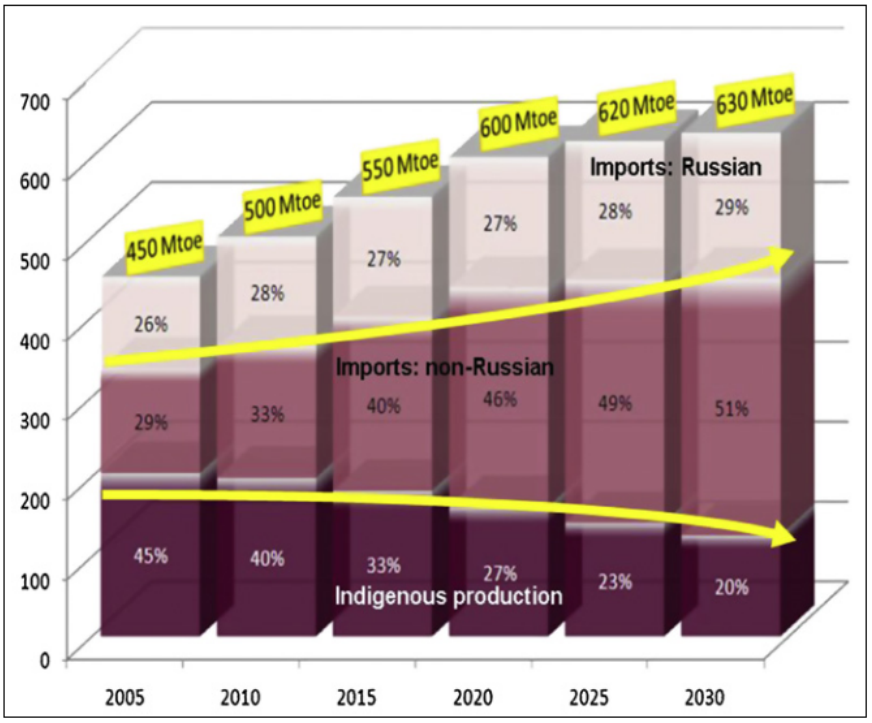

FIGURE 2.4: Share of EU gas imports [54]

2.1.2 Production of shale gas

Shale gas are unconventional resources and unconventional technologies are applied to shale gas reservoir to extract shale gas. As shale gas reservoir has very low permeability, production of shale gas is very difficult and also very expensive than the conventional reservoir. Conventional gas reservoirs has free gas in interconnected pores from where it flows through well bore. While Shale gas has very low permeability and often gas is adsorbed on organic material. So, It is necessary to stimulate reservoir by fracturing the reservoir to interconnect the pores containing the shale gas[17].

The Advancement in horizontal drilling and hydraulic fracturing technologies played a key role in development of shale gas resources. Both of these technologies were used and developed to enhance recovery of conventional reservoir, however, the application of these two technologies to unconventional reservoirs enhance the potential of recovery of trillion cubic foot of natural gas present in shale gas plays. A schematic of the horizontal drilling & fracturing operation is shown in the figure 2.5 Oil and gas drilling rig begins in the same fashion for both vertical and horizontal drilling well. In the case of horizontal drilling, the drilling starts turning or kicking off when the top surface of the production zone arrives and then runs through the formation horizontally. The horizontal drilling can be proceeded up to 10,000 feet through the production Zone formation. Once the drilling completed, the production casing is perforated with the help of explosive at the

points where the hydraulic fracturing has to carry out for the production of shale gas [58].

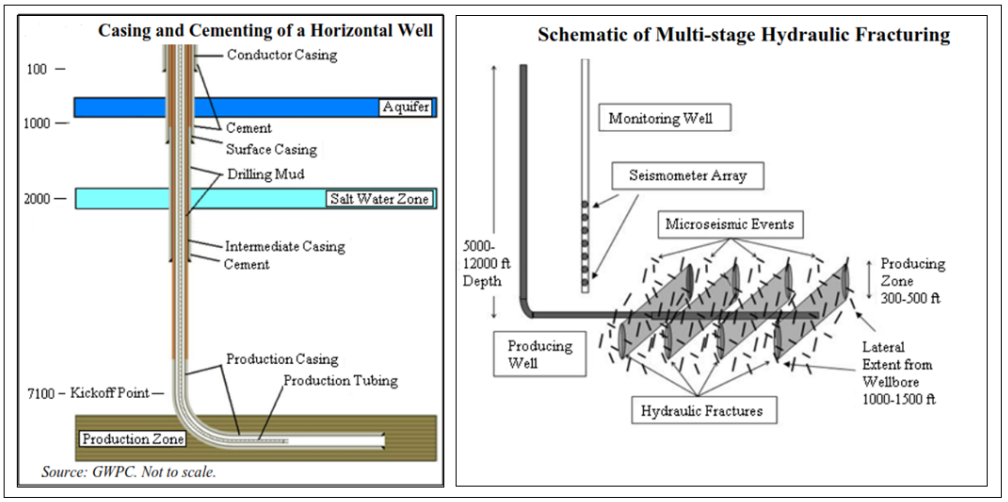

FIGURE 2.5: Horizontal Drilling with Hydraulic Fracturing [58]

Water is among the most important part of the hydraulic fracturing process. Availability of water is distinguishing factor for the development of the shale gas resources. Ten of thousands of barrels of water is required for each stage during the hydraulic fracturing operation. Along with the water, some granular materials known as proppants are also added to keep open once the propped fractures. The most commonly used proppants are sands with some other resin coated ceramics. The successful hydraulic fracturing process is carried out at higher viscosity, therefore, some gel material, polymer and crosslinking agents are also added in the fracturing fluids. Some scale, corrosion inhibitor, and gel breaker are also part of the fracturing fluid . An overview of hydraulic fracturing fluid constitutes is given in the figure 2.6. The improved hydraulic fracturing fluid composed of slick water instead of polymer gel material in the fracturing fluid. Slick water is more dilute, low viscosity water based fluid which allows gas to pass through it. Slickwater works better in shale gas formation because of its low viscosity which allows fracturing fluid to reach into many small naturally occurring fracture in the formation [3] .

2.1.3 Environmental Concerns

Shale gas production is viewed to be controversial with environmental risks and impact on human. Hydraulic fracturing is considered to be main concern because it uses large quantity of water and extraordinary pressure created deep in the subsurface. The major environmental threats associated with hydraulic fracturing are surface and subsurface

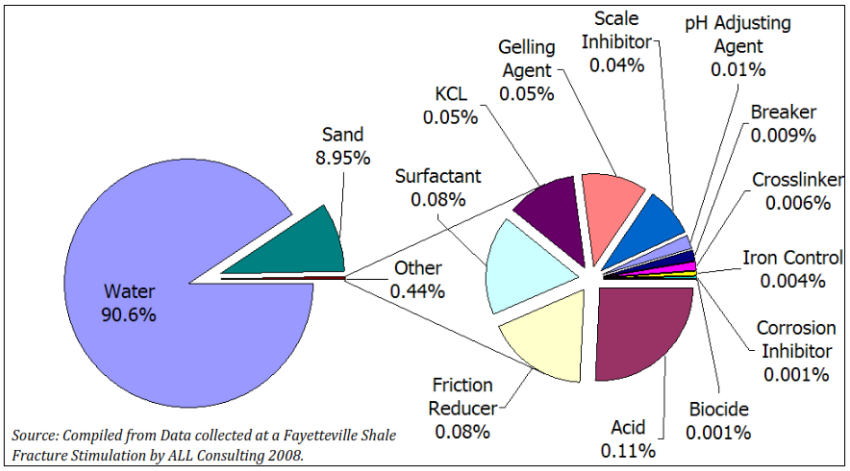

FIGURE 2.6: Composition of Proppants Laden Fracturing Fluid [3]

water contamination, artificial earthquakes and air pollution. Some environmental challenges of shale gas production are discussed as follow.

2.1.3.1 Water Contamination

The hydraulic fracturing creates fracture which can be propagates hundreds of feet from the fracture point. The common debated concern associated with shale gas production is the risk of extension of fracture from target formation to water aquifers and contamination of drinking water with flow methane. However, with few exceptions, the natural gas bearing shale formation is thousands of feet separated from the base of the formation containing water aquifers. Therefore, the methane mixing with drinking water placed thousands of feet above the shale formation is very less likely. Seismic Monitoring system is very effective tool to make sure that hydraulic fracturing is carrying out within the shale formation and it cannot propagate outside the shale formation. However, failure in cementing or casing around the wellbore may cause severe risks to water aquifers. The leakage through casing or cementing may lead to flow of hydrocarbon, fracturing fluid or produced water and mix with water formations which may pose major concern to quality of water along with other environmental issues [58]. With the gas leakage, the methane as major component of shale gas mixes with water. It has very low water solubility with 26 mg/L at 20C, therefore, considering methane as solute in water is not considered as health hazardous for ingestion. However, methane can be oxidized by bacteria in water and cause depletion of oxygen. Low oxygen contents in the water results in higher solubility of iron and arsenic elements [50].

Hydraulic fracturing process requires huge volume of water which is also considered to be the environmental concern. A comparison of water consumption of different shale

TABLE 2.2: Comparison of estimation of water needed for hydraulic fracturing for different Shale play [51]

Shale Play	**Formation Depth (ft)**	**Porosity (%)**	**Fracture Water (mln gal/well**
Bernett	6500 - 8500	4 - 5	2.2
Fayetteville	1000 - 7000	2 - 8	2.9
Haynesville	10,500 - 13,500	8 - 9	2.7
Marcellus	4000 - 8500	10	3.8

plays is given in the table **??**. However, the major environmental concerns are chemicals used in the hydraulic fracturing fluids which have been discussed before. The chemicals accounts for only 0.5 to 2 %d of total volume of fracturing fluid. Its looks small component of fracturing fluid, however, when we compare it with 2-4 million gal of water used for fracturing operation then it accounts for 80 to 330 tons of chemical. Even a small quantity of chemical used in fracking process tends to contaminate million gal of water. The very large quantity of water also pose sever concerns when it flow back after completion of fracturing operation. One to five million gal water of which 25 to 100% is returned back to surface tend to contaminate the surface. The flow back fluid in addition to chemical also contains total dissolved solids TDS for example Marcellus operation contain TDS around 70,000 to 250,000 mg/L. The direct release of these chemical on the surface may cause adverse effect on human health and environment quality. Reverse osmosis and distillation techniques can be used for the waste fracturing fluid treatment, however, these techniques are considered to be very expensive for such a large quantity of fracturing fluid used. So, other techniques for fracture fluid waste handling are not considered to be sustainable [51]. Therefor handling of chemicals in the flow back fluid is an area of concern for development of shale gas resources.

2.1.3.2 Seismic Risks

Shale gas production operation also has major concern of generation of earthquake as result hydraulic fracturing activities. Hydraulic fracturing operation can change the stress and strain mechanism deep in the rock. Below few kilometers, the whole earth crust is under stress and these natural stresses help to propagate the fractures. Injection of fluid strikes the faults and fracture reduced the stresses by creating space which have tendency to trigger the earthquake [51]. For example, a town in Texas experienced earthquake in 2008 and 2009, however, there was no earthquake observed for the recorded 142 year history. It was believed that seismic activities related to hydraulic fracturing operation resulted in the earthquake. The team of seismologist investigated the causes of earthquake but no solid link was found between hydraulic fracturing activities and

causes of earthquake, however, concerns were raised over the seismic activities related to injection of waste fluid from the shale gas operation into disposal well [58].

2.2 Proppants

Proppants are small particles that are used with hydraulic fracturing fluid to keep fracture open with an ultimate goal to create a high-permeability and high surface area conduit that may access oil and gas in the reservoir. The proppants settle in the rock fissures as closed packing or as a single layer to keep fissure open while ensuring adequate permeability as illustrated in figure 2.7 [13].

The proppant particle has to bear extreme stresses within the rock, therefore, it should be composed of very high strength material. During service and operation, a pack of proppants is subjected to forces, a compressive force from the rock of the fracture and other transverse shear force due to pressure difference as well as drag force exerted by the fluid flowing. The compressive force tries to crush the proppants, thereby reducing the permeability and conductivity of the proppant. The transverse force may cause proppants flowback which may result in erosion and interrupt production[38]. Poppants work underground and they have to bear every type of harsh environment such as high temperature, high pressure, HF-HCLmixture used for removal of blockage and corrosive media in crust and fracking fluid. So, the quality of proppant is very crucial to the success of hydraulic fracturing operation [17].

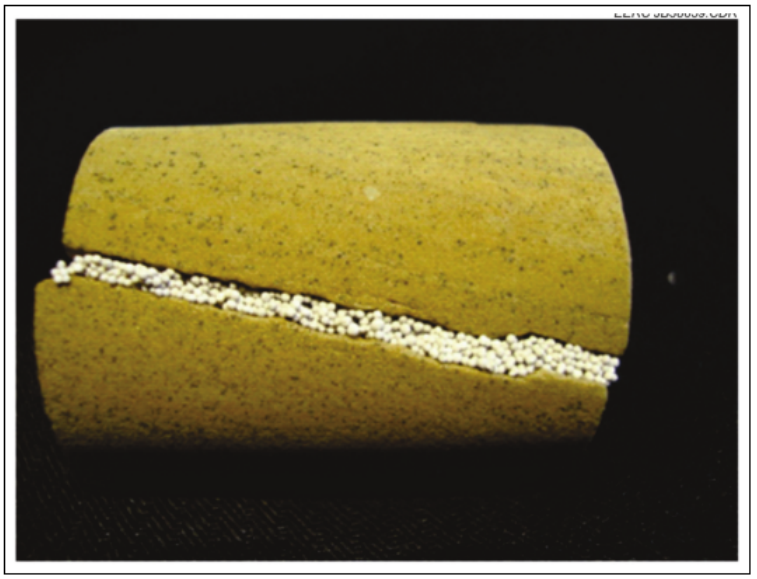

FIGURE 2.7: Propped Fracture [6]

2.2.1 Types of Proppants

Proppants are prepared in various form with variation in properties according to specific applications. Selection of proppants is based on reservoir conditions, economics of the operation and properties such as strength, chemical resistance, and density of proppants. Proppants are available in two major types

1. **Sand Proppants**
2. **Ceramics Proppants**

2.2.1.1 Sand Proppants

When economics of operation and low cost of proppants is main consideration, then there is no better choice than the use of sand. Sand is not only cheapest choice among proppants, it is also abundantly available material as proppants. Therefore, sand is most commonly used proppants material in past and also in recent proppants application. However, There are some limitations attributed to sand as proppant which restrict its vast application. Sand is not ideal proppant, at above 5000 Psi closure stress, sand is not normally employed because it start to disintegrate into its fragments. The resulting material from disintegration is in the form of fines or pellets, it migrate and plug the flow passage of shale gas in the propped fracture. These migrated fines particle of sand silica drastically reduce the permeability of the propped fracture. Since closure pressure varies directly with the depth, so sand is not recommended to be used as proppant for depth greater than 5000 ft[39]. The sharp decrease in permeability of sand is given in table 2.3.

TABLE 2.3: Quartz sand proppants permeability data [23]

Closure stress (psi)	**Permeability (darcy)**
2000	88
4000	65
6000	34
8000	16

Sand proppants has very poor chemical resistance and resistance against the attack of corrosive acid. So, the sand proppants limitations prompt for development of new proppants or some treatment of sand proppants to achieve desirable properties for vast applications. Resin coating is considered to be effective treatment to enhance sand ability to bear harsh conditions. Resin coated particle show greater resistance to closure and improve the stability of proppants. Sand is coated with infusible resin such as

epoxy or phenolic resins. These proppant show better stability than sand and may be used at closure pressure not higher than 8000 psi[23]. Resin coating also imparts geochemical stability to the sand proppants and helps spread stress over the large area of the grain reducing the point loading. Proppant consisting of sand with coating of precured phenol famaldehyde resins had been used in subterranean formations. However, at high temperature and high stress level these resin coated sand proppants still showed decrease in permeability. During the rapid closure of fracture, the proppant crushed before the resin coating cured it[57]. This problem was overcome by dual resin coating having a reinforcing agent interspersed into inner boundary of the resin[42].

2.2.1.2 Ceramics Proppants

For application in harsh condition of extreme stress, more sophisticated, especially prepared proppants are employed and ceramics proppants are considered to be among best choices. Ceramics proppants are very high strength proppants. Ceramics proppants are becoming widely used proppants in hydraulic fracturing of oil and gas due to their higher strength and resistance to closure stress. The ceramics are considered to be stronger, less deforming , and tougher, less breakage, as a result of mineralogy composition high in aluminium and silicon oxide. Chemical robustness is also reported for oil and gas field application. Ceramics proppants are commonly reported in three types Light weight, Intermediate strength proppants (ISP), High strength proppants (HSP). Intermediate strength proppants (ISP) have strength greater than sand and light weight ceramics and has application in operating condition 5000 to 10000 psi. High strength proppants (HSP) mostly consist of bauxite is proved to be strongest proppant and has application in operating condition 10000 to 15000 PSI [26].

For use in 10,000 ft or deeper into the earth, the proppant have to withstand more than 10000 Psi, to keep open the fracture. Currently only ceramics material such as Bauxite and alumina have sufficient high compressive and flexural strength to bear high pressure and temperature deep into the earth. Bauxite with 85% alumina is strong enough to resist crushing stress at well depth of 20000 ft. Table 2.4 shows high permeability of sintered bauxite proppants and decrease in permeability with the increased in closure stress. But it is evident that permeability of bauxite still higher of 103 Darcy at 12000 psi than the permeability of sand of 88 at 2000 psi [23].

The performance of ceramics proppants is not comparable with the sand proppants, similarly the cost of ceramics proppants is also not comparable with the sand. The sand proppants are naturally present but the ceramics proppants are especially manufactured product. Therefore, the ceramics proppants are too expensive than the sand proppants.

TABLE 2.4: Sintered Bauxite proppants permeability data [23]

Closure Stress (Psi)	Permeability (darcy)
6000	169
8000	137
10000	120
12000	103
14000	86

The ceramics proppants prepared from alumina and bauxite are very high strength but they are very expensive because limited supply of raw material and higher requirement of purity. It is reported that sintered bauxite is much more expensive than sand even in some case 10 times the cost [6]. In addition these ceramics material provide higher strength at the expense of increase weight. They have specific gravity higher than 3.0 which is highly undesirable for proppant application [8]. Higher density of ceramics can leads to higher erosion and also higher settling. So, the selection of proppants for a specific application is an compromise between cost, strength, density and other important properties.

2.2.2 Properties of Proppants

The properties of proppants are very critical for hydraulic fracturing process. As discussed earlier, the selection of proppants largely dependent upon the properties of proppants. As proppants have to use under harsh condition, therefore ideal properties are expected from proppants. The main properties of upon which the performance of proppants are greatly dependent are weight or density of proppants, high mechanical strength and chemical resistance of proppants material.

2.2.2.1 Light Weight

The weight or density of the proppants is very important regarding the transportation and placement of proppants deep in the reservoir. The proppants are ideally quoted as they should be lighter than air. The proppants have to be transported along with the fracturing fluid, and it desirable that proppants should be suspended within the fracking fluid and they should not be allowed to settle down. If very high density proppants are to be used, there is possibility of settling down of proppants during initial stages of proppants placements in the reservoir. There is also possibility for synthesis of ultra light weight proppants. The ultra light weight proppants designed with the porous structure particles with pores filled with the encapsulated air. But the porous structure resultrd in decreased mechanical strength [45].

TABLE 2.5: Comparison of proppants density [2]

Proppants type	**Specific gravity**
Sand	2.65
Resin coated ceramics	2.6
Light weight Ceramics	2.72
Resin coated light weight ceramics	2.66
Intermediate strength proppants	2.27
High strength proppants	3.56

However, in order to get minimum density, a compromise has to be made on the strength of the proppants. A comparison of densities of different types of proppants is elaborated in the table 2.5. The table 2.5 represent an increase in density with the moving towards the high strength proppants [2]. So, high strength proppants are used at the expense of increased density and ultimately with the higher settling velocity. The settling velocity similarly showed in the figure 2.8 an increase with the density for the higher strength materials [44]. Therefore, it is usually hard to suspend the high strength higher density proppants. In order to achieve higher suspension of the proppants within the fracturing fluid, a most commonly employed technique is the use of polymer gelling material to make the viscous fluid. The polymer gelling agent assisted with some cross linking agent, help the viscous fracking fluid to make proppants suspended [19].

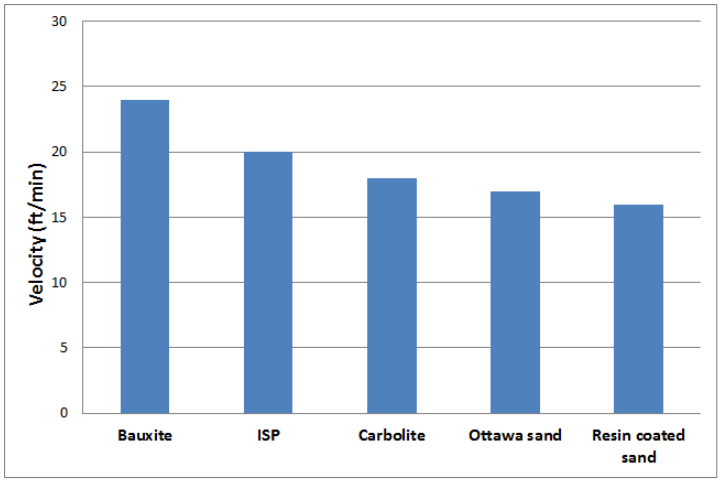

FIGURE 2.8: Comparison of proppants settling velocity [44]

However, with the higher density proppants more gelling agents have to be added to make fluid more viscous. The higher viscosity fluid require higher pumping rate and

higher pumping cost. Erosion is another opeerational problem caused by the use of higher density proppants. Higher density proppants contain higher momentum due to turbulent fluctuations. The higher momentum carrying proppants can strike with tubing and piping with more force resulting in higher damage and erosion [12]. So, the density of proppants is an important factor in a deciding application of the proppants.

2.2.2.2 High Mechanical Strength

The strength of proppants is the most important properties of the proppants. Its ultimately is the strength of proppants which keep the fracture open and provide resistance against the two closing rocks. The forces which applied on the proppants are far filed stresses which apply normal to the fracture plane and try to close the fracture. In response to the applied closure forces on the proppants, the proppants particles within the fracture also apply stresses to the walls of the fractures which tries to keep open the fracture. In order for safe operation of the hydraulic fracking process, the applied stresses by the proppants on the walls of the fractures should be higher to keep open the fracture [47].

The early proppants were prepared from sand, glass and walnut shell which were of very low strength material. When low strength materials are employed deep in the reservoir, once they are broken cause not only closure of fracture but also generate fine particles. The fine particles try to fill the intra particle porosity and block the flow of oil and gas [4]. For application in very high stress reservoirs, the high strength ceramics proppants are considered to be preferred choice. The alumina contents in the ceramics proppants impart very high strength to the ceramics proppants, however, very high alumina contents also result in higher density. As discussed earlier, the very high density of proppants is not a desirable phenomena.

The conductivity or permeability of the fractured reservoir is the most important criteria for evaluation of the performance of the proppants. It is the conductivity of the fracture reservoir which measure the extent of oil & gas flow rate through the reservoir and ultimately measure of production of oil & gas. The mechanical strength of the proppants is very critical for the conductivity a decrease in strength of the proppants result in reduction of permeability or conductivity. As discussed in the table 2.3 show sand proppants as low strength material and there is sharp decrease in permeability with the increased applied stress. However, the ceramics proppants are very high strength material than the sand [23] and represent a much higher conductivity than the sand proppants as discussed in the table 2.4. The decrease in conductivity with the applied stress is due to the generation of fines. Its is reported that for 20/40 mesh proppants,

an increase in 5% fine in proppants pack could result in 60 % reduction in conductivity of the proppants pack [9]. The strength of the proppants can further be increased with the coating of the proppants with some polymer resin.

2.2.2.3 Chemical Resistance

Proppant have to be in contact with chemical containing fracking fluid, along with corrosive environment of crust and HF-HCl mixture, so prppant must be resistant to chemical.The proppants are specially designed to bear very harsh condition underground however, conditional changes such as reservoir souring, CO_2 for EOR and injection well retrofitting may challenge the chemical integrity of proppants. Proppants particle are susceptible to geochemical affects because of high surface area and high flow rate of the fluid flow in the fracture[6]. Pressure solution controlled by gradient of potential difference between stressed sites and free pore spaces is one of the important factors in chemical degradation of the proppants. The degradation of proppants begins with the creation of defects on the surface of the proppants which open the reactive surface. The presence of reactive surface on the proppants may lead towards dissolution of the proppants [41]. Pressure solution and compaction is schematically shown in the figure 2.9.

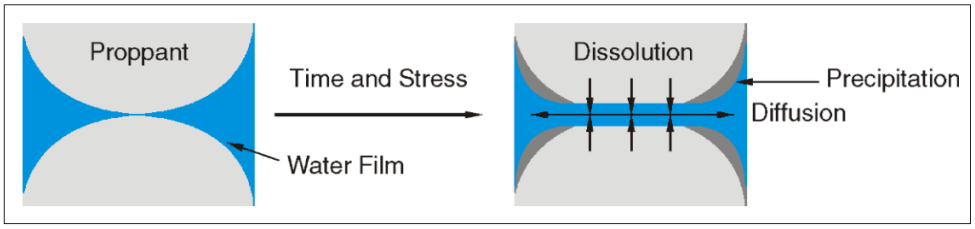

FIGURE 2.9: Pressure compaction mechanism [52]

In the pressure solution mechanism, the stress level is extremely high at the contact point of the two proppants in a fluid under very high mechanical load. In the presence of water the solubility of the proppants is much higher at the contact point where stress is very high than the region where there is no stress. So the dissolution of the proppant material occurs at the contact point of the proppants. The dissolved proppant material diffuses into the fluid, precipitate on to the pores, cause decrease in porosity, permeability and finally conductivity of the reservoir. Moreover dissolved material also create reactive surface on the surface of the proppants to cause further damage [28] .

Proppants may have to be contact with CO_2 and H_2S while EOR and reservoir souring. Further research on chemical effect on proppants revealed a loss of strength of proppannts

on contact with H_2S and CO_2. A loss in strength of 8 %, 7% and 25% is reported for the fine grain sized ceramics, sintered bauxite and sand respectively in a brine as fluid. Furthermore, strength loss from exposure CO_2 is 5 times more than the loss in strength in case of H_2S and sand is reported stronger than the ceramics on contact with gasses [52]. Low permeability and deep well are increasingly drilled using acidification, which required proppants with very high acid resistant. Tingtu et al, 2013 research showed that poor acid resistant is due to silicon containing compounds in proppants raw material. Silicon compounds are amorphous and decrease the acid resistant[56].

2.3 Scale Inhibition

Scale are deposits which formed by the precipitation of chemical species present in the water at reservoir conditions. The scale formed inside tubing, pumping equipment and the reservoir which cause the blockage of flow of oil and gas with other different production problems. Scaling is phenomena which originate from super saturation of dissolved solid present in the water. This supersaturation can occur either by water present in the reservoir or originate from incompatibility caused by mixing of different water. Water is a good solvent and has capacity to dissolve many chemical species and can result in a complex fluid which is rich in different ions through contact with different minerals. Subsurface water can be enriched with ion on contact with sedimentary minerals such as carbonate and sandstone reservoir contain rich Ca^{+2}. and Mg^{+2} cations sandstone contain Ba^{+2}, Sr^{+2}. In reservoir condition the total dissolved solid can reach 4000,000 mg/L [10].

Scaling is very disturbing phenomena for continuous production of oil & gas. The scale can be removed either mechanically or chemically. The chemical scale removal is more convenient especially for places where access is comparatively difficult. The hydrochloric acid is considered to be the first choice for chemical treatment of the scale, however, spent acid has tendency to further initiate the scaling process. The ethylenediamenetetraacetic acid (EDTA) is chemical reagent which has capacity to dissolve and chelate the calcium carbonate by breaking the precipitation cycle. However, EDTA treatment is much more expensive and slower than the HCl treatment [10].

Preventing scale formation is considered to be much more effective approach than once the scale formed and then costly removal of it. Therefore scale inhibitors are employed in the oil & gas production to inhibit the scale formation in the reservoir. The scale inhibitors prevent scale formation by poisoning the scale crystal growth phenomena. The main area of interest for the present research work is the investigation of solid scale inhibitor.

2.3.1 Phosphonates

Phosphonates are compounds of phosphonic acid with Lewis acid moiety R-CP(O)(OH)2. The phosphonates consist of stable covenant bond of carbon with phosphorous. Phosphonates can be in form of single phosphonic group or multi phosphonic group. Methylphosphonic acid (MP), hydroxymethylphosphonic acid (HEDP), Nitrolotris-methylphosphonic acid (NTMP), Ethylenedinitrolotetrakismethylene phosphonic acid (EDTMP), diethylenedinitrlopentakismethylene phosphonic acid (DTPMP) consist of mono, di, tri, tetra and penta phosphonic acid group respectively which represented in the figure 2.11 [35]. Phosphonates are highly water soluble, have ability for complex formation with metals, strong adsorbent and their ability to inhibit scale formation distinguish them for different industrial applications. Stability of phosphonates complexes with metals is represented in figure 2.10. The stability of phosphonates complexes increases with the increased number of phosphonic acid groups present in phosphonates for example, AMPA has the lowest stability with the only phosponate group, and EDTMP have the highest with the four phosphonates group. For the metals with $logK$ value for stability of complexes varies according the Irving-William series $Mn^{+2} < Fe^{+2} < Co^{+2} < Ni^{+2} < Cu^{+2} < Zn^{+2}$ [35].

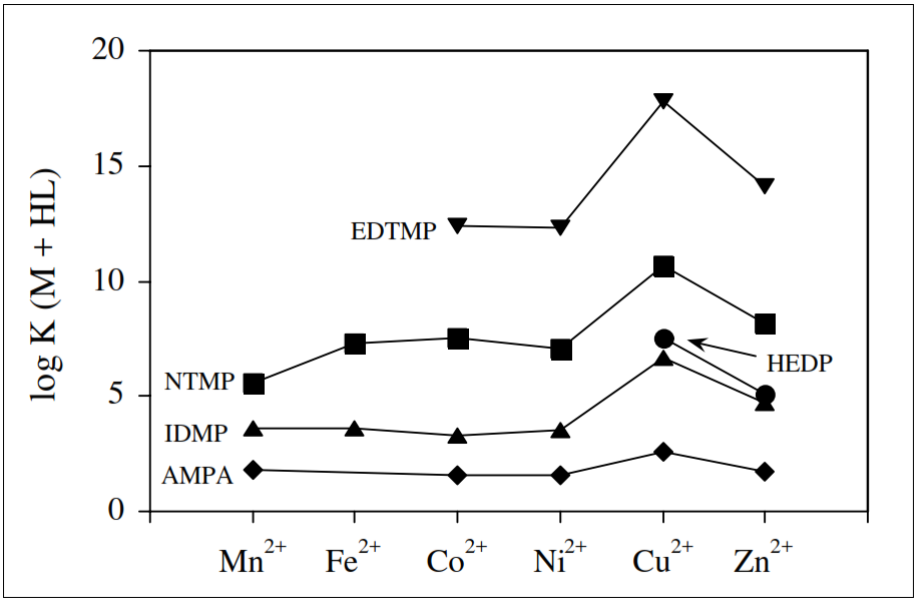

FIGURE 2.10: Stability constant of 1:1 complex (M+HL) of phosphonates with transition metals [35]

Phosphonates find application in petroleum production, in cooling water system, boiler and desalination system as scale inhibition agent, in the textile industry for stabilization of peroxide bleaching agent, detergent formulation and in nuclear medicine as bone

seeking carrier for radionuclides [35]. Scale inhibition applications of phosphonates are discussed in detail in this report.

Abbreviation	Name	Structure
MP	Methylphosphonic acid	CH_3-$PO(OH)_2$
AMP	Aminomethylphosphonic acid	H_2N-CH_2-$PO(OH)_2$
HMP	Hydroxymethylphosphonic acid	HO-CH_2-$PO(OH)_2$
HEDP	1-Hydroxyethane-(1,1-diphosphonic acid)	$(OH)_2O\,P$ | HO-C-CH_3 | $(OH)_2O\,P$
IDMP	Iminodi-(methylenephosphonic acid)	$(OH)_2OP$-CH_2 \ N — H / $(OH)_2OP$-CH_2
NTMP	Nitrilotris-(methylenephosphonic acid)	$(OH)_2OP$-CH_2 \ N — CH_2-$PO(OH)_2$ / $(OH)_2OP$-CH_2
EDTMP	Ethylenedinitrilotetrakis-(methylenephosphonic acid)	$(OH)_2OP$-CH_2 \ / CH_2-$PO(OH)_2$ N-CH_2-CH_2-N / $(OH)_2OP$-CH_2 \ CH_2-$PO(OH)_2$
DTPMP	Diethylenetrinitrilopentakis-(methylenephosphonic acid)	$(OH)_2OP$-CH_2 \ / CH_2-$PO(OH)_2$ N-CH_2-CH_2-N-CH_2-CH_2-N / $(OH)_2OP$-CH_2 \ CH_2-$PO(OH)_2$ | CH_2 | $PO(OH)_2$

FIGURE 2.11: Name abbreviation and structures of phosphonates [35]

2.3.2 Mechanism of Scale Inhibition

Precipitation of dissolved solid to form scale occurs when the solubility limit of chemical species achieved. However, the dependence of solubility of dissolved solid on different factor is a complex phenomenon and is governed by changes in temperature, pressure, PH and incompatibility of mixing water. Mostly the solubility increases with the increase in temperature but there are some compounds which show decrease in solubility with the increase in temperature. For example the solubility of Calcium Carbonate decreases with the increase in temperature. The scale growth within the supersaturated solution initiated by formation of unstable atoms clusters. The atoms clusters form small seed crystals which grow further by adsorption of ion on the seeds extending the crystal size. This homogeneous nucleation process results in the growth of scale [10]. A schematic representation of crystal growth process of scale is illustrated in the figure 2.12.

Several theories about mineral scale growth and inhibition were presented, however, the most successful theory about kinetics and precipitation of scale is Burton-Caberrara-Frank mechanism. In this mechanism, the kinks sites are considered to be continuously

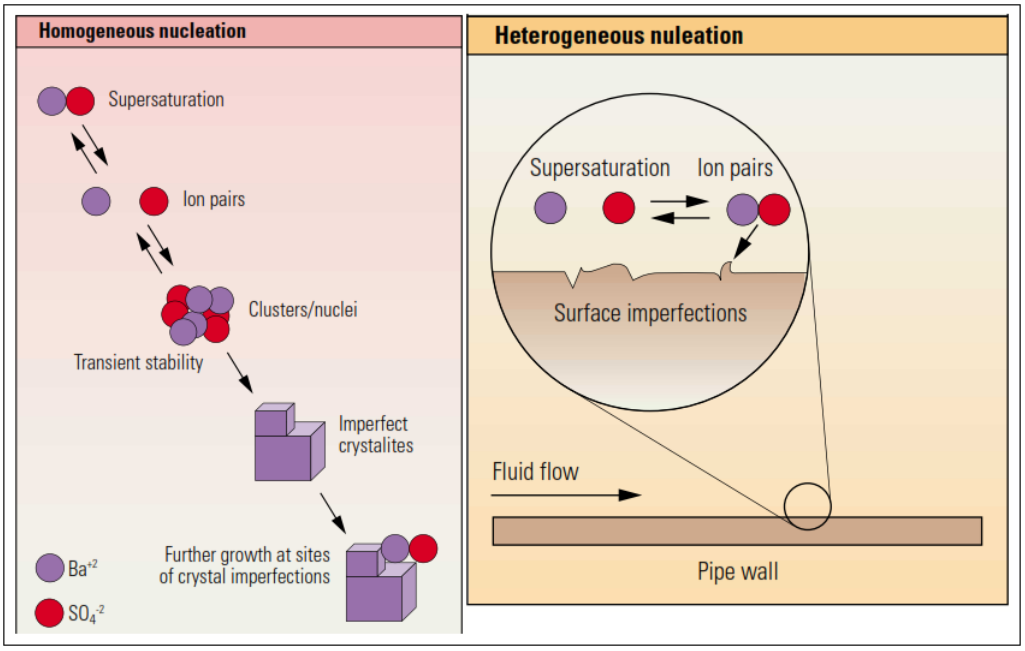

FIGURE 2.12: Nucleation & crystal growth process [10]

grown in a spiral form to overcome the activation energy for nucleation. With the calcite scaling, the spiral growth mechanism was observed at larger reaction time and near equilibrium conditions. At shorter reaction time, the growth follows the polynuclear birth and spread mechanism where nuclei quickly grow and coalesce with layer growth [14]. Scale inhibitors are employed which perform inhibition by poisoning the crystal growth mechanism and cause defect in growth process. It is generally believed that inhibitor adsorbed on the active sites of crystal growth of the surface and stop further growth. So, the scale inhibitor adsorb on the kinks site and stop the further spiral or polynuclear birth & spread mechanism resulting in prevention of scale formation. In the case of calcite, the phosphonates are considered to be adsorbed on the Ca^{+2} and form Ca-phoshohonates complexes. For efficient scale inhibition, there should be sufficient inhibitor coverage of nuclei and crystal growth sites. Seed growth studies evident that there should be 5 to 25 % coverage nuclei or crystal site necessary to prevent growth mechanism. In order to cover 5 to 25 % surface of nuclei, there should be 0.05 to 0.25mg/m2 of inhibitor is required [49].

As discussed earlier the adsorption of phosphonates is very important phenomena in scale inhibition mechanism. The linear adsorption constant Kd for calcite and barite is 0.27 and 0.22 L/m2 respectively. Therefore adsorption of phosphonates is higher for calcite than barite resulting in higher efficiency of scale inhibition in case of calcite. The linear adsorption constant is also observed to increase in order of $NTMP < HEDP < DTMP < BHPMP$ and scale inhibition efficiency also follow the same order [49].

Nowak et al, 1999 investigated the adsorption behavior of phosphonates over goethite (FeO(OH)). The adsorption reaction of phosphonates was very fast and achieved equilibrium within few minutes. As the PH increased the adsorption became less significant and resulted in desorption of phosphonates with the increase in PH as reversible process to adsorption. The adsorption behavior of Phosphonates with change in PH value was investigated with five phosphonates MP, IDMP, NTMP, EDTMP, and DTPMP possessing one, two, three, four and five phosphonates group. The phosphonates showed strong adsorption at lower PH value and desorption trend started at PH value higher than 8 irrespective of number of phosphonates attached the compounds as illustrated in figure 2.13.The methylenphosphonic acid (MP) with mono phosphonic group showed sharp decrease in adsorption with increase in PH. However, the compounds containing multiphosphonic group shows comparable rate in decrease of adsorption with PH [36].

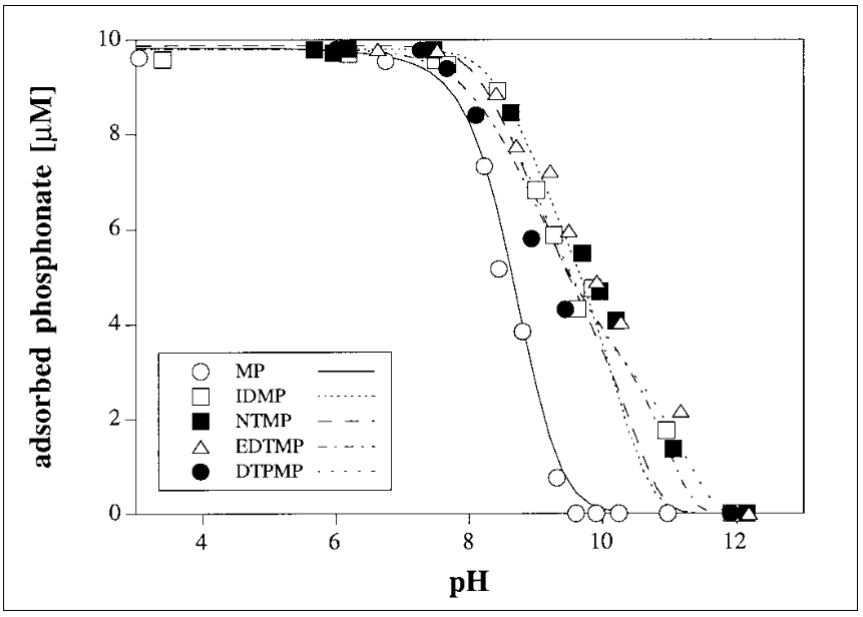

FIGURE 2.13: Comparison of adsorption of 9.8 uM Phoshphonates on goethite [36]

2.3.3 Chemical Scale Inhibitor Placement

Effective placement of chemical and scale inhibitor is very critical for efficient performance of the reservoir for oil and gas production. Sustainability of propped jfracture is largely dependent upon effective placement of scale inhibitor in the produced fractures. If some fractures or some parts of fractures are without scale inhibitor treatment, may result in scaling on contact with mineral scales which cause damage in conductivity and reduction in production [10]. Bullhead scale squeeze operation is considered to be

conventional technique for scale inhibition operation. In Bullhead scale inhibitor operation, liquid scale inhibitor are injected in the reservoirs after intervals and repeated this process several time according to need. This is non-selective operation and is not very effective because there is likelihood that some parts of water production zones left without scale inhibition treatment.The formation face is considered to be very large. The liquid inhibitor injected in the reservoir has the possibility to be lost before reaching the target area. This phenomena leads to poor placement of inhibitor and ineffective scale inhibition process [34].

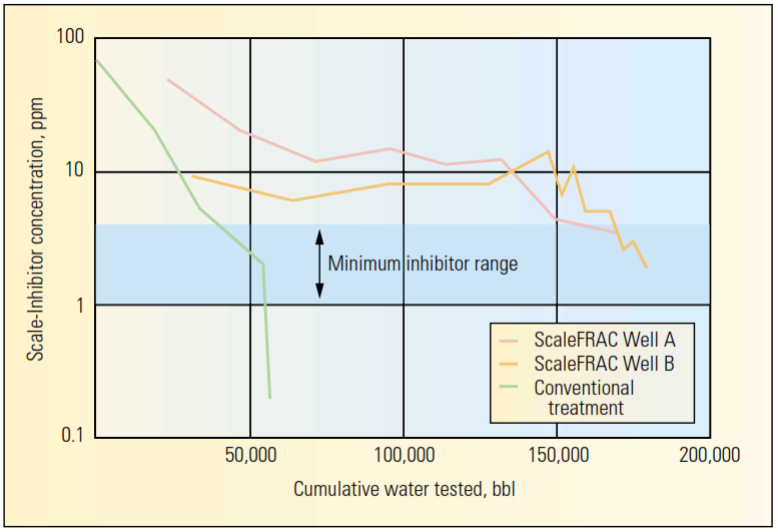

FIGURE 2.14: Comparison of Bullhead convention inhibitor injection method with ScaleFRAC system [10]

An alternative technique is employed by Schlumberger known as ScaleFRAC in which cracking process and scale inhibition treatment process are combine in a single step operation . In the new approach, the scale inhibitors are mixed with fracking fluid which leads the scale inhibitor everywhere in the fracture points in the reservoir [10]. A Comparison of Bullhead convention inhibitor injection method with ScaleFRAC system is depicted in the figure 2.14. The figure showed an improved performance of ScaleFRAC operation compare to conventional Bullhead approach. However, the ScaleFRAC approach has limitations in applications due to interaction of ScaleFRAC with fracking fluid. The acidic behavior of scale inhibitor may interact with fracking fluid gel and cause breakdown of gel cross-linking structure which may cause the decrease in viscosity thereby poor performance of the proppants transport. Therefore, careful testing and evaluation of interaction of fracking fluid with inhibitor is necessary to ensure no compromise on success of proppants placement in the reservoir.

Solid Scale inhibitors provide opportunity for scale inhibition deep the reservoirs. The solid scale inhibitors present very effective performance during early stages of water

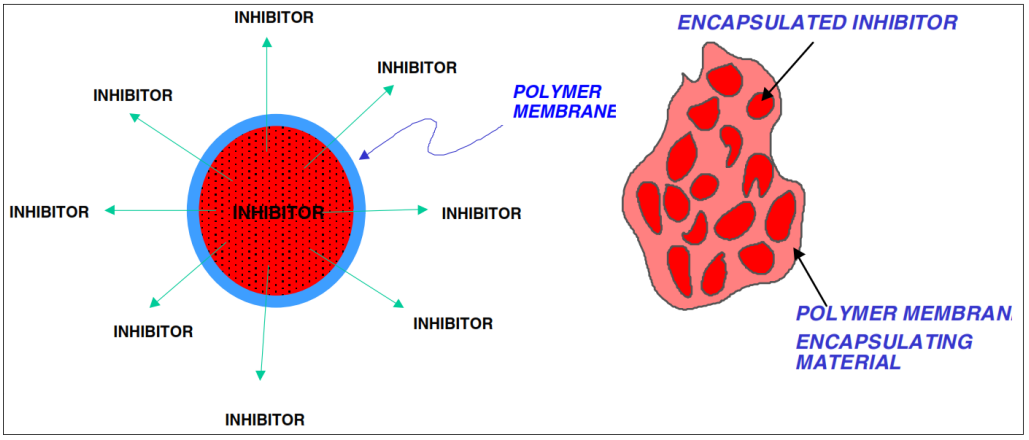

FIGURE 2.15: Encapsulated Scale Inhibitor [5]

breakthrough and also provide opportunities for scale inhibition in dry or near dry well. However, solid scale inhibitor present the drawback of very quick reaction of acidic scale inhibitor with the carbonate result in precipitation of Ca-phosphonates near the formation face. The phenomena of quick precipitation near wellbore result scale inhibition operation for only a limited distance near the wellbore [7].In order to slow down the quick reaction and slow release of inhibitor , the phosphonates inhibitors are encapsulated in a permeable polymer membrane as represented in the figure 2.15. The active scale inhibitor release was controlled with this approach through the polyemr membrane into solution. The rate of release through the membrane depend upon PH, temperature, surface area, flow rate and inhibitor concentration gradient. The inhibitor release rate increase with increase in PH, temperature and chloride concentration [5]. Flow back is another operational problem associated with chemicals and inhibitor deep in the reservoir. During flow back condition large quantity of phosphonates inhibitors returned back and after few days quantity decrease to a value below the minimum inhibitor concentration (MIC) where inhibitor are not capable of scale inhibition [7]. So, the operational challenges of scale inhibition techniques bring motivation for effective placement of chemical in the reservoir and further research and development in scale inhibition processes.

2.3.4 Development of Multifunctional Proppants

Development of multifunctional proppants is considered to be an opportunity to resolve challenges related placement of scale inhibitor and other chemicals deep in the reservoir. Development of scale inhibitor impregnated proppants by AEA technologies was major breakthrough in development of idea of multifinctional proppants. The scale inhibitor were impregnated on specially prepared porous proppants, which on contact with water

slowly release into water. Scale inhibitor inside the porous proppants first dissolve, then diffuse through the proppants followed by diffusion of inhibitor from the surface of the proppants to the flowing water. The scale inhibitor release rate and performance of impregnated porous proppants have been investigated in different fields and the field trial of Alaska field and Valhall field is given in the figure 2.16. The early stages of the operation showed very high release of scale inhibitor, however, the release rate slowed down with the passage of time [53] . So, there were significant achievements in slow release of scale inhibitor from the porous proppants and effective placement of scale inhibitor in the reservoir.

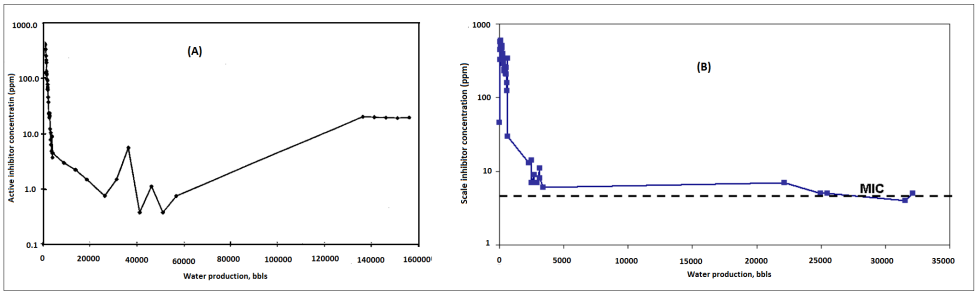

FIGURE 2.16: Scale Inhibitor Return Profile (A)Alaska Field Trial (Webb). (B)Valhall Field Trial [34]

However, the application of porous proppants are limited due to loss of mechanical strength and ultimately loss of conductivity of proppants. The comparison of conductivity of multifunctional porous proppants with conventional proppant ans sand proppant represented in the figure 2.17 . The figure depicts a decrease in conductivity of impregnated porous proppants compare to conventional proppants. The drawback of porous proppants is compensated by employing porous proppants in combination with the convention stronger proppants in order to optimize the conductivity. The mixing approach showed some improvements in application of porous impregnated proppants [53]. So, the porous impregnated multifunctional proppants open new window of opportunities for effective delivery of chemical deep in the reservoirs. This technique of chemical infused proppants can also be advantageous for effective placement of gel breaker, asphalt inhibitor, corrosion inhibitor along with other chemicals.

2.3.4.1 CNT Developed Multifunctional Proppants

Carbon nanotubes are of very high mechanical strengtjh with stiffer than the diamond and young modulus five time higher than the modulus of steel. Carbon nanotubes also have the ability to be functionalized and make bond with other contacting chemicals. So carbon nanotubes have the potential application in development of multifunctional

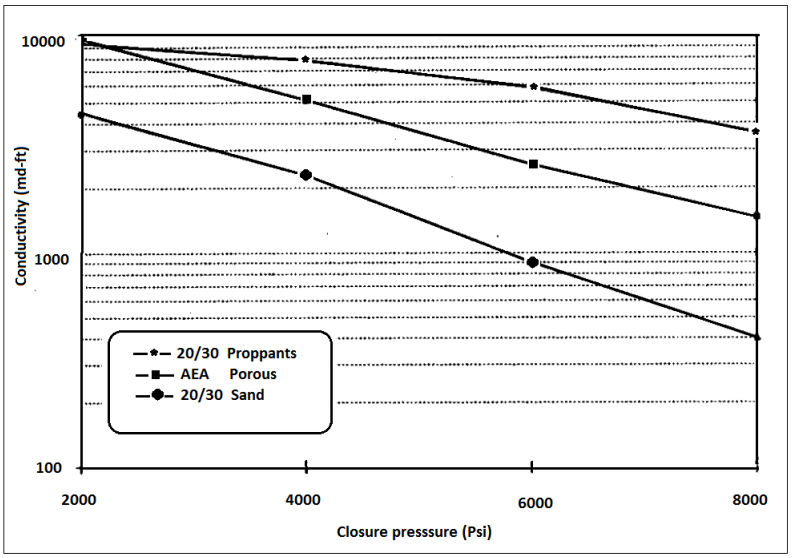

FIGURE 2.17: Conductivity Comparison of Porous Impregnated Proppants [53]

proppants. So the new approach for development of multifunctional proppants consists of coating of proppants particle or sand particle with carbon nanotubes using chemical vapor deposition method. The coated proppants particle further treated with chemicals such as scale inhibitor, asphaltene inhibitor or gel breaker for impregnation of chemical over the surface of the coated proppants particles as shown in the figure 2.18. This technique allow the opportunity to place inhibitor in the well where water production occurs .The solid inhibitor attached to the surface of proppants then dissolved slowly on contact with produced water. The dissolved inhibitors then prevent precipitation of scaling agents. The approach will not have any negative impact on the strength of the proppants or on other properties of proppants as seen in the proppants developed with the AEA technologies.

Carbon nanotubes can be functionalized by covalent or noncovalent technique. During covalent functionalization, the carbon nanotubes functionalized with the help of water-solubilizing agent. However, the covalent chemistry changes the atomic and electronic structure of carbon nanotubes thereby resulting in electrical and mechanical properties loss. The phosphonates scale inhibitors can also be attached to carbon nanotubes by nocovalent appraoch. However, noncovalent approach require an aromatic group attached to the phosphonates in order to be attached to carbon nanotubes. As discussed before phosphonates have high tendency to adsorb on the surfaces and variation of adsorption with PH, it will be interesting to investigate the potential for development of multifunctional Proppants.

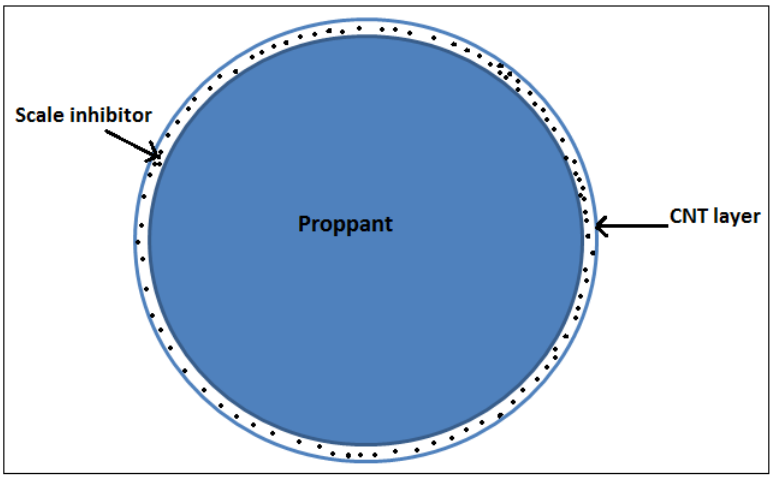

FIGURE 2.18: Scale Inhibitor Impregnated CNT Proppants

2.4 Carbon Nanotubes

Carbon nanotubes consist of sp^2 tubular structure of carbon discovered first time by Iijima in 1991. The nanotube composed of graphene sheet round into circular form [22].

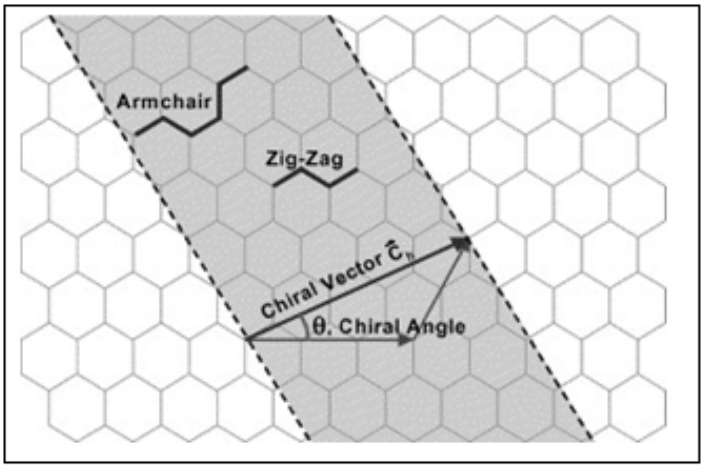

FIGURE 2.19: Schematic diagram for graphene sheet [48]

2.4.1 Types of Carbon Nanotubes

Carbon nanotubes are allotrope of carbon and carbon nanotubes can be divided into two main types.

- Single wall carbon nanotubes (SWCNTs)

- Multi wall carbon nanotubes (MWCNTs)

The schematic of types of carbon nanotubes is illustrated in figure 2.20. Single wall carbon nanotuebes (SWCNTs) can be considered as a sheet of graphene rolled into a circular form. Single wall carbon nanotubes has smaller diameter in the normal range from 0.4 to 4 nm. Single wall carbon nanotubes shows the properties as metallic and semiconductor based on the chirality vector. On average one third of the single wall carbon nanotubes are metallic when (n-m) is multiple of 3 and two third are of semiconductor when (n-m) is not a multiple of 3. Carbon nanotubes can be considered as perfect crystalline material when there is no variation in hexagonal structure of carbon atoms in the graphene sheet [33].

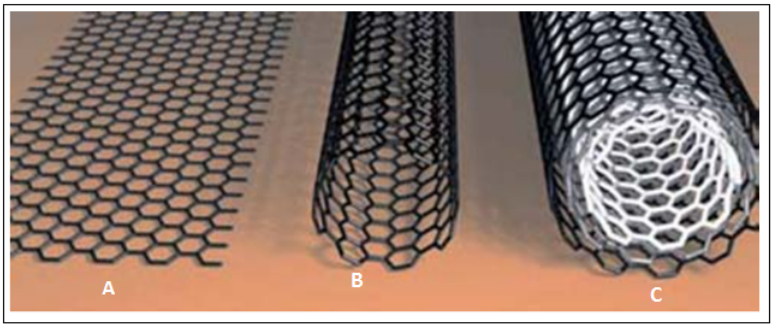

FIGURE 2.20: Types of carbon nanotubes (A)graphene sheet (B)SWCNTs (C) MWCNTs [18]

Multiwall carbon nanotubes can be visualized as concentric rolled up tubes of graphene sheets. The multiwall carbon nanotubes have number of tubes ranging from 2 to less than hundred. The multiwall carbon nanotubes have normally larger diameter than the single wall and diameter for MWCNTs range from 1nm and rarely increase 100 nm. The distance between two graphene sheet in graphitic is 0.34nm, therefore the inter tube distance is also 0.34nm in multiwall carbon nanotubes. The multiwall carbon nanotubes are considered to be metallic if only a single tube in the bundle is metallic. [33].

2.4.2 Molecular Structure of Carbon Nanotubes

The molecular structure of carbon nanotubes is considered to be a graphitic sheet which is rolled into to form a tubular structure. Similar to graphitic structure, each carbon atom in the tube has bonding with three neibors. The carbon nanotubes has sp2 hyberdization bonding like with a small s character because of curvature.

The atomic structure of carbon nanotube is described in term of tube chirality or helicity, which defined as chiral vector Ch and chiral angle. The chiral vector can be visualized

by cutting the graphite sheet as shown in the figure and rolling the tube in such a way that tip of the chiral vector touche its tail. The chiral vector is also known as roll up vector which can be described as following relation[48].

$$\vec{C_h} = n\vec{a_1} + m\vec{a_2} \tag{2.1}$$

Where interger (n,m) are the number of steps along the zigzag carbon bond in the hexagonal sheet and n $\vec{a_1}, \vec{a_2}$ are unit vectors.

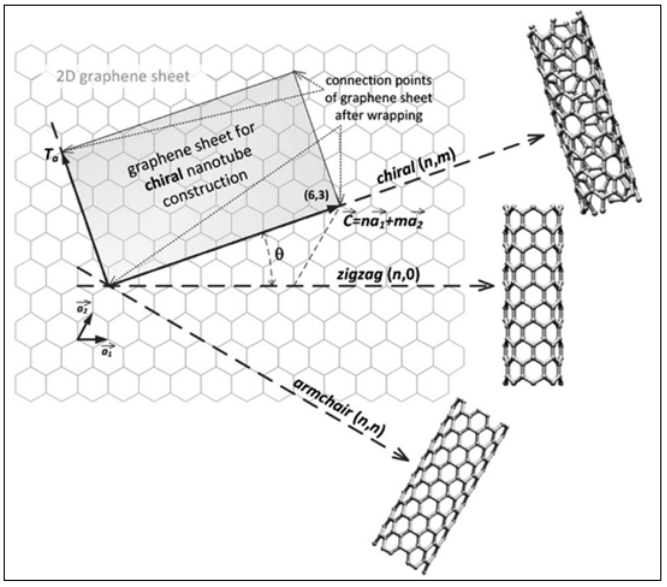

FIGURE 2.21: Structure of Carbon Nanotubes [40]

However it is not easy to classify these structure and guess their properties. The high symmetry structure of carbon nanotubes are classified in the following forms

- Zigzag
- Armchair
- Chiral

Chirality vector can be used to classify carbon nanotubes structure. In term of roll up vector or chirality vector, the carbon nanotube structure is referred as zigzag when chirality vector is (n,0) means when m=0. The carbon nanotube structure is armchair with the chirality vector of (n,n) means with m=n. For all other cases the structure of tubes is chiral. The physical property of the carbon nanotubes are senstive to the chirality of carbon nanotubes. The tube chirality has very strong influence on the

electrical properties of carbon nanotubes and also the effect is also observed on the mechanical properties of the tubes [29].

2.4.3 Synthesis of CNTs

Initially carbon nanotubes were synthesized with high temperature techniques such as arch discharge and laser ablation method. However, these method are now replaced with comparatively lower temperature technique known as chemical vapor deposition method (CVD). The chemical vapor depostion method have advantage of control over orientation, alignment, length of tube, diameter of tube, density and purity of the tube.

All currently employed method produce carbon nanotubes with impurities. Only a fraction of the synthesised material contain carbon nanotubes and remaining is carbonaceous material such as nanocrystalline graphite, amorphous carbon and metals that were introduced as catalyst. Therefore there is need of purification and commonly used purification method for carbon nanotube is acid treatment. There are three major lab scale synthesis method

1. Arc-discharge
2. Laser Abalation
3. Chemical Vapor Deposition

2.4.3.1 Chemical Vapor Deposition (CVD)

Chemical Vapor Deposition technique for the synthesis of carbon nanotubes has now become the standard method for the synthesis. The CVD method usually produces longer carbon nanotubes but with more defects as compared to arc discharge or laser ablation method. CVD process is based on the decomposition of carbon containing gasses over a catalyst at higher temperature. The temperature normally is ranged from 600 to 900 C. The catalysts usually employed are transition metals (Fe, Ni, Co) in the form of film or nanoparticle deposited on a support material. The catalysis in the CVD can be heterogeneous as in the case metal catalyst deposited as thin film or nanoparticle over a substrate. The CVD catalysis can also be the homogeneous in which gas phase contain carbon gas and catalyst particles as in the case of ferrocene [33].

The most widely used carbon source gasses used are acetylene, methane, ethane, crbon monoxide, ethylene. The carbon precursor gas is used with hydrogen diluted with some inert gas. The commonly used inert gasses are nitrogen and argon. The flow rate of

carbon source gas is typically between 10 to 30 ml/min. The flow rate of inert gas is kept higher than the carbon precursor. CVD process consists of a furnace with resistive or inductive heater as energy source which is used to decompose the carbon containing gasses [33].

Parameters Affecting CNT CVD synthesis

The most important catalyst for the synthesis of Carbon nanotubes through chemical vapor deposition are Iron, Nickel, cobalt. Their catalytic activity is related through decomposition of carbon precursor, formation of meta-stable carbide, diffusion of carbon and formation of graphite sheet[21]. The effect of different catalyst on the synthesis of carbon nanotubes has been reported in the literature. The performance of catalyst is observed in the order of $Ni > Co > Fe$. It is reported that catalyst activity of Nickel is better with with more uniform and stable across the catalyst which gives straight aligned carbon nanotubes perpendicular to the substrate while catalyst activity and carbon segregation of Co and Fe is non uniform and very slow. At a site of reduced catalytic activity, segregation of carbon may be extremely slow which can open the wall of tube which gives crooked or twisted carbon nanotubes [27].

The carbon nanotubes growth is much related with Carbon segregation and carbon diffusion through the catalsy. As discussed before carbon segregation of nickel is much higher while diffusion rate of Ni, Co, Fe are $1.1 \times 10^{-7}, 8 \times 10^{-7} and 1.6 \times 10^{-7} cm^2/s$ with order of $Ni > Fe > Co$. Another important factor for synthesis of carbon nanotubes is the dispersion of carbon nanotubes. Large particles which are in aggregate form are inactive for CNT growth in comparison to the fines and fully dispersed catalyst particles [27].

The temperature also has profound influence on the catalyst synthesis by chemical vapor deposition method. CNT synthesis at lower temperature than the optimum results in lower yield of CNT. It has also been reported in literature that temperature also effect the alignment and diameter of the synthesized carbon nanotubes.

Chapter 3

Material & Method

3.1 Catalyst Preparation

Different techniques are used for the preparation of catalyst depending upon support material, catalyst and their interaction. Incipient wetness impregnation is very commonly employed technique for catalyst preparation when the support material has high surface area. The incipient wetness has possibility of very efficient application of catalyst on the support material with minimum wastage of catalyst. With the incipient wetness technique the metal oxides groups on the surface of the support are generated through calcination at high temperature and the metal oxides are reduced to metal catalyst form with reduction through flow of Hydrogen. However, Incipient wetness technique has limited application because it is used for support material which has very high surface area. Our proppants material has extremely low surface area even lower than $1m^2/g$. So, it is not wise to use Incipient wetness technique for extremely low surface are proppants. Therefore, deposition-precipitation approach was preferred for the preparation of Nickel and Iron catalyst on the proppants material as support. In the deposition-precipitation method catalyst is forced to deposit on the very low surface area support. In the precipitation deposition method, the catalyst precursor e.g $Ni(NO_3)_2.6H_2O$ decomposed into metal oxides during the process and deposition of catalsyt on the support takes place in the form of metal oxides. Therefore, the deposition precipitation technique do not require calcination step after the preparation of the catalyst.

Deposition-precipitation was carried out in batch reactor equipped with magnetic stirrer and oil bath for heating . 5 g of sand proppants were added with 225 ml of water in the batch reactor. A separate solution of catalyst precursor Nickel nitrate hexahydrate $Ni(NO_3)_2.6H_2O$ was prepared with urea. The solution was continuously stirred and 3 to 4 drops of HNO_3 were added in the solution to maintain acidic PH. The solution

containing $Ni(NO_3)_2.6H_2O$ was then mixed with support material sand in the batch reactor. The whole mixture in the reactor was stirred for 20 minutes. The batch reactor was then installed in the oil bath and magnetic stirrer was placed inside the reactor. Temperature was maintained at 100 C and stirring was started for homogeneous deposition of Nickel on the sand support. A condenser was installed at top of the batch reactor to cool and return back the water vapors coming from the mixture.

Magnetic stirring was continued for about 7 hour at 100 C. After 7 hours, stirring was stopped and stirrer was removed from the batch reactor and temperature was lowered to 94 C. The batch reactor was kept placed in the oil bath for 11 hour at temperature of 94 C. After 11 hour of heating, temperature was dropped to room temperature and kept for 1 hour at room temperature. The mixture from the batch reactor was filtered and washed thoroughly with fresh water. The weight of the precipitate was measured again and the weight of nickel deposited on the sand was calculated for exact measurement of catalyst loading. The supported catalyst was then dried and stored for the further experiments [16].

Precaution

- In order to measure extremely low loading on proppant surface, very high accuracy in weight measurement of proppant support before and after catalyst preparation is required.
- Proper washing with water is required in order to eliminate any catalyst particle which is not attached the proppants surface. The detached catalyst particles result in higher proportion of detached carbon nanotubes.

3.2 CNT Synthesis

Carbon nanotubes were synthesised using chemical vapor deposition (CVD) method in a quartz reactor schematic diagram of which is shown in the figure 3.1. In chemical vapor deposition carbon source gas e.g CO is decomposed in the presence of some inert gas Argon or Nitrogen, which deposit on the surface of catalyst resulting in tubal structure of carbon. The CNTs synthesis set up consist of a quartz reactor, high temperature furnace, gas containing cylinders along with flow meter and temperature controller. The quartz reactor is equipped with thermocouple to control temperature, with inlet and outlet of gasses and a support to hold the catalyst material. In the experiment 1 g of catalyst was placed on the support of the reactor. Carbon nanotubes were grown using nickel catalyst on sand, iron catalyst on sand and with pure sand without using any catalyst.

Inlet and outlet of the reactors were tightly connected to the gas cylinders. Flow meters were used to control the flow of H_2, CO and argon flow rate and temperature controller was used to program the temperature profile for the synthesis of CNTs. Soap leak test was first applied allowing flow of argon through the reactor followed by hydrogen leak test with the help of Hydrogen, CO detector.

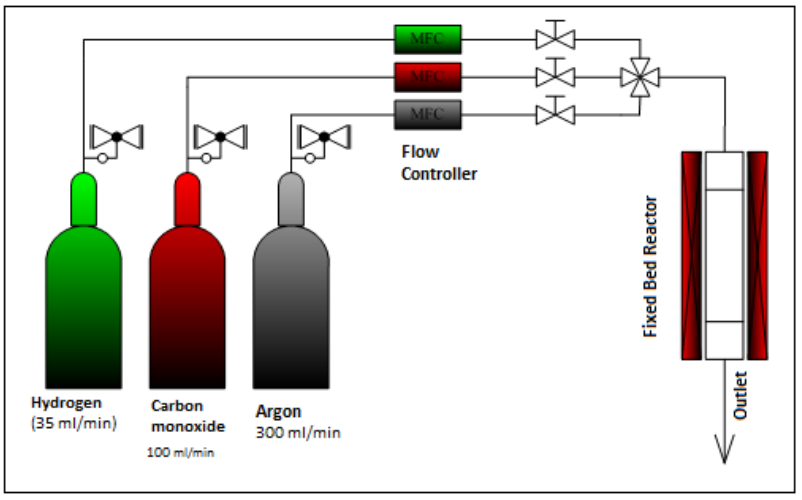

FIGURE 3.1: Chemical Vapor Deposition synthesis [32]

3.2.1 Reduction

Catalyst was first reduced in flow of hydrogen diluted with Argon at 625 C for 2 hours. The flow of hydrogen and argon was maintained with the ratio of 20 and 80 %. During reduction 40 ml/min and 160 ml/min argon was allowed to flow past through the reactor at 625 C. The temperature was raised from room temperature to 625 C at 7C/min heating rate.

3.2.2 Synthesis

After the reduction, temperature was lowered to 571 C at rate 5C/min. For the synthesis of carbon nanotubes ethane was used as carbon source combine with the hydrogen and argon. The ratio between ethane and hydrogen was maintained at 20 to 7 %. The 80 ml/min of carbon monoxide was passed with 27 ml/min of hydrogen and 160 ml/min of argon [31]. Synthesis was carried out for different intervals 2, 4, 6, 8 and 13 hours. After the specified time period, flow of carbon monoxide and hydrogen was stopped and flow of argon was slow down to cool down the reactor at room temperature. When the temperature of the reactor reached room temperature the flow of argon stopped, inlet,

outlet and thermocouples were removed from the reactor. The reactor was disassembled from the installation, the grown carbon nanotubes were removed from the reactor. The carbon nanotubes were weighed to calculate yield of the growth and then stored for further characterization and applications.

Precaution & Safety

- It should be ensured the thermocouple wire must touch the bottom of the thermocouple holding tube before reactor installation for efficient control of temperature
- Efficient insulation of the reactor should be ensured
- High degree of cleaning of outlet joint is required before employing lubricant grease to ensure not a single particle remain in between joint
- Soap & CO leakage testing must be employed to prevent any leakage for safe running of the synthesis experiment
- After completion of synthesis experiment, only flow of hydrogen H_2 and carbon source gas should be stopped. The flow of inert gas Argon must be continued until the reactor is cool down, otherwise vacuum created at high temperature in the reactor suck back the oil in the reactor from the vent cylinder.
- High level of accuracy in weight measurement is required to calculate yield of CNT

3.3 Characterization

Characterization techniques were used to study the characteristics of proppants, prepared supported catalyst and grown carbon nanotubes.

3.3.1 N_2 Physisorption

Surface area of proppants and carbon nanotubes grown is determined with N_2 physisorption technique. The reactor tubes were first cleaned with acetone and dried in oven. The weight of the tube was first measured with the help of balance. The tubes were filled with 0.5 to 1 g of proppants sample. The sample containing tubes were then fixed in degasification apparatus where they were degasified overnight at 200 C. The weight of the samples measured accurately after overnight degasification. The sample tube were fitted in N_2 physisorption apparatus and liquid N_2 is filled in N_2 jar upto a required mark. Analysis condition were chosen in Micrometric software and experiment was started to get the required data for analysis.

3.3.2 X-ray Diffraction XRD

X-Rays Diffraction performed to study the the structural analysis and to identify phased present in the sample. Xrd data is collected using $CuK_{\alpha}1$ radiation in the range of 2θ from $15 - 75^{o}$.

3.3.3 Scanning Electron Microscope

The morphology of samples is studied with the help of scanning electron microscopy and transmission electron microscopy. Hitachi S-5500 S(t)EM located in NTNU nanolab was used for the study of the nanotubes. Synthesized carbon nanotubes along with proppant support material were deposited on the carbon tape placed on the holder. The holder was fixed into sample holder and inserted into the SEM. The currents and voltage were adjusted to get clear images of samples with information including them.

3.4 Scale Inhibitor Adsorption

Phosphonates are commonly used as scale inhibitor and find applications in reservoir scale inhibition for oil and gas production. The adsorption of scale inhibitor on carbon nanotubes was analyzed by placing the carbon nanotubes coated sand proppants in a solution containing inhibitor. For the adsorption experiment 2ml of water was mixed with 1 ml of ethanol. Ethanol was used in the solution mixture to increase the wettability of the carbon nanotubes. The phosphonates have no solubility in ethanol, therefore, it could not be used alone rather used as mixture with water. 0.05 go of phosphonates inhibitors were dissolved in the solution containing water and ethanol. When the phosphonates were fully dissolved, 0.2 g of carbon nanotubes were poured into the phosphonates solution.

Different yield of carbon nanotubes were employed to test the effect of yield upon the adsorption behavior of phosphonates. The experiment was carried out for different time period. After, desired reaction time, the spent solution was poured out completely. The samples were kept overnight at room temperature for drying and then placed in oven overnight for complete removal of any moisture left. The procedure was also repeated with variation PH of solution with the addition of acid and base.

Precaution & Safety

- Very minute changes in adsorption is measured which required extra care during the whole procedure
- Very accurate weight balance should be used to count very small changes
- Should be dried for longer time period to remove any fraction of moisture present, so that it would not effect the weight calculations

3.5 Proppants Testing

Different testing standards were used for the characterization of proppant in past. The API recommended practice RP 56, RP 58 and RP 60 were commonly used standards for analysis of characteristics of sand, gravels and high strength proppants. A committee from American Petroleum Institute (API) and International Organization for Standardization introduced new standard ISO 13503-2 "Measurement of properties of proppants used in Hydraulic fracturing and gravel packing operation" and ISO 13503-5 "Procedure for measuring the long term conductivity of proppants" [24].

3.5.1 Acid Solubility

API RP 56, RP 58 ad RP 60 also defined procedure for acid solubility testing of proppants, in which the proppants treated with solution of 12:3 HCl:HF for 30 min at 150 C. RP 56 comprised acid treatment of sand for 30 minutes, RP 60 acid treatment of gravel for 30 minutes and RP 60 acid treatment of high strength material with no time restriction. ISO 13503-2 composed of previous standards for acid treatment of solution of 12:3 HCl:HF but for only fixed time of 30 min at 150 F for any type of proppants used [24].

A 3% solution of HF was prepared from 5 % HF solution and 12% solution was prepared from 25% solution. The acid solutions were mixed in Teflon beakers. A careful measured weight of 0.5 g of proppants were placed in teflon beaker containing 15 ml of prepared acid solution for 30 min at 150 F. Acid solubility of sand and ceramics proppants was also measured at 60, 90 and 120 min. After specified time, the acid solution is drained and proppants particle are carefully stored. The stored proppants particles are dried overnight at 100 C to remove any moisture present in it. Weight after acid treatment was measured with high accuracy and used for calculation of acid solubilities [24] .

$$S = [1 - m_{treated}/m_{untreated}] \times 100$$

Safety

- HF is highly corrosive acid, and extra high care is required while handling HF
- NTNU nanolab has extra care personal protective equipment, the proper use of PPE is required to avoid any contact of human body with the HF
- After the treatment of the sample with HF, the sample is required to wash thoroughly with the water to eliminate any HF with the sample.
- A buddy should be there in the surrounding area to accompany in case of any incident while working with the HF

3.5.2 Density Measurements

Density is very important characteristic of proppants due to its pronounce effect on transport behavior of proppants in the reservoirs. ISO 13503-2 defined standard procedure for measurement of density of the proppants. There are three different types of densities known as bulk density, apparent density and absolute density. Bulk density is calculated by measuring the weight of material in a specified volume. Apparent density is determined by measuring the displaced volume of low viscosity liquid with the addition of proppants of known weight [24].

Bulk density was measured by filling $2cm^3$ of a graduated cylinders with the proppants material. The weight of proppants materials was measured in $2cm^3$ volume of cylinder to calculate bulk density. Bulk density was also measured by filling $3cm^3$ volume of cylinder to check accuracy and reproducibility of results. Apparent density was calculated by measuring the $3cm^3$ of water in a graduated cylinder, then 2.00 g of proppants were added in the cylinder. The increased in water level inside the cylinder represented the volume of water displaced equivalent to volume of proppants particle. The density is calculated according to the formula

$$Density = \frac{Mass of Proppants}{Volume of water}$$

3.5.3 Sphericity & Roundness

Sphericity & roundness is another important property of proppants. The sphericity of proppants was determined with Camsizer XT particle analyzer from Statoil. In the Camsizer XT particle analyzer, thousands of images of the particles are analyzed before final statistical value. Two measurements of each sample were taken to get more reliable

statistical data. With the help of Camsizer XT particle analyzer mean value sphericity SPHT, symmetry Symm and mean value of width to length ratio b/l was calculated.

3.5.4 Mechanical Testing

Mechanical strength is most important property of proppants which was measured with the help Instron mechanical testing machine. The machine consist of an upward and an downward plate. Upward plate is equipped with a load frame which apply stress to the sample material placed on the downward plate. The accurate diameter of each sample was first estimated with the help of SEM. Particles of known diameter were stressed with upward load frame till the breakage of the particles. The load against deformation data was plotted with the help of software. Stress and strain data was calculated from the load deformation curves.

Chapter 4

Results & Discussion

4.1 Proppants Testing

Standard methods are commonly used for testing of proppants which provide guideline for accurate and reproducible standard measurements for proppants testing. The data for the report was calculated from the guidelines defined by ISO 13503-2 "Measurement of properties of proppants used in hydraulic fracturing and gravel packing operations" [24]. The testing of important properties of proppants are discussed following.

4.1.1 Surface Area of Proppants

The proppants are generally available as very strong compact particles with extremely low porosity particles. Due to nonporous structure of proppants particles, the surface area of proppants particles are considered to be extremely low. A comparison of surface characteristics of proppants particle is given in the table 4.1. The proppants particles follow a trend of extremely low surface area material with the exception of alumina proppants. The data in the table is based on measurement of surface area of grounded proppants particles and still it is below $1m^2/g$ for most of the proppants. The surface area of ungrounded bigger particle was so low that it was not measurable with the conventional N_2 Physiosorption measurements. The pore volume of the proppants material also measured to be extremely low with the exception of pore volume of alumina proppants.

The very low surface area of proppants is due to very compact structure of proppants particles to give very high mechanical strength. However, the surface area of the alumina proppants is very high with more than 200 time more than the surface area of other proppants and it is not comparable with the surface area of other proppants in any

Table 4.1: Surface measurement of proppants

Proppants	**Surface area** (m^2/g)	**Pore volume** (cm^3/g)	**Pore Size** ($\AA$)
Sand	0.5580	0.001164	83.4360
Ceramics	0.3732	0.000936	87.1856
Alumina	200.8940	0.216459	98.4212
Carbolite	0.963	0.002231	89.2170
Limgrus	0.0017	-	-

respect. SEM analysis of alumina proppants revealed it as specially designed porous structure with some bigger pores. So, the highly porous structure resulted in very high surface area and other surface characteristics different than the other proppants.

4.1.2 Mechanical Strength

The proppants have to face extreme conditions deep in the reservoir and extreme level of stresses. The mechanical strength is the property of proppants which provides resistance against closing rocks and keep open the propped fracture. So, the proppants particle are designed as very high strength material. A comparison of the mechanical behavior of proppants when load is applied is given in the figure 4.1. The ceramics proppants depicted an excellent performance and show resistance to five time more load than the sand particles. Ceramics proppants also showed much more deformation than the other proppants showing more ductility and tendency for more compression before breakage. Carbolite proppants showed strength lesser than ceramics but better strength against the applied load compare to other proppants. However, the carbolite proppants showed higher slope of the curve which represent lesser deformation against the applied load. The better mechanical properties of ceramics and carbolite proppants is result of very high strength structure of alumino silicate in the ceramics proppants material.

The worst behavior against the applied load was observed in the case of sand proppants which were only capable to withstand against applied load of 45 N. The sand proppants behave like a brittle material and break after very low deformation compare to other proppants. The brittle behavior of sand proppants is attributed to higher silica contents in sand proppants. The poor performance of sand proppants invites initiative to improve the strength of sand particle with the application of very high strength material such as carbon nanotubes. Alumina proppants has much larger size almost more than double the size of other proppants. According to their size, alumina proppants should show higher mechanical strength. However, alumina proppants were only capable to withstand a load of 45 N which is very low compare to ceramics and carbolite proppants. The porous structure of alumina proppants resulted in decrease in mechanical performance of alumina proppants. However, alumina proppants depicted very high deformation which

can also be due to porous structure of alumina proppants, which provide the alumina proppants space to squeeze. So, the proppants such as ceramics and carbolite represented good mechanical strength along with some poor performance of sand proppants which need to be improved.

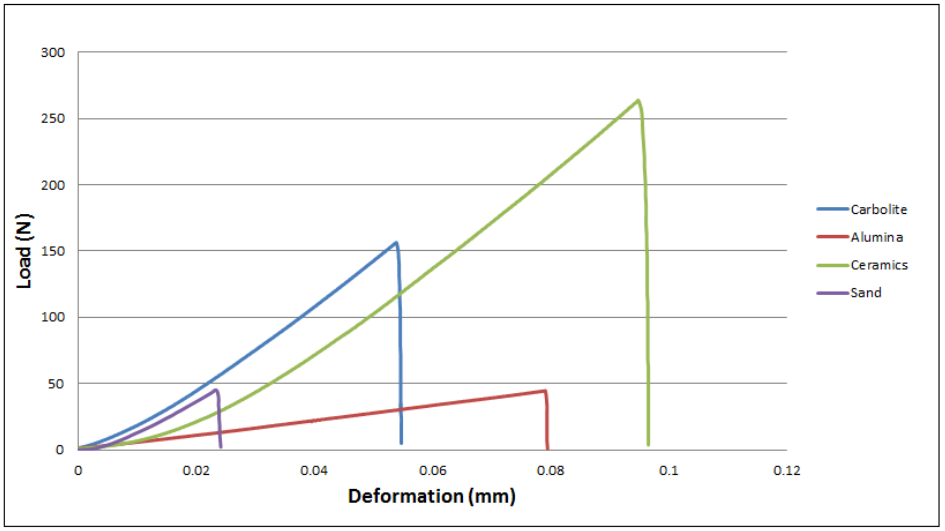

FIGURE 4.1: Load deformation curves of proppants

4.1.3 Acid Solubility

Acid solubility is an important property to evaluate the chemical effect on the surface of the proppants used in the fracking operation.Proppants have to encounter with corrosive acids for example with HF and HCl during the scale removal opertion. Acid solubility testing provide important information about strength and resistance of proppants material against the corrosive acid and other corrosive agents. The acid solubility analysis of proppants is given in the figure 4.2. The ceramics proppants gave very low acid solubility even less tha 0.1 % which represent very high resistance of ceramics proppants against the acid treatment. The very low solubility of ceramics qualify ceramics proppants to be used in very harsh and corrosive conditions. The very good performance of ceramics proppants against corrosive acids like HF & HCl is the result of polymer resin coating around the ceramics proppants. The polymer coating around ceramics proppants avoid contact of alumino silicates with acid solution and provide itself resistance to corrosive behavior of acid solution.

The effect of acid treatment was also investigated for longer time than the standard 30 min to allow corrosive acid to destroy the polymer coating and further study the acid resistance of aluminosilicates. The figure 4.3 shows a small increase in acid solubility for ceramics after 60 min, 90 min, 120 min. The increase in acid solubility can be result of

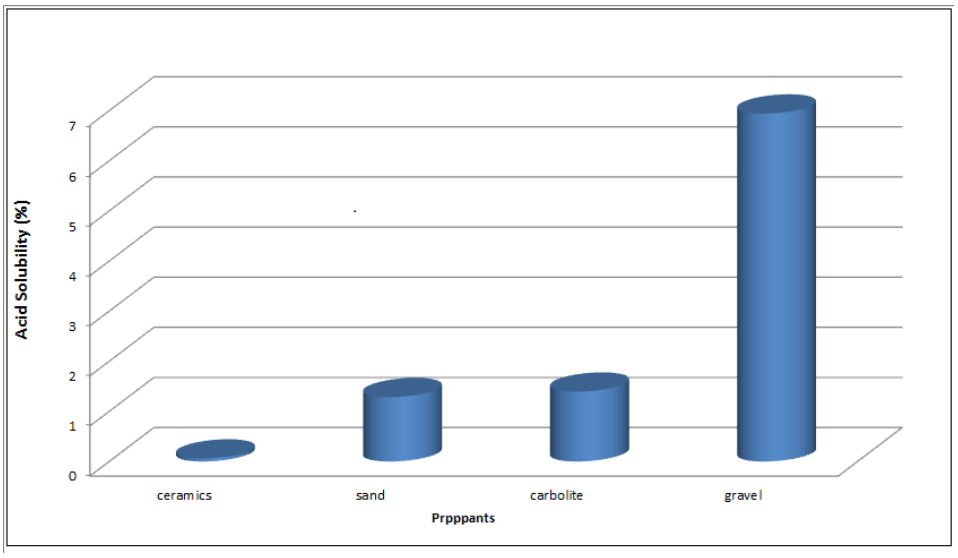

FIGURE 4.2: Acid solubility of proppants

destruction of polymer coating and contact of acid solution with aluminosilicates in the ceramics proppants. Although ceramics proppants showed some acid solubility at longer time than the standard 30 min, however, its effect was still not very pronounced with acid solubility value even less than 0.5 %. Silica contents with ceramics proppants are susceptible to corrosive behavior of acids. The presence of silica in the ceramics form a silica-rich glassy phase which is an easy target for acid attacks [56]. Therefore with the breakage of polymer coating for longer time, ceramics proppants although very less but show some acid solubility.

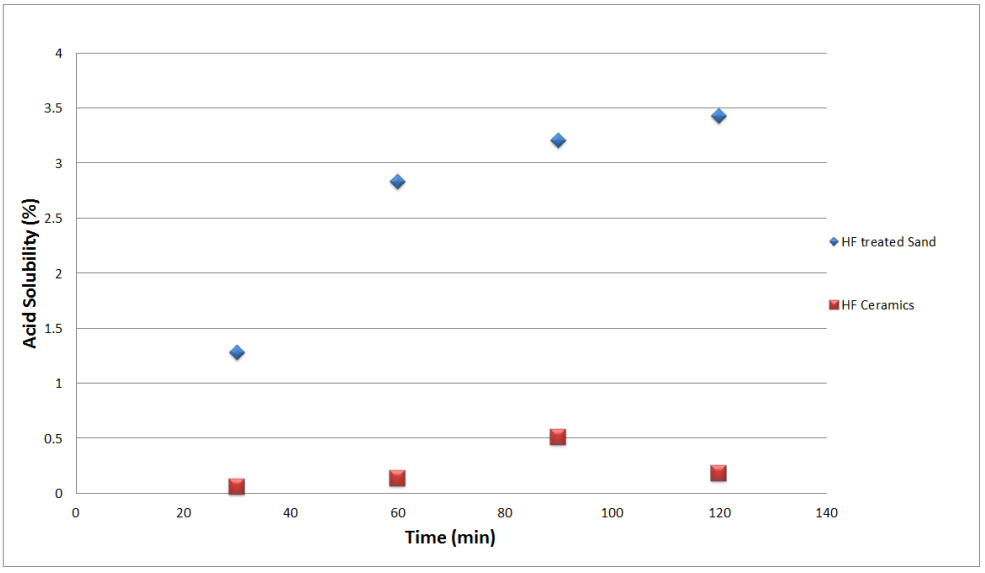

FIGURE 4.3: Acid solubility variation with time

The sand particles showed much higher acid solubility than the ceramics indicating poor performance and resistance against corrosive acids. The much increase in acid solubility was also observed with the increase in acid treatment time. The increase in acid solubility compared to ceramics is due to unavailability of polymer coating surrounding the sand particles and presence of silica as major component in sand particle which is easily attacked by acid. So, the application of sand particles are limited in the reservoirs where excessive acid treatment is required or acid resistance of sand can be improved with coating of sand particles with polymer resins. Very high percentage of acid solubility was observed in the case of gravel particles. The acid solubility of alumina proppants was so high that more than one third of the proppants was dissolved in acid. The very high solubility of alumina proppants is due to very high porous nature of alumina proppants.

4.1.3.1 SEM Analysis

Corrosive nature of acid has main focus on the surface of the proppants and it will be worth to visualize surface characteristics after the acid treatment. SEM is an effective tool for qualitative analysis of surface structures. The SEM analysis of sand proppants surface is shown in the figure 4.4 . The figure depicted effect of acid treatment following a leaching mechanism. The whole sand surface was not smoothly removed rather acid was in search of specific component on the sand surface. Acid left some portion of the sand surface and went deep to dissolve more soluble component which made the sand surface as more rough surface. It can be assumed that silica is more soluble in acid and acid tried to leach silica from the surface.

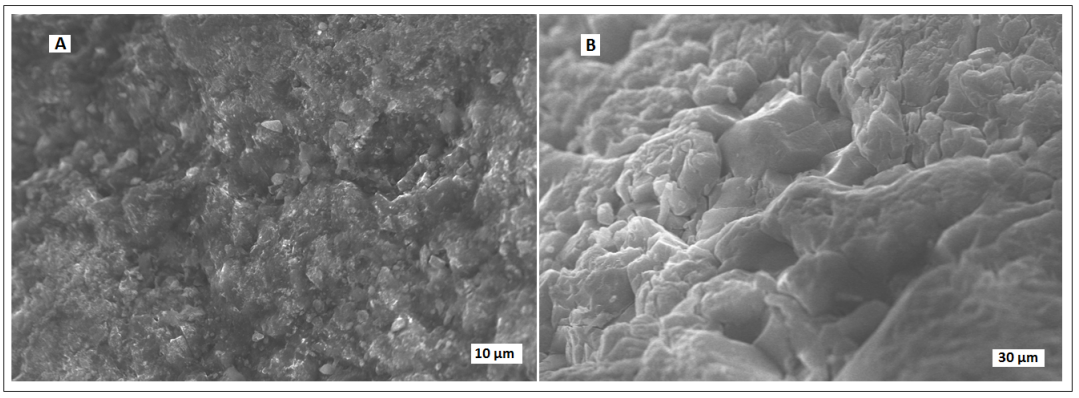

FIGURE 4.4: SEM analysis of acid treated surfaces

4.1.3.2 Xrd Analysis

X-ray diffraction technique was employed for evaluation of structural changes within the sand particles after acid treatments. The SiO_2 peak analysis of Xrd pattern is illustrated in the figure 4.5. The xrd pattern of pure sand and acid treated sand particle is quite similar with very minute changes. The peak intensities are also similar, however, right side downward moving part of the acid treated peak become more smooth. The acid used for treatment were 3% HF and 12% HCl with treatments lasted for only one hour for the analyzed sample. So, it can be concluded that the effect of acid treatment was only limited to the surface of the proppants and it did not really cause damage to the internal proppants structure.

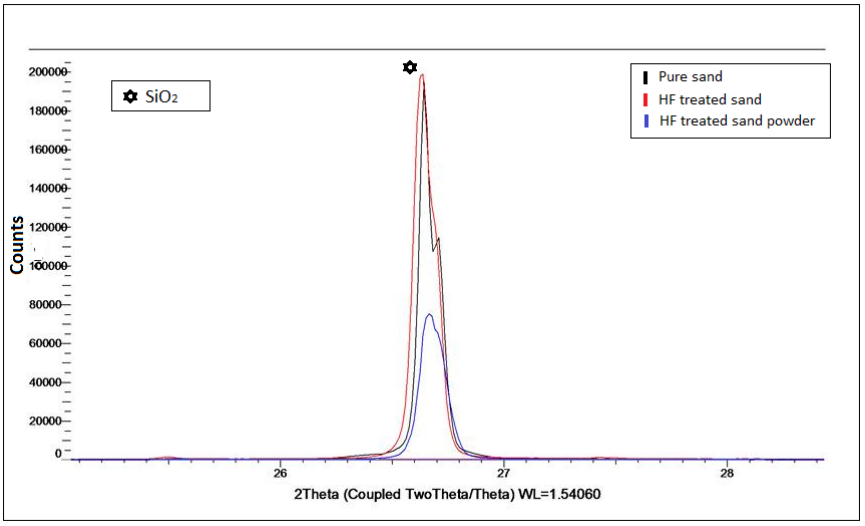

FIGURE 4.5: Xrd analysis of acid treated surfaces

The x-ray diffraction analysis was also carried out to check the effect of acid treatment on the grounded sand. For the analysis the sand particles are broken and after acid treatment analyzed with Xrd. There are bigh changes in xrd pattern of grounded sand compare to pure sand as visible in the figure 4.5. The intensity of the peak reduced from the 200000 counts to just around 65000 counts. The change in pattern could be due to structural changes of sand material after the treatment of acid. The SiO_2 is more soluble in acids and usually leached during the acid treatment. The decrease in intensity of SiO_2 could be result of reduction in SiO_2 content from the sand material. So from Xrd results, it can be concluded that there is no sever threat to structure of sand particle for acid treatment at low concentration. However, when higher surface area of sand with broken particle is exposed to acid or sand is treated under sever conditions then the structural changes become area of concern.

4.1.4 Proppants Density Measurement

The density of proppants is among the most important properties of proppants. The density of the proppants should be very low and it is quoted that the ideal proppants should be lighter than air. The density of the proppants has direct effect on the transport properties of proppants towards target point in the reservoir. A comparison of density of proppants is given in the table 4.2 with the results based upon three measurements for each type of proppants. Apparent density and bulk density, two different types of densities were calculated. The bulk density was calculated taking into account the volume of particles plus volume of inter particle spaces. The apparent density or particle density is calculated taking into account only the volume of particle sphere and is measured from displaced volume of water with the addition of proppants particles.

TABLE 4.2: Proppants density measurement data

Particles	**Apparent density** (g/cm^3)	**Bulk density** (g/cm^3)	**Fractional Voidage**
Sand	2.5358	1.64	0.35328
Alumina	2.06233	0.5754	0.721
Ceramics	2.5195	1.5754	0.37353
Gravel	1.68806	1.1085	0.3434
Carbolite	2.5393	1.649	0.35063
Limgrus	1.9896	1.605	0.19331

The density of sand particles was calculated to be $2.53 g/cm^3$ which is close to literature value of density of sand which is $2.65 g/cm^3$ [2]. The density of ceramics and carbolite is comparable with the density of sand particles. The high strength paroppants have general drawback of higher density. Our results conclude that the ceramics and carbolite proppants proved to be higher strength material than sand, however, their density is not much higher than the sand particles. So, the better performance of ceramics proppants in term of higher strength and comparable density assume that their properties are specifically controlled while designing and manufacturing of ceramics proppants.

The Voidage or intra particle porosity was another important property calculated from the density data. Voidage or intra particle porosity is the inter particle spaces left without filling when the particles pack in the form of bed. The calculated fractional voidage for the proppants is between 0.35 to 0.37 as given in the table which is close to literature value of 0.393 for a packed of 0.794 mm particles. The voidage between the proppants particles actually provide permeability for flow of oil and gas through the proppants packed bed within the fractured rocks. The voidage has direct relation with permeability through the spherical particles and with the particle size. The particles having higher voidage give us higher permeability coefficient [43]. So, the ceramics

proppants having higher voidage should allow more flow of oil and gas than the sand proppants having lower voidage.

4.2 CNT Proppants Synthesis & Characterization

The study on proppants testing as discussed earlier revealed the ceramics proppants are especially material with properties much better than the sand proppants, even not comparable with the sand. The poor performance of sand as proppants prompts initiative to improve the performance of sand particles. So, the application of carbon nanotubes with its exceptional properties opens the research area to improve the performance of proppants material used in hydraulic fracturing.

Synthesis of carbon nanotubes on proppants sand particles carried out with the help of chemical vapor deposition method. Carbon monoxide was preferred as carbon source for better quality nanotubes on the surface sand particles. Carbon monoxide was also preferred to generate some oxygen group on the surface of carbon nanotubes during the synthesis process.

4.2.1 % Yield

The measurement of % yield is an effective tool to estimate the quantity of carbon nanotubes grown over the surface of the sand particles. The yield of carbon nanotubes grown over the surface of the sand can be calculated with the following formula

$$\% \text{ Yield} = (1 - M_i \ / \ M_f) * 100$$

M_i = Initial mass of catalyst before synthesis

M_f = Final mass after synthesis

The synthesis of carbon nanotubes was carried out with different time interval using nickel as catalyst supported on sand along with pure sand particles without catalyst. A comparison of variation of the carbon nanotubes yield with time is illustrated in the figure 4.6. The nickel catalyst loading over the pure sand particles was very low, however, it showed good yield of carbon nanotubes around the Ni supported sand surface.There was also an increase in % yield with growth time when nickel supported on sand was used as catalyst. The increase in yield of carbon nanotubes with time also give control to get desired yield of CNT on sand. However, the higher yield also resulted in some unbound carbon nano fiber which are not attached to the particles. The unbound carbon

nanotubes were present in the powder form along with the proppants and was considered to be main limitation moving towards high yield CNTs proppants. The phenomena of unattached carbon nanotubes is highly undesirable. It is possible toh achieve desired high yield of carbon nanotubes allowing more reaction time. However, the unbound carbon nanotubes put constraints to keep the yield of CNTs around the sand proppants within limits.

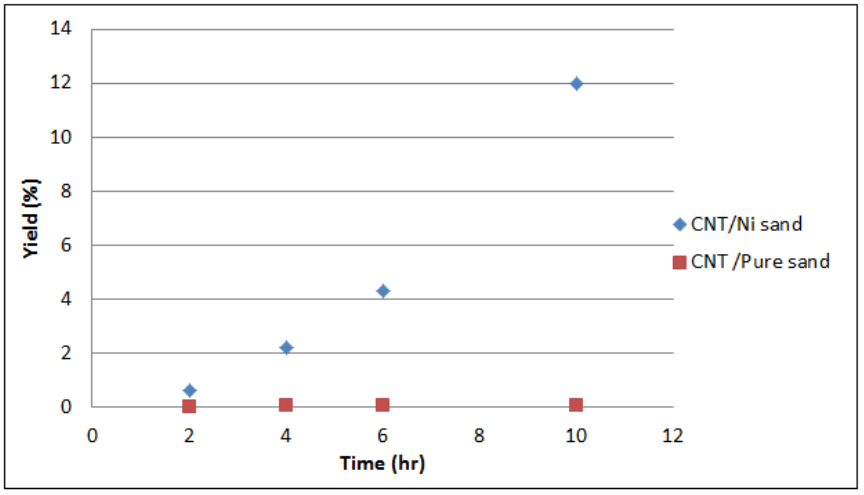

FIGURE 4.6: Variation of % CNT yield with time for pure sand and Ni supported on sand

Pure sand particles also contain traces of iron on the surface of particle. The naturally presence of iron can be used as source of catalyst for carbon nanotubes synthesis over the surface of pure sand. So, pure sand was also employed for the synthesis of carbon nanotubes. There was very small yield of carbon nanotubes observed on the surface of pure sand and SEM results also confirmed the presence of CNT on pure sand. However, there was no significant observable increase in yield of carbon nanotubes with the time obtained in the case carbon nanotubes grown over the surface of pure sand. In case of pure sand used for the synthesis, the iron which is already present in the sand is utilized during the synthesis process. However, only traces of iron are present in the sand surface, which can give only limited growth of carbon nanotubes and yield cannot be boosted up than a limit even not more than 1 % with increase in growth time. This is the limitation of using pure sand that we cannot get our required yield, if higher yield is needed. In order to get higher yield of carbon nanotubes of own desire, the use of catalyst sand is considered to be the prefer option.

4.2.2 SEM Characterization

Scanning electron microscopy technique was employed for qualitative study of surface characteristics of carbon nanotubes grown over the surface of the sand. A comparison of the surface of sand particles with different growth time is represented in the figure 4.7. With the increase in yield and growth time, the increase in particle size was observed with SEM. With the higher growth time, the increase in the layers of carbon nanotubes over the surface of the sand was also observed which resulted in increased roughness of the particle surface.

The figure 4.7 illustrate, there are large number of layers of carbon nanotubes with the 10 hour growth time. Only first few layers are strongly attached with the sand particles. With the increase in time & yield, the additional layers try to attach through entanglement with the first few layers of carbon nanotubes directly attached to the sand particles. Subsequent carbon nanotubes further try to attach with already attached carbon nanotubes. The upper most layers of carbon nanotubes give soft loosely packed structure which can easily be removed from the surface. Therefore, very high yield of carbon nanotubes give detached or unbound carbon nanotubes which are present in powder form. The phenomena of unbound powder form carbon nanotubes is highly undesirable according to proppants point of view.

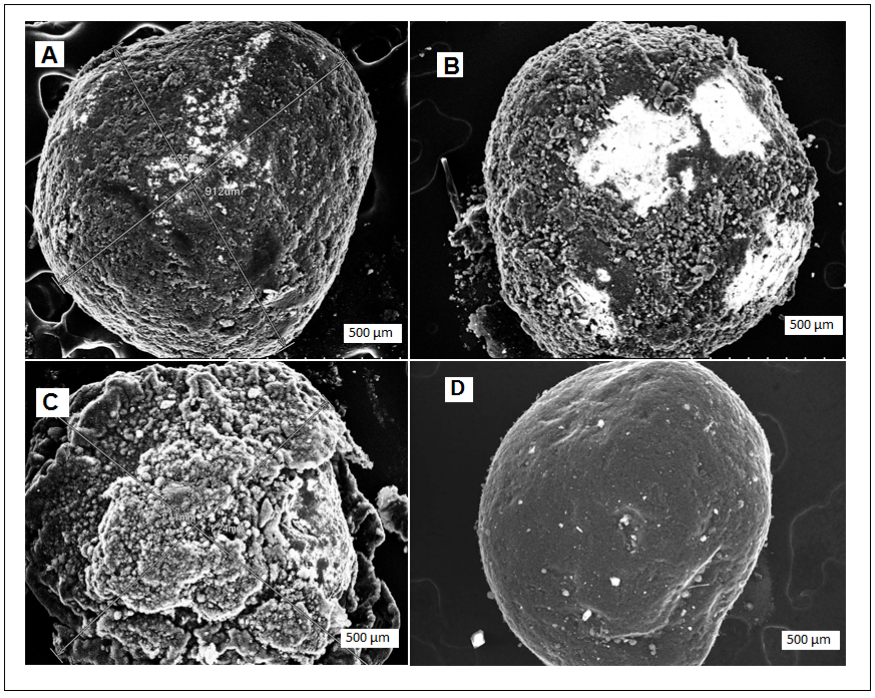

FIGURE 4.7: Low resolution SEM of CNT sand surface A) 2hr growth time with 0.6 % yield B) 4hr growth time with 2.2 % yield C) 10 hr growth time with 12% yield D) CNT on pure sand for 12 hr with 0.1 % yield

With the lower yield for 2hr growth time, the carbon nanotubes are bonded with the sand particle in more compact form. There are very less loosely attached CNTs at the upper most surface of the particle. Therefore, the 2hr growth time surface has very small quantity of unbound carbon nanotubes compared with CNT surface for 4hr growth time. The growth of carbon nanotubes around the pure sand without catalyst resulted in thin layer of carbon nanotubes around the particle. The most of the individual carbon nanotubes are directly attached with the sand particle. Therefore, there is no point of creation of detachment of carbon nanotubes layers from the surface and production of unbound carbon nanotubes. So,the generation of unbound carbon nanotubes is an important criteria for the optimization of require yield for the desired applications. If other properties are not concerned, the yield of carbon nanotubes around 1 to 2 % should be sufficient to minimize the powder form detached carbon nanotubes phenomena.

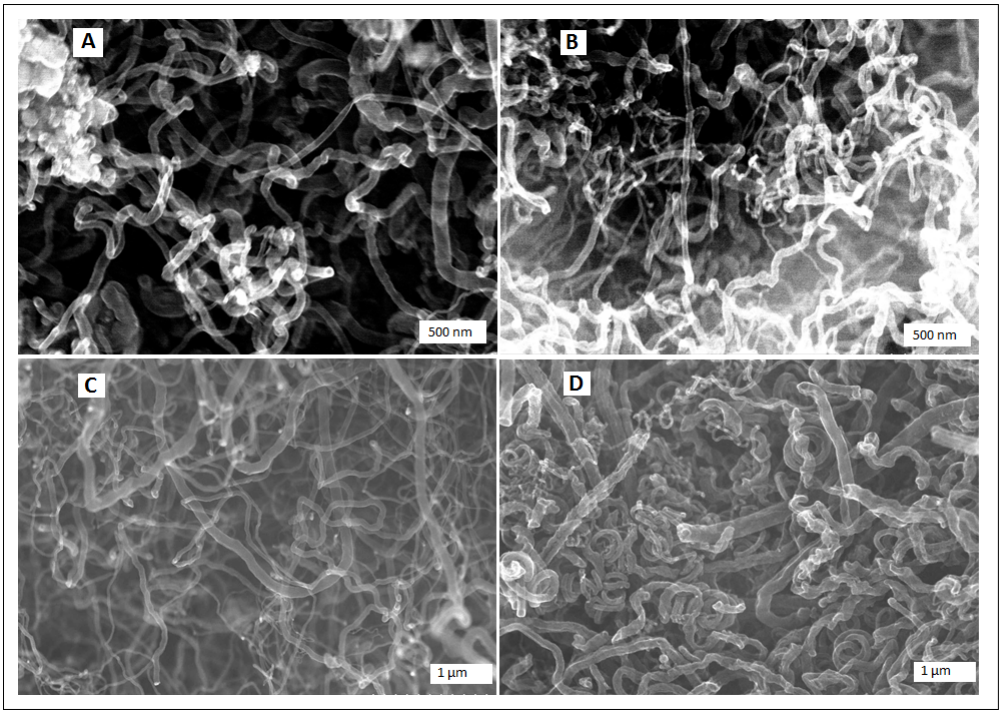

FIGURE 4.8: High resolution SEM of CNT sand surface A) 2hr growth time with 0.6 % yield B) 4hr growth time with 2.2 % yield C) 10 hr growth time with 12% yield D) CNT pure sand for 12 hr

The high resolution SEM images of carbon nanotubes growth over sand for different yield is illustrated in figure 4.8. The carbon nanotubes around Ni deposited sand at low yield for 2 hr synthesis time appear more separated with less densely packed giving less degree of entanglement. With the increase in time & yield, the tubes are more closely packed with more bending structure and increased entanglement of carbon nanotubes with each other. The carbon nanotubes around the pure sand particles without the

deposited Ni, depicted very densely packed larger diameter carbon nanofibers with more twist structure. It looks the carbon banotubes formed in search of very small fraction of naturally catalyst on the surface of sand. Once carbon found the iron, then the carbon atoms were in competition to grow carbon nanotubes around the iron catalyst resulting in bending and closely packed structure. The carbon nanotubes around the pure sand particle were synthesized with very reduced catalyst activity. At very low catalyst activity the segregation of the carbon is extremely low which can result in opening of the wall of tubes which gives crooked or twisted carbon nanotubes [27]. Therefore, the synthesis of carbon nanotubes around the pure sand particles resulted in very twisted and larger diameter carbon nanotubes. After initial growth of carbon nanotubes , the catalyst activity is also reduced as in the case of 12 % yield CNTs, the tubes opening starts which result in larger diameter carbon nanotubes as shown in figure 4.8 (C).

4.2.3 CNTs Surface Area Measurement

Proppants are of very low surface area materials, therefore, it is important to analyze the surface area variation with the growth of carbon nanotubes on the surface of the sand. N_2 physiosorption technique is commonly employed for the surface area measurement. The surface area variations with the yield of carbon nanotube on the surface of the sand is illustrated in figure 4.9. The figure 4.9 show an increase in the surface area of cnt grown sand particle with the increase in yield. There is an smooth increase in surface area until for yield around 6% . However, there was very high surface area reported at around 10 % yield which is more than 4 times the surface area reported for 6% yield.

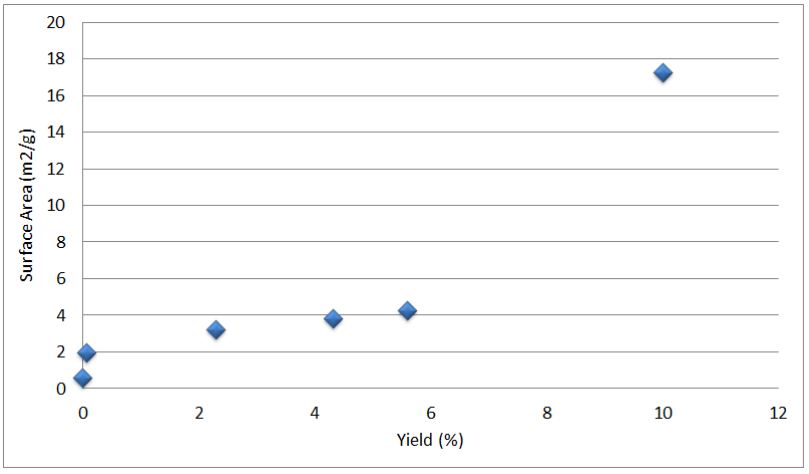

FIGURE 4.9: CNTs surface area variation with % yield

The higher surface area is only due to the layers of carbon nanotubes surrounding the sand particles but has no effect from the inner enclosed sand particle. The increase in

yield can be result of soft structure of carbon nanotubes layers around the sand particles. As reported in the SEM charecterization that the carbon nanotubes are loosely packed on each other with distance between individual nanotubes. Therefore, they packed in such a way to give enhanced surface area. The very large value of surface area for high yield of 10%, was result of detached, unbound CNTs, which gave their own value rather than the whole particle. The pure sand particles has extremely low surface area of even below than $1m^2/g$ because of very compact crystalline structure of SiO_2. The normal proppants trend is to have very low surface area. The large increase in surface area of cnt grown sand particles compare to pure sand particle adds no significant advantages to proppants preformance. However, the increase in surface area can be exploit for transport and effectively utilization of chemical deep in the reservoir. The pore volume of carbon nanotubes is also represented in the figure 4.10 with the variation of yield. There was also an increase in pore volume observed with the carbon nanotube growth over the sand particle compare to pure sand. The increase in pore volume can be interesting for movement of solvent within the carbon nanotubes layer.

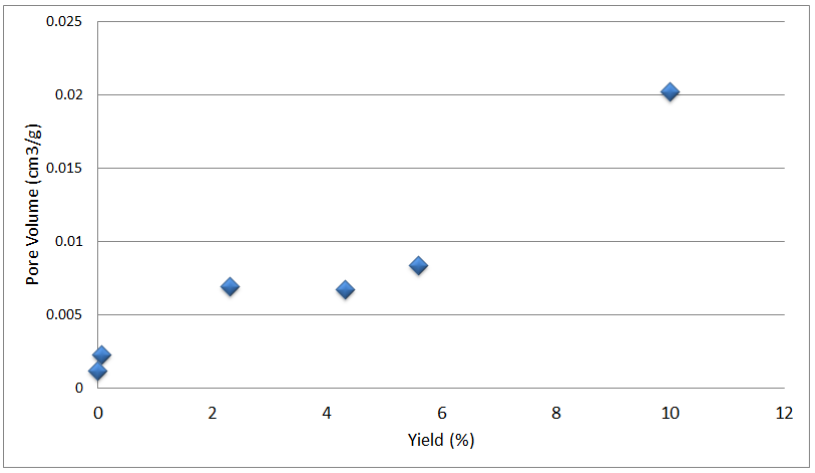

FIGURE 4.10: CNTs pore volume variation with yield

4.2.4 CNT Density Analysis

The density of the proppants is the most important property when transport of proppants deep in the reservoir is under consideration. The proppants have to be suspended within the fracturing fluid, therefore, it is very important the density of the proppant should be very low. The density variation with the growth of carbon nanotubes was also investigated and results are represented in the figure 4.11. The figure depicted the decrease in density with the growth of carbon nanotubes and even decrease in density with the increase in yield of carbon nanotubes around the surface of the sand particle. The figure show an decrease of 21 % for 7% yield CNTs and 25 % for 10% yield CNTs in

particle density compared to pure sand particles. Similarly, bulk density was decreased 33% for 7% yield CNTs and 36% for 10% yield CNTs as compared to sand particles.

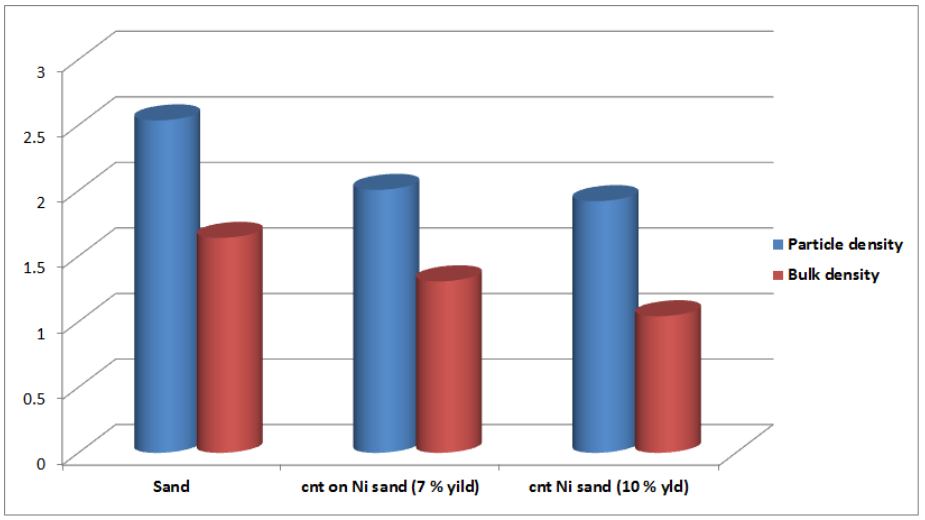

FIGURE 4.11: Density variation with CNT growth

The high resolution SEM characterization of the carbon nanotubes revealed that the carbon nanotubes placed on each other with the distance among them, resulted in loosely packed structure. The presence of soft layers of carbon nanotubes around the sand particle resulted in expanded volume which give decrease in density. So, with the growth and variation of yield of carbon nanotubes around the surface of sand particle, it is possible to improve the performance of sand particles by decreasing desity of proppants. However, there are again constraints to achieve yield in a limited range due to the generation of unbound or detached carbon nanotubes. So, it is possible to increase performance of proppants sand particle but up to limited extent.

4.2.5 Sphericity & Roundness

Proppants are commonly used as spherical particles and there is more focus to prepare proppants particle as perfect spheres. Spherical particles are very effective to reduce erosion behavior and abrasiveness of proppants during transport of proppants and production of oil & gas. The variation of sphericity of proppants with the growth of carbon nanotubes on sand was analyzed with Chemsizer and results are given in the Table 4.3. The chemsizer require large quantity of material for analysis and due to limitation of quantity of carbon nanotubes synthesis, only two samples with 0.1 % yield of CNT on pure sand and 7 % yield of carbon nanotubes on Ni sand were analyzed.

The results are quite surprising which depicted a decrease in symmetry and sphericity with the synthesis and with the increase in yield of carbon nanotubes. With the SEM analysis of only few particles of CNT grown sand, it was thought that carbon nanotubes surround sand particles with layers making it more circular and considered CNT little but improved spehericity of the sand particles. However, the results from the chemiszer are opposite and much more reliable to follow because chemsizer consider thousand of particles for analysis. It can be considered that the carbon nanotubes growth followed the distribution of catalyst particles around the surface of the sand during synthesis processs. The natural distribution of iron on the surface of the pure sand can be uneven. There can also be possibility of uneven deposition of catalyst particles while deposition precipitation method because during the preparation method sand try to settle down in the form of bed. One side of single sand particle within the bed likely to get more catalyst deposition than the other side of particle. So, the part of single sand particle with more proportion of catalyst get more growth which can be resulted in non-homogeneous growth of carbon nanotubes giving less spherical particles. The random removal of soft layer of CNTs on the surface of sand at high yield could also be cause of decrease in spehricity. Along with powder CNTs formation, the decrease in sphericity with the increase in yield also restricts synthesis of CNTs on sand particles with limited yield.

Table 4.3: Spehricity and roundness variation with CNTs coating on sand

Particle	**Symmetry**	**Sphericity**	**b/l**
Sand	0.926	0.936	0.775
CNT pure sand (0.1 % yield)	0.926	0.935	0.774
CNT Ni sand (7% yield)	0.921	0.907	0.773

The chemisizer analysis also gave very important information about the particle size and increase in particle size with the carbon nanotubes growth. The analysis of 83853 particles with 8564 images of pure sand particles gave us statistical particle size of 606.83 micrometer for pure sand particle, similarly the analysis of thousands of particles of 0.1 % and 7 % yield of carbon nanotubes gave statistical particle size of 638 and 736 micrometer respectively. The particle size of pure sand particle and increase in particle size with carbon nanotubes growth on sand particle provide an opportunity to calculate thickness of the carbon nanotubes layer surrounding the sand particle as given in table 4.4. The thickness of carbon nanotubes layer increase from 32 micrometer for the CNTs on pure sand with 0.1 % yield to 4 times with thickness of 132 micrometer for CNTs on Ni sand with yield of 7 %. So, the chemisizer is an important technique for tuning of thickness of carbon nanotubes layer around the surface of the sand particles with variation in yield and with the time.

TABLE 4.4: Spehricity and roundness variation with CNTs coating on sand

Particle	**Particle size (micrometer)**	**CNT Thichhkness (micrometer)**
Pure Sand	606.83	0
CNT pure sand (0.1 % yield)	638	32
CNT Ni sand (7% yield)	736	130

4.2.6 X-rays Diffraction Analysis

X-ray diffraction technique is common to use for determination of number phases present in sample material. The x- ray diffraction results of sand and sand with carbon nanotubes grown over it are shown in figure 4.12. Sand showed a large peak of SiO_2 at 2Θ of 26.6 which depicts that sand is composed of SiO_2 as major part. The large peak of SiO_2 with high intensity of 200000 counts represents higher crystallinity of sand particles. The results for CNT over sand also gave SiO_2 peak as major part which also depicted SiO_2 is major part of CNTs sand. However, the height of the peaks decreased in the case of carbon nanotubes over the sand particles which gives idea of decrease in either composition of SiO_2 or structural changes of sand particle with the carbon nanotubes grown over sand. The decrease in intensity of the peak is attributed to high temperature treatment of sand during the carbon nanotubes synthesis process.

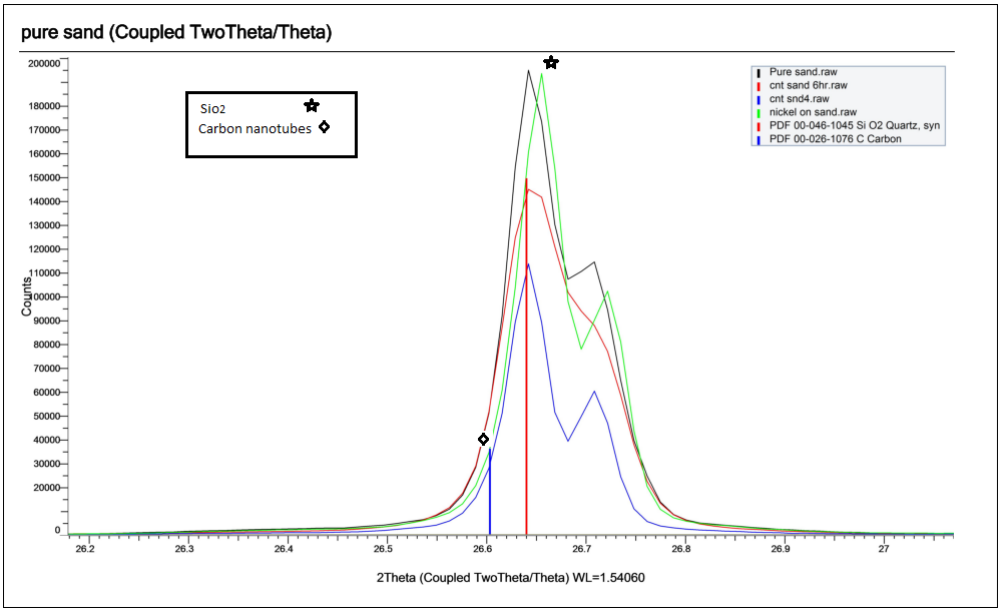

FIGURE 4.12: Xrd for sand with CNTs on sand

The effect of heat treatment on the structure of sand and intensity of Xrd peaks was further studied. The figure 4.13 represent the Xrd analysis of heat treated sand. The heat treatment was carried out at 600 C for 8 hr and 13 hr. It is evident in the figure, the decrease in intensity of peak with the heat treatment which represent structural changes in the sand particle with the heat treatment. The atoms within the solid particle undergo vibration from their mean position with the increase in temperature. The amplitude of the vibration become larger at high temperature which result in agitation. The agitation smear the lattice plane resulting in ill defined thickness of plane which causes decrease in intensity of Xrd peaks [11]. So, for application of carbon nanotubes for development proppant, it is important that CNTs synthesis conditions has minimum impact on the structural or other main properties of proppants.

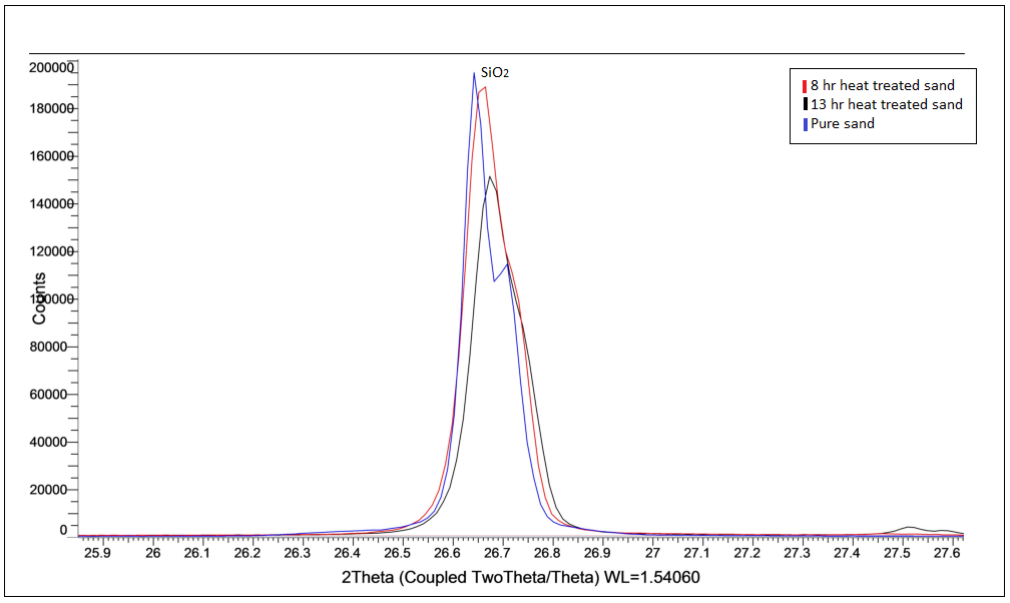

FIGURE 4.13: Xrd analysis for heat treated sand

4.2.7 Mechanical Strength of CNT Sand

The mechanical properties of proppants are very critical for efficient performance of proppants in the reservoir under extreme and very stressed conditions. Conductivity and permeability of flow of oil and gas in the fractured reservoir ultimately dependent on mechanical properties of the proppants. The effect of carbon nanotubes on the mechanical properties is compared with the load deformation curve in the figure 4.14. Initial phases of the curves of 8 pure sand particles did not show a very sharp increase in stress compared to deformation until deformation of 0.0005 mm, after deformation of 0.0005 mm the curves of all the particles symmetrically gave straight lines with sharp slope of the curves. The initial less sharp curve can be due to top surface show some

soft behavior or can be due to touching effect of plates with the sand particle. With the specific applied load, the particles after certain deformation break into pieces, the point at which particle break down occurs known as fracture point. The fracture points for most of the sand particles were between 30 to 45 N load.

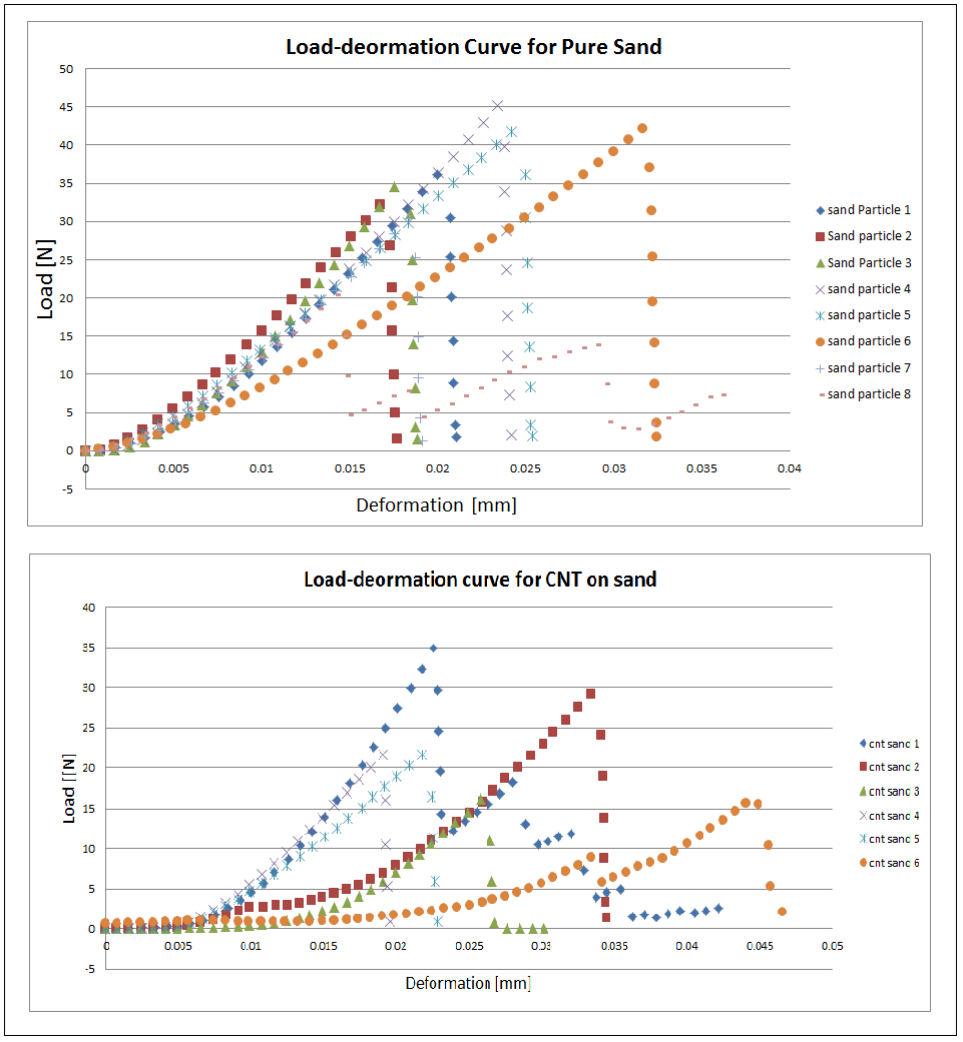

FIGURE 4.14: Load deformation curve for sand & CNT sand

The initial phases of the curves gave extremely low slope for the curves with very low deformation against the applied load for CNTs sand particles as illustrated in figure 4.14. Apart from the initial phases of curves, the later part of curve did not show sharp slopes as observed in the case of pure sand particles. The lesser slopes represents a high deformation of the shape of proppants against the applied load as compared to pure sand particles. The higher deformation was the result of coating of less dense soft layers of carbon nanotubes around the sand particle. As depicted in SEM results, the CNTs laid down upon each other with some free spaces between them. So, when load is applied the carbon nanotubes layers are compressed giving more deformation against applied stress.

It is also possible that the heat treatment of sand particles during the CNTs synthesis process brought changes in the internal structure of the sand particle as discussed earlier with the Xrd analysis. The structural changes of the sand particles possibly decreased the brittleness of the sand particles and resulted in more deformation.

Another important phenomena observed during the mechanical testing of the carbon nanotubes grown sand was the multiple fracture of the CNT sand particles which is also evident in the load deformation curves of CNTs sand. Multiple fracture phenomena was not observed in the case of pure sand and pure sand particles preferred to break down in a single step process which is considered to be the property of a brittle material. The multiple fracture could be result of structural changes within the sand particle with the growth oc CNTs which causes decrease in brittleness. Another possibility of multiple fracture can be the carbon nanotubes surrounding the sand particle do not allow to break the particle at once. After the initial break down of the sand particle, the carbon nanotubes around the sand particle tried again to combine the sand particle and provided enough strength against the second fracture, similarly provided strength for third, fourth and so on fracture points. However, the carbon nanotubes fracture point at very low load compared to fracture points of pure sand. The young modulus of pure sand and sand with carbon nanotube growth were compared in the table 4.5 at 8000 kpa and 14000 kpa. The result shows an distinct decrease in young young modulus with the growth of carbon nanotubes compare to pure sand.

The no distinct increase in strength of sand proppants as represented in the results is quite concerning. In case the mechanical testing equipment available in future, the detailed investigation of the strength testing will be informative for generalization of the impact of carbon nanotubes on the strength of the sand proppants.

Table 4.5: Young modulus of sand and CNT grown sand proppants

Particle	**Sand modulus at 8000 (Kpa)**	**CNT modulus at 8000 (Kpa)**	**Sand modulus at 14000 (kpa)**	**CNTs modulus at 14000 (kpa)**
1	876661.8	901119	974921	0
2	876987	584926.1	969240.9	0
3	1012474	0	1137211	0
4	819073	571665	895694	0
5	695782	0	749966	0

4.3 Scale Inhibition

Scaling phenomena is very common problem, petroleum industry faces in routine daily life for production of oil and gas. The scaling problem in the reservoir begins with the

decrease in solubilities of mineral total dissolved solid in the produced water to minimum limit that they starts precipitation. Scales are usually removed once they formed with the treatment of acid. It is preferable to prevent scale formation rather than allowing them to form and then removing them. So, for the prevention or inhibition of scale, some solid phosphonates chemical are used in the reservoir. Scale inhibitors are normally added in the fracturing fluid for their transport into reservoir, however, the industry is still facing issues of efficient placement of scale inhibitor at the target points. So, it is designed to study the adsorption of scale inhibitor to proppant with the help of carbon nanotubes for controlled transport of scale inhibitor in the reservoir which is discussed following in detail.

4.3.1 Inhibitor Adsorption with CNTs yield

Phosphonates are considered to be with very good adsorption properties. As discussed earlier the proppants particle are non porous with extremely low surface area. For loading of chemical on the proppants surface, the proppants must have higehr surface area which can be achieved by making particle as porous structure. For example AEA technologies loaded scale inhibitor on proppants with a porous structure particle to achieve higher surface area [53]. However, increasing surface area with the porous proppants structure has limitation of decrease in mechanical properties. The results given in the figure 4.9 showed an increase in surface area with the growth of carbon nanotube around the surface of the proppants. The increase in surface area with CNTs propmts idea to adsorb phosphonates on the surface of CNTs proppants instead of making it porous. So, the adsorption of phosphonates scale inhibitor on the surface of the CNT sand particles are represented in the figure 4.15 which shows positive attitude towards the increase in phosphonates loading with the growth of carbon nanotubes. The evidence of some phosphonates adsorption on CNT sand particle is attributed to the availability of higher surface area for inhibitor to adsorb.

There was also increased in phosphonates loading observed with the increase in yield of carbon nanotubes. With the higher yield of CNTs, the sand particle is coated with more layers of carbon nanotubes which provide more surface area to phosphonates resulting in higher loading of phosphonates. The higher loading of phosphonates is possible with increasing yield of carbon nanotubes around the sand particles. However, it is not possible to get high yield of carbon nanotubes even more than 1 % on pure sand without using catalyst as discussed earlier. Therefore, it is difficult to adsorb phosphonates with higher loading in simple way for CNTs grown over pure sand particles. The high yield of CNTs on sand particles results in unbound, detached CNTs powder. So, it is critical

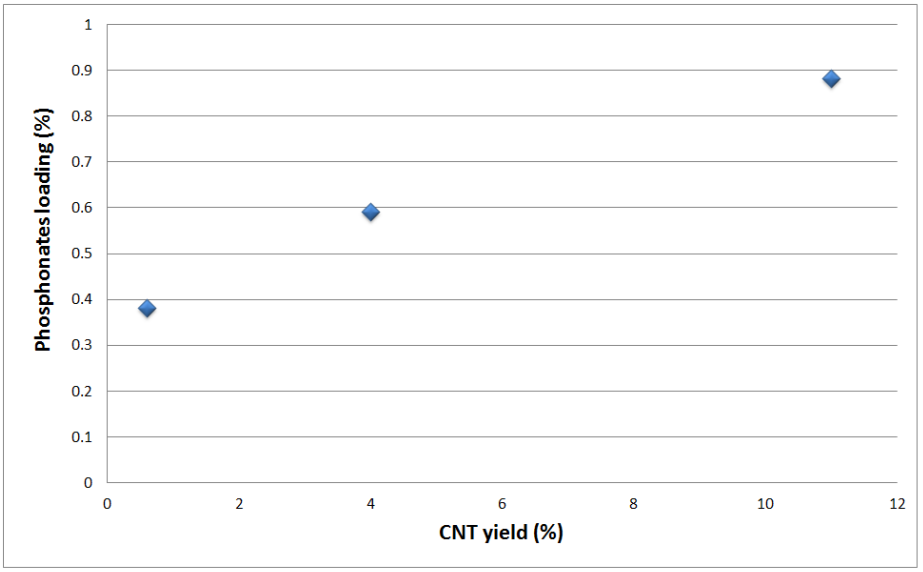

FIGURE 4.15: Phosphonates loading with variation of % yield of CNT over sand

to optimize the yield of CNTs on sand particle with higher loading of phosphonates and minimum powder CNTs.

Loading for 0.6 % CNT Yield

Phosphonates inhibitor loading over the CNT sand particles is further investigated with the variation of time for a fixed % yield. The variation of phosphonates loading with time is given in the figure for 0.6 % cnt yield on pure sand particles. After a time period of one day, 0.39 % loading of phosphonates was observed, however, there was no distinct increase in loading was observed with the further increase in time in days. Even after a time period of 4 days the phosphonates loading is same as of $1st$ day. So, from the results, it can be concluded that with 0.6 % yield of cnt on sand, there is only very limited coating of carbon nanotubes with the limited increase in surface area. With the low yield, the phosphonates find only limited surface area which they saturate within a day.

The chemisizer results show a thin layer of carbon naotube of 32 micrometer for 0.6 % yield of cnt on pure sand. So, the presence of thin layer of cnt coating the phosphonates containing solution has to penetrate into very thin layer, which the solution cover in short time and saturate whole the layers of carbon nanotubes coating. So, the loading of phosphonates on low yield CNTs sand particle can not be achieved for more than a certain limit even with the increase in time for adsorption reaction. So, in order

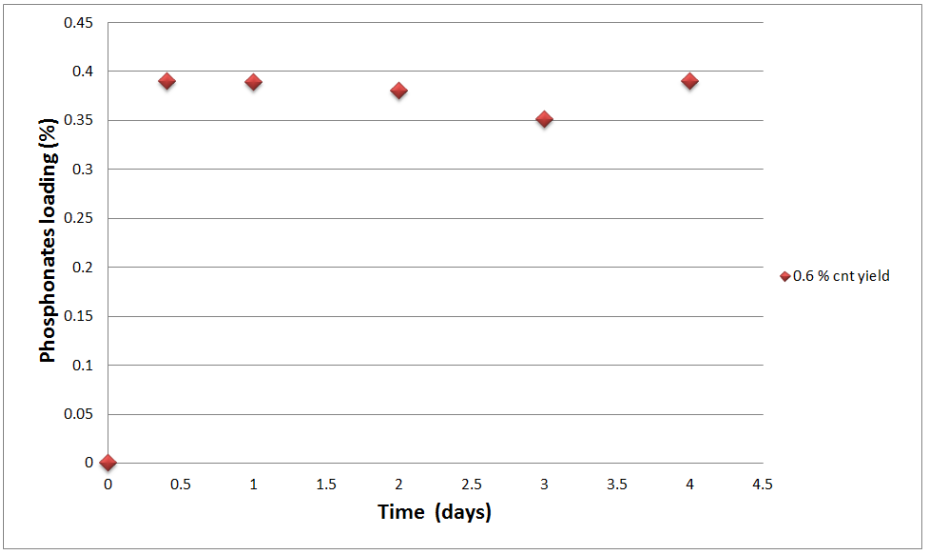

FIGURE 4.16: Phosphonates loading with variation of time for 0.6 % yield of CNT

to get higher loading of phosphonates on low yield CNT sand, the factors controlling adsorption of phosphonates other than the time should be sought.

Loading for 4 % CNT yield

With the higher yield of carbon nanotubes more coating of cnt is achieved resulting in higher surface area and thicker cnt layer around the sand particles. The results of phosphonates loading over the CNT Ni sand with 4 % loading are represented in the figure 4.17. There was little but increased in phosphonates loading over the surface of cnt sand observed with the variation of time in days. With the shorter time for adsorption reaction, the phosphonates containing solution could not penetrate through the comparatively thicker cnt layer. There was surface area available which still had to saturate after one day. So, with the increase in reaction time, more of carbon nanotube layers become accessible to phosphonates solution and more of surface area tried to be saturated which resulted an increase in phosphonates loading.

Loading for 12 % yield

The 12 % yield of carbon nanotubes around the sand particles means presence of thick layer of carbon nanotubes with higher surface area available for phosphonates adsorption. So, the figure 4.18 shows phosphonates adsorption on 12 % yield CNT surrounding sand particles. It was evident an higher loading of inhibitor along with an increase in adsorption with the increase in time in days. It can be concluded that with shorter time

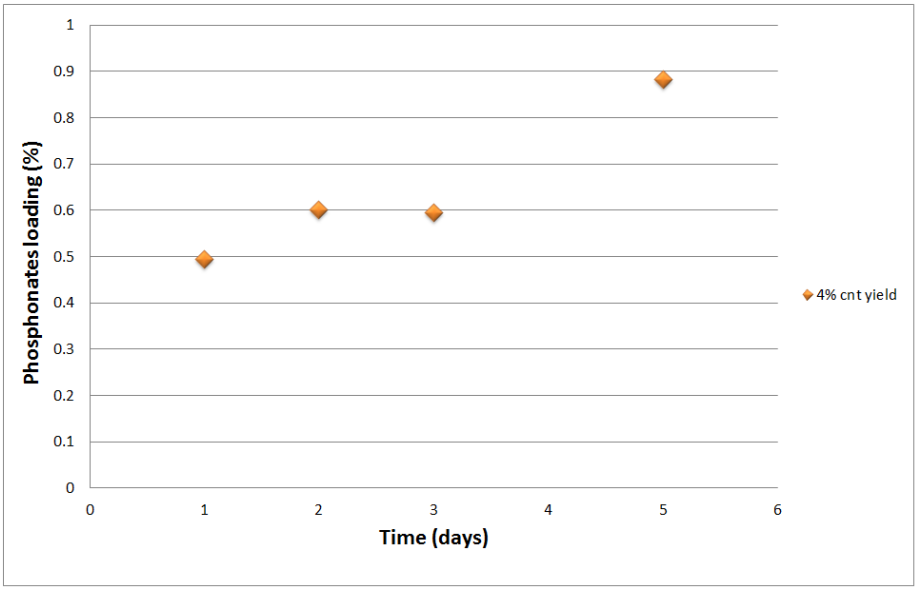

FIGURE 4.17: Phosphonates loading with variation of time for 4 % yield of CNT

of one day, the complete surface area of thick layers of carbon nanotubes around the sand particles was not fully saturated. The adsorption is observed without stirring, so it need more time to fully saturate the carbon nanotubes with the inhibitor. Therefore, it shows an increase in inhibitor loading with the increase in time.

So, in contrast to low yield CNT sand, the time of adsorption reaction can be one of the controlling factor for the loading of phosphonates for higher yield CNTs sand particles. Brown et al, 2011 reported the 1 to 2 % loading of scale inhibitor on the proppants considered to be sufficient for most of chemical demand calculations [7]. The results of the present research work showed a loading of phosphonates higher than the 1 %. However, the comparatively higher loading achieved is with the use of very high yield CNTs on sand particles but high yield has limitations of generation of powder form carbon nanotube and soft layers of CNTs on sand particles. Therefore further research work is required to get higher loading of phosphonates at lower yield of very compact CNTs composite with the sand particle.

4.3.2 Inhibitor Adsorption with PH variation

The phosphonates scale inhibitor with different number of attached phosphonic groups are good adsorbent and their adsorption is reported to be varied with the changes in PH. The adsorption variation with PH is considered to be good factor for further analysis of adsorption of phosphonates inhibitor on carbon nanotubes. The results of inhibitor loading over the 13 % yield CNTs for changing PH are represented in the figure 4.19

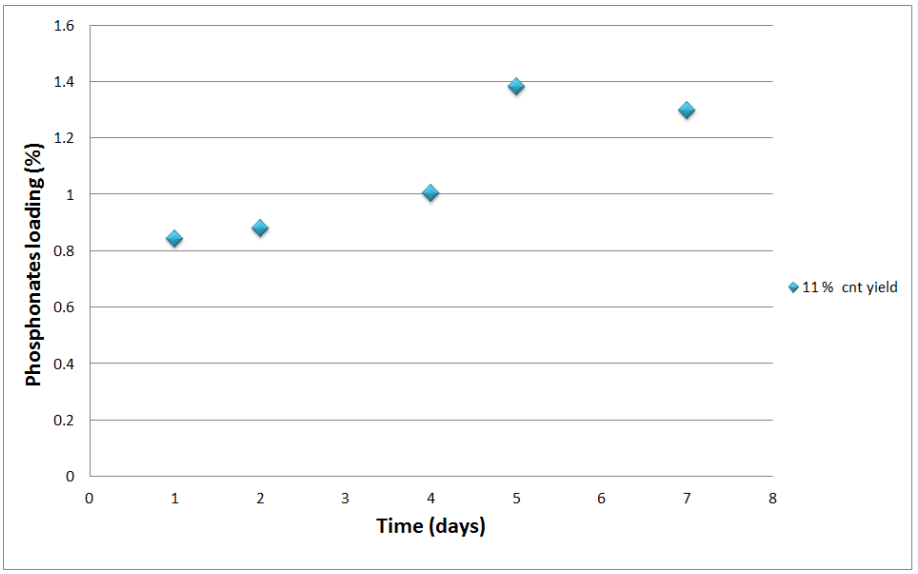

FIGURE 4.18: Phosphonates loading with variation of time for 12 % yield of CNT

and results are based upon the 48 hour reaction time. The higher yield cnts were chosen to distinguish minute changes in yield with the change PH. Therefore, results depicted a higher loading of phosphonates inhibitor in most of cases.

There was little but higher loading of inhibitor observed at very low PH of 1 and 3 in acidic region. However, the phosphonates loading little bit decreased at higher PH in basic region. The very low loading of inhibitor, reported at PH 4, is quite astonishing and create some uncertainty in the observed results. There may be some lost of material during measurement or some error in weight measurement, which resulted in strange value at PH value of 4. It needs further detailed investigation of the impact of PH on the loading before making final conclusion. However, it seams from the result that it is possible to control the adsorption , desorption behavior of phosphonates on CNTs with the PH variations.

4.3.3 SEM Analysis of Inhibitor Adsorption

The SEM analysis was carried out to visualize the adsorption of phophonates inhibitor on the surface of CNT sand particles. A comparison of high resolution images of phosphonates inhibitor adsorbed CNTs with the before treatment CNTs is illustrated in the figure 4.19. The pure CNTs indicated with C) & D) look more separated and laid upon each other with the distance apart between them. The phosphonates inhibitor adsorbed CNTs indicated with A) & B) look density packed with smaller distance between individual tubes. The inhibitor adsorbed The closely packed carbon nanotubes could be due

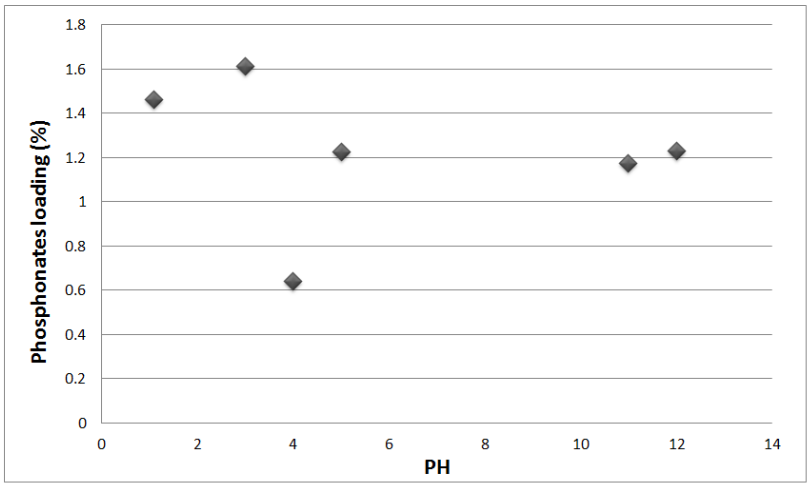

FIGURE 4.19: Phosphonates loading with variation of PH for 13 % cnt yield

to penetration of the solution from surface to inside the carbon nanotubes layer which brought the carbon nanotube close to each other.

CNTs are visible with more bending structure and more entanglement. The adsorption of the phosphonates could disturb the structure of individual carbon nanotube and resulted in more twisted structure. The carbon nanotubes after inhibitor adsorption seam to be thicker with the increase diameter. It can be concluded that increased diameter carbon nanotube indicate the adsorption of phosphonates inhibitor on the surface of the carbon nanotubes.

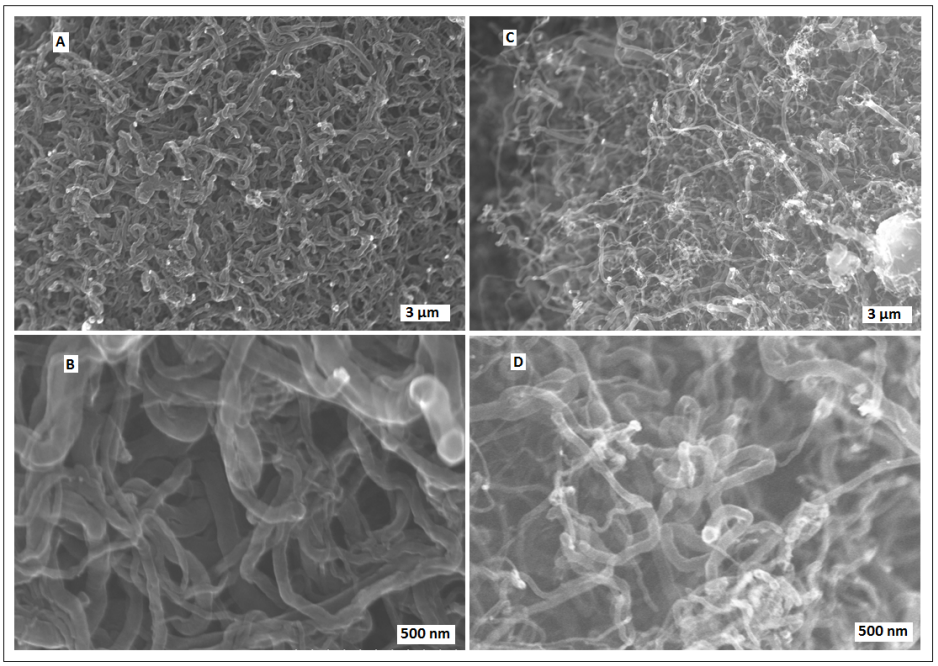

FIGURE 4.20: Phosphonates inhibitor adsorption: A) & B) 1.14% inhibitor loading, C) & D) without inhibitor loading

Chapter 5

Perspective & Future Work

The carbon nanotubes has potential to improve the performance and functionality of proppants used in the reservoir for the enhanced oil & gas production. The application of carbon nanotubes for development of multi-functional proppants seams very interesting idea and hopefully expanding shale gas industry will use the idea in future. However, the focus of research & development is required to develop the multi-functional proppants. The present research work is an exploration of key area of interest for the application of carbon nanotubes but with limited resources to some extent. These areas can be focused in future for the desired application of carbon nanotubes for development of proppants.

The present research included the density measurement along with measurement of sphericity & roundness. These measurement required comparatively larger quantity of carbon nanotube for experiments. However, the carbon nanotubes could be synthesized in a limited quantity in limited time. Therefore, only limited amount of data was obtained for these measurements. The future work can include the detailed analysis of variation of density and sphericity with the variation of yield of carbon nanotubes having more time to synthesize more quantity of CNTs. If the mechanical testing machine "Instron" will be available again it will be interesting to investigate the reason how the CNT grown sand bear less load than the pure sand particles. It can be investigated in future work if there is influence of heat treatment on mechanical strength of sand during the CNT synthesis. The carbon nanotubes grown sand gave multiple fracture phenomena in mechanical strength testing. It will be very interesting to record the break down process of sand particle with the high speed camera. It was tried with the simple camera but was not capable to give information about very minute small scale particle break down phenomena.

Conductivity is very critical for evaluation of the performance of proppants. However, the availability of conductivity or permeability testing set up is still a question mark. If

the conductivity measurement set up available for future work, it will be of great worth for evaluation of carbon nanotubes grown proppants. Settling velocity in fluid closely related with density of proppants is very important for evaluation of transport behavior of proppants. It was tried to measure the settling velocity with the simple camera, but again camera was unable to detect the motion of small particle within the fluid. So, if the high speed camera available for future work, settling velocity measurement will be interesting area of investigation and can be related with density variation with CNT synthesis.

The author thinks high potential of carbon nanotubes for development of multi-functional proppants especially the use proppants for the efficiently placement of chemical in the reservoir. It was investigated the potential of CNTs grown proppants as scale inhibitor carrier with the adsorption of phosphonates scale inhibitor on the surface of the CNTs grown sand particles. The adsorption behavior can be further investigated in future work. The report is badly lacking the scale inhibition testing and evaluation of the phosphonated CNTs sand proppants. It was relied on titration method as simple way with notably two method one involved with the use of electrical conductivity meter and other complexometry titration with EDTA. Unfortunately, the electrical conductivity meter set up was not found. The concentration of scale forming calcium ion is usually found with EDTA titration which make complex with Ca^{+2}. However, the phosphonates also form complex with the Ca^{+2} and it is not possible to quantify Ca^{+2} with EDTA in the presence of phosphonates. Therefore, It was not possible to get some scientifically reliable results for scale inhibition testing for the present work. It will be very interesting to employ some sophisticated equipment for release and inhibition efficiency of phosphonates inhibitor in future work. Future work can also include development of self suspended proppants, another potential area for development of multifunctional proppants.

Chapter 6

Conclusion

The proppants are important part of hydraulic fracturing process & different aspect of proppants were explored in the present research work. It include proppants testing, application of carbon nanotubes for development of proppants and development of multifunctional proppants. The proppants testing gave deep insight into the properties of proppants. The proppants particles resulted in extremely low surface area even lower than $1m^2/g$ which is indication of very compact nonporous structure of proppants material. The alumina proppants has porous structure, therefor, resulted in very high surface area more than 200 time more than the other proppants. So, it was concluded that the nonporous structure of proppants was one of the reason of extremely low surface area. The ceramics proppants exhibited very high mechanical strength compare to strength of other proppants. The strength behavior of sand proppans was worst compare to other proppants. Moreover, the acid resistance of ceramics was excellent with acid solubility of 0.06% but the performance of sand particle was again very poor to resist the acid attack with the acid solubility of 1.28 %. The ceramics proppants generally have drawback of very higher densities compare to sand proppants which is highly undesirable. However, the density measurement data depicted comparable density $2.51g/cm^3$ of ceramics proppants with the $2.53g/cm^3$ of sand . Therefore, the ceramics proppants proved to be very good proppants material with high strength, high acid resistance along with comparable densities with sand which indicate that they do not need much improvements. The sand is still mostly used proppants in industry and very poor performance of sand proppants raise concerns and motivation for research & development work for improvement of its performance.

In order to improve the properties of sand proppants, the applications of carbon nanotubes with excellent properties were explored. The carbon nanotubes synthesis with the Chemical Vapor Deposition, depicted an increase in CNTs yield with the time for Ni

supported sand but there was no significant increase in CNTs yield with the pure sand. The very high yield also resulted in detached powder form carbon nanotubes which restrict to go beyond a certain limit of yield. If powder form CNTs are concerning, the results showed the yield of 2% is sufficient. There effect of synthesis reaction conditions on the structural properties of sand was also observed with the X-ray diffraction analysis. There was no observable increase in strength of the proppant and even sphericity reduced little bit with the application of carbon nanotubes around the sand proppants. However, there was 21 to 25 % decrease in particle density and 33 to 35 % decrease in bulk density for the 7% and 10% yield of CNTs respectively. The decrease in density is considered to be an improvement in the properties of sand proppants. There was also an increase in surface area with the growth of carbon nanotubes, it has no impact on the performance of proppants. However, increase in surface area can be used for adsorption of the chemical on the surface of the proppants and use as vehicle for efficient delivery of proppants in the reservoir.

The phosphonates inhibitor adsorption on CNTs sand particles showed an increase in loading with the increase in yield of CNTs on the sand surface. The increase in loading of phosphonates with the increase in adsorption reaction time was also observed except in the case of very low yield CNTs sand proppants. So, it can be concluded that the loading of the phosphonates on CNTs sand can be controlled with the variation in yield and time. The phosphonates loading with the PH variation needed more investigation to make final conclusion. The higher yield CNTs sand particles showed phosphonates loading higher than the 1 %. Literature reported 1 to 2 % of inhibitor loading on the proppant is sufficient for inhibitor demand calculations. So, It can be concluded that the CNTs proppants has potential to be use for multipurpose along with its main purpose to keep open the fracture.

Bibliography

[1] World energy outlook 2009. *International Energy Agency*, 2009.

[2] R. S. Aboud, R. C. B. De Melo, et al. Past technologies emerge due to lightweight proppant technology: Case histories applied on mature fields. In *Latin American & Caribbean Petroleum Engineering Conference*. Society of Petroleum Engineers, 2007.

[3] J. D. Arthur, B. Bohm, B. J. Coughlin, M. Layne, D. Cornue, et al. Evaluating the environmental implications of hydraulic fracturing in shale gas reservoirs. *ALL Consulting. http://www. all-llc. com/publicdownloads/ArthurHydrFracPaper-FINAL. pdf*, 2008.

[4] R. L. Bienvenu Jr. Lightweight proppants and their use in hydraulic fracturing, July 2 1996. US Patent 5,531,274.

[5] H. Bourne, S. Heath, S. McKay, J. Fraser, L. Stott, S. Müller, et al. Effective treatment of subsea wells with a solid scale inhibitor system. In *International Symposium on Oilfield Scale*. Society of Petroleum Engineers, 2000.

[6] J. M. Bremer, B. Mibeck, B. L. Huffman, C. D. Gorecki, J. A. Sorensen, D. D. Schmidt, J. A. Harju, et al. Mechanical and geochemical assessment of hydraulic fracturing proppants exposed to carbon dioxide and hydrogen sulfide. In *Canadian Unconventional Resources and International Petroleum Conference*. Society of Petroleum Engineers, 2010.

[7] J. M. Brown, D. Gupta, G. N. Taylor, D. Shen, R. Self, et al. Laboratory and field studies of long-term release rates for a solid scale inhibitor. In *SPE International Symposium on Oilfield Chemistry*. Society of Petroleum Engineers, 2011.

[8] D. K. Chatterjee, R. D. Skala, C. E. Coker, J. R. Loscutova, et al. Low surface friction proppants, July 13 2012. US Patent App. 13/548,243.

[9] G. Coulter, R. Wells, et al. The advantages of high proppant concentration in fracture stimulation. *Journal of Petroleum Technology*, 24(06):643–650, 1972.

[10] M. Crabtree, D. Eslinger, P. Fletcher, M. Miller, A. Johnson, and G. King. Fighting scale—removal and prevention. *Oilfield Review*, 11(3):30–45, 1999.

[11] B. D. Cullity and S. R. Stock. *Elements of X-ray Diffraction*. Pearson, 2001.

[12] J. L. Daniels, G. A. Waters, J. H. Le Calvez, D. Bentley, J. T. Lassek, et al. Contacting more of the barnett shale through an integration of real-time microseismic monitoring petrophysics and hydraulic fracture design. In *SPE Annual Technical Conference and Exhibition*. Society of Petroleum Engineers, 2007.

[13] S. Darin, J. Huitt, et al. Effect of a partial monolayer of propping agent on fracture flow capacity. 1960.

[14] P. M. Dove and M. F. Hochella Jr. Calcite precipitation mechanisms and inhibition by orthophosphate: In situ observations by scanning force microscopy. *Geochimica et Cosmochimica Acta*, 57(3):705–714, 1993.

[15] U. EIA. Annual energy outlook 2011 with projections to 2035. *Washington DC: Energy Information Administration, United States Department of Energy*, 2011.

[16] E. O. Fernández. Carbon nanofibers supported ni catalyst. *Faculty of Chemistry and Biology, Department of Chemical Engineering, NTNU*, 2003.

[17] J. F. Gale, R. M. Reed, and J. Holder. Natural fractures in the barnett shale and their importance for hydraulic fracture treatments. *AAPG bulletin*, 91(4):603–622, 2007.

[18] A. Graham, G. Duesberg, W. Hoenlein, F. Kreupl, M. Liebau, R. Martin, B. Rajasekharan, W. Pamler, R. Seidel, W. Steinhoegl, et al. How do carbon nanotubes fit into the semiconductor roadmap? *Applied Physics A*, 80(6):1141–1151, 2005.

[19] J. Gulbis, G. Hawkins, M. King, R. Pulsinelli, E. Brown, and J. Elphick. Taking the brakes off proppant-pack conductivity. *Oilfield Review*, 3:18–26, 1991.

[20] S. A. Holditch. Unconventional oil and gas resource development–let's do it right. *Journal of Unconventional Oil and Gas Resources*, 1:2–8, 2013.

[21] Z. Huang, D. Wang, J. Wen, M. Sennett, H. Gibson, and Z. Ren. Effect of nickel, iron and cobalt on growth of aligned carbon nanotubes. *Applied Physics A*, 74(3):387–391, 2002.

[22] S. Iijima et al. Helical microtubules of graphitic carbon. *nature*, 354(6348):56–58, 1991.

[23] D. Kamat, I. M. Saaid, and I. Dzulkarnain. Comparative characterization study of malaysian sand as proppant.

[24] P. B. Kaufman, R. W. Anderson, M. A. Parker, H. D. Brannon, A. R. Neves, K. L. Abney, S. A. Joyce, M. J. Ziegler, G. W. K. d. P. Cortes, G. S. Penny, et al. Introducing new api/iso procedures for proppant testing. In *SPE Annual Technical Conference and Exhibition*. Society of Petroleum Engineers, 2007.

[25] G. E. King et al. Hydraulic fracturing 101: What every representative environmentalist regulator reporter investor university researcher neighbor and engineer should know about estimating frac risk and improving frac performance in unconventional gas and oil wells. In *SPE Hydraulic Fracturing Technology Conference*. Society of Petroleum Engineers, 2012.

[26] R. Kothamasu, Y. K. Choudhary, K. Murugesan, et al. Comparative study of different sand samples and potential for hydraulic-fracturing applications. In *SPE Oil and Gas India Conference and Exhibition*. Society of Petroleum Engineers, 2012.

[27] C. J. Lee, J. Park, and J. A. Yu. Catalyst effect on carbon nanotubes synthesized by thermal chemical vapor deposition. *Chemical Physics Letters*, 360(3):250–255, 2002.

[28] D. S. Lee, D. Elsworth, and Yasuhara. Experiment and modeling to evaluate the effects of proppant-pack diagenesis on fracture treatments. *Journal of Petroleum Science and Engineering*, 74:67–76, 2011.

[29] C. Li and T.-W. Chou. A structural mechanics approach for the analysis of carbon nanotubes. *International Journal of Solids and Structures*, 40(10):2487–2499, 2003.

[30] Y. Min-Feng. Tensile loading of ropes of single wall carbon nanotubes and their mechanical properties. *Physical review letters*, 2000.

[31] N. Muthuswamy, J. L. G. de la Fuente, P. Ochal, R. Giri, S. Raaen, S. Sunde, M. Rønning, and D. Chen. Towards a highly-efficient fuel-cell catalyst: optimization of pt particle size, supports and surface-oxygen group concentration. *Physical Chemistry Chemical Physics*, 15(11):3803–3813, 2013.

[32] M. Navaneethan. Introduction to carbon nanofibers. In *Training for project for project student*. Department of Chemical Engineering, NTNU, 2013.

[33] G. D. Nessim. Properties, synthesis, and growth mechanisms of carbon nanotubes with special focus on thermal chemical vapor deposition. *Nanoscale*, 2(8):1306–1323, 2010.

[34] M. Norris, D. Perez, H. Bourne, and S. Heath. Maintaining fracture performance through active scale control. *Journal of petroleum technology*, 53(12):42–43, 2001.

[35] B. Nowack. Environmental chemistry of phosphonates. *Water Research*, 37(11):2533–2546, 2003.

[36] B. Nowack and A. T. Stone. Adsorption of phosphonates onto the goethite–water interface. *Journal of colloid and interface science*, 214(1):20–30, 1999.

[37] A. E. Outlook. Us energy information administration (eia). *Department of Energy (DoE)*, 2012.

[38] M. Parker, J. Weaver, and D. Van Batenburg. Understanding proppant flowback. In *SPE annual technical conference*, pages 681–693, 1999.

[39] J. E. Patchett and R. A. Rowse. Low density proppant for oil and gas wells. European Patent No. EP 0101855, 1984.

[40] J. Prasek, J. Drbohlavova, J. Chomoucka, J. Hubalek, O. Jasek, V. Adam, and R. Kizek. Methods for carbon nanotubes synthesis—review. *Journal of Materials Chemistry*, 21(40):15872–15884, 2011.

[41] A. Revil. Pervasive pressure-solution transfer: A poro-visco-plastic model. *Geophysical research letters*, 26(2):255–258, 1999.

[42] L. J. I. Richard and A. R. Sinclair. Composite and reinforced coatings on proppants and particles, June 6 1995. US Patent 5,422,183.

[43] J. F. Richardson and J. H. Harker. Chemical engineering-volume 2: Particle technology and separation processes. pages 191–193.

[44] A. R. Rickards, H. D. Brannon, W. D. Wood, C. J. Stephenson, et al. High strength ultra-lightweight proppant lends new dimensions to hydraulic fracturing applications. In *SPE annual technical conference and exhibition*. Society of Petroleum Engineers, 2003.

[45] H. B. Rickards, Allan and W. Wood. High strength, ultralightweight proppant lends new dimensions to hydraulic fracturing applications. pages 212–221, 2006.

[46] H. Rogers. Shale gas—the unfolding story. *Oxford Review of Economic Policy*, 27(1):117–143, 2011.

[47] S. Schubarth, S. Cobb, R. Jeffrey, et al. Understanding proppant closure stress. In *SPE Production Operations Symposium*. Society of Petroleum Engineers, 1997.

[48] E. T. Thostenson, Z. Ren, and T.-W. Chou. Advances in the science and technology of carbon nanotubes and their composites: a review. *Composites science and technology*, 61(13):1899–1912, 2001.

[49] M. Tomson, G. Fu, M. Watson, A. Kan, et al. Mechanisms of mineral scale inhibition. *SPE production & facilities*, 18(03):192–199, 2003.

[50] R. Vidic, S. Brantley, J. Vandenbossche, D. Yoxtheimer, and J. Abad. Impact of shale gas development on regional water quality. *Science*, 340(6134):1235009, 2013.

[51] Q. Wang, X. Chen, A. N. Jha, and H. Rogers. Natural gas from shale formation–the evolution, evidences and challenges of shale gas revolution in united states. *Renewable and Sustainable Energy Reviews*, 30:1–28, 2014.

[52] J. D. Weaver, R. D. Rickman, H. Luo, R. Logrhy, et al. A study of proppant formation reactions. In *SPE International Symposium on Oilfield Chemistry*. Society of Petroleum Engineers, 2009.

[53] P. Webb, T. Nistad, B. Knapstad, P. Ravenscroft, I. Collins, et al. Advantages of a new chemical delivery system for fractured and gravel-packed wells. *SPE production & facilities*, 14(03):210–218, 1999.

[54] R. Weijermars, G. Drijkoningen, T. Heimovaara, E. Rudolph, G. Weltje, and K. Wolf. Unconventional gas research initiative for clean energy transition in europe. *Journal of Natural Gas Science and Engineering*, 3(2):402–412, 2011.

[55] R. Weijermars and C. McCredie. Assessing shale gas potential. *Petroleum Review*, 65(777), 2011.

[56] T. Wu, B. Wu, and S. Zhao. Acid resistance of silicon-free ceramic proppant. *Materials Letters*, 92:210–212, 2013.

[57] R. Youngman, P. R. Okell, and S. Akbar. Proppant composition for gas and oil well fracturing, Apr. 16 2002. US Patent 6,372,678.

[58] M. Zoback, S. Kitasei, and B. Copithorne. *Addressing the environmental risks from shale gas development*, volume 21. Worldwatch Institute, 2010.

Appendix A

Catalyst Preparation

For 15% of Nickel supported on proppants the required amount of precursor salt is calculated as follow. For 5g of support the mass of Ni needed is given as

$$m_{cat,Ni} = m_{cat,total} - m_{cat,support} = 5/(5 - 0.15) = 0.8823$$

$$n_{Ni} = m_{cat,Ni}/M_{Ni} = 0.8823/58.7 = 0.01503$$

the mass of $Ni(NO_3)_2.6H_2O$ is given by

$$m_{Ni(NO_3)_2.6H_2O} = n_{Ni}.M_{Ni(NO_3)_2.6H_2O} = (0.01503).290 = 4.371179477$$

For deposition precipitation method the urea was also used. Urea is used in excess and mole of the urea should be 3 time than that of nickel. The mass of urea used is calculated as follow

$$m_{urea} = n_{Ni}.3.M_{urea} = 2.7372$$

Appendix B

SEM Results

FIGURE B.1: SEM images of sand proppants particle

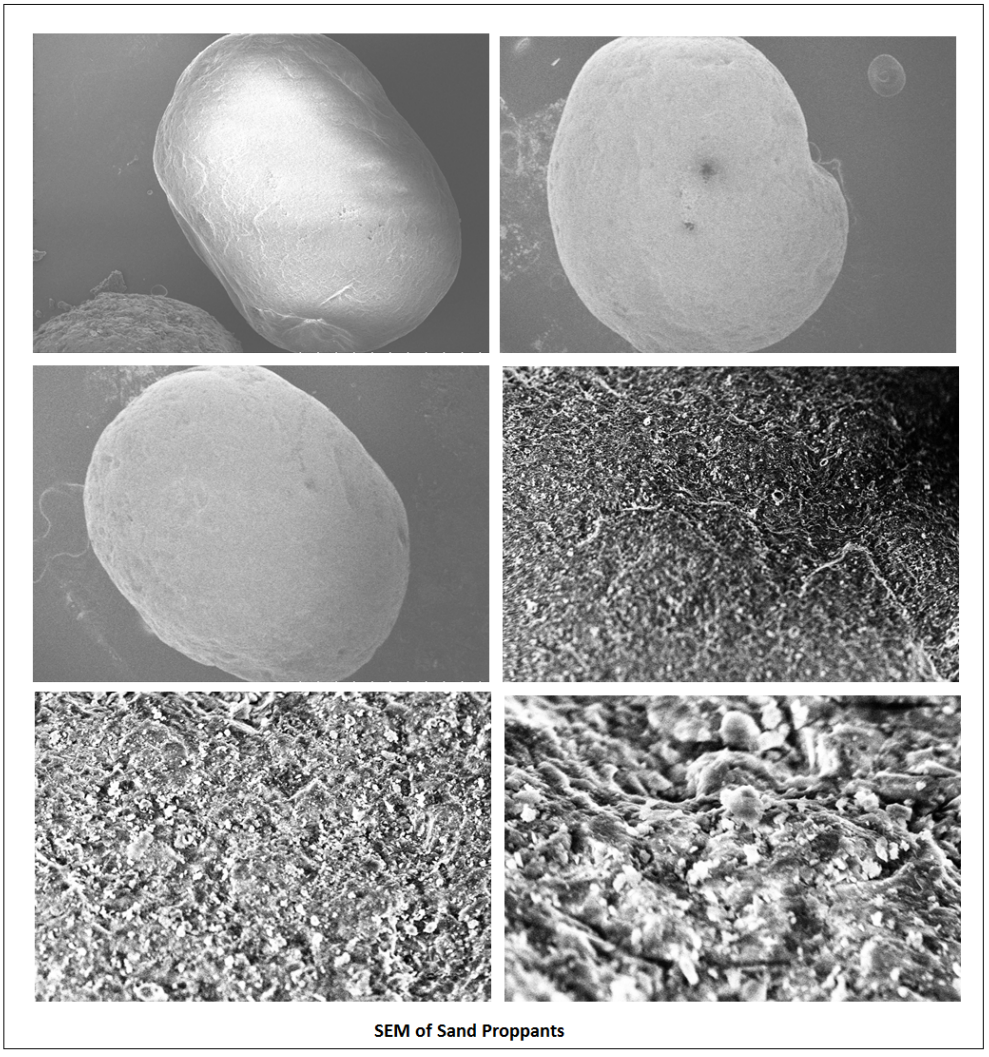

FIGURE B.2: SEM images ofAlumina proppants particle

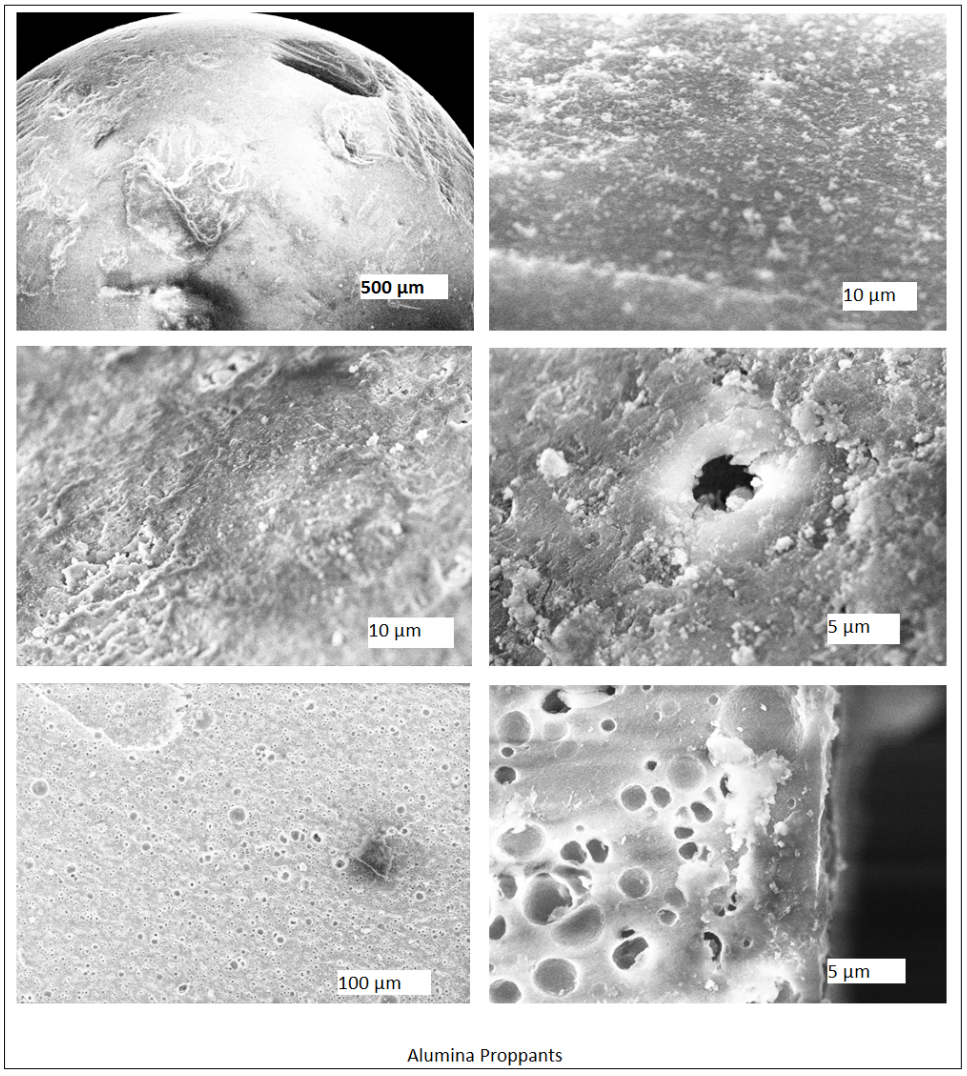

FIGURE B.3: SEM images of carbolite proppants particle

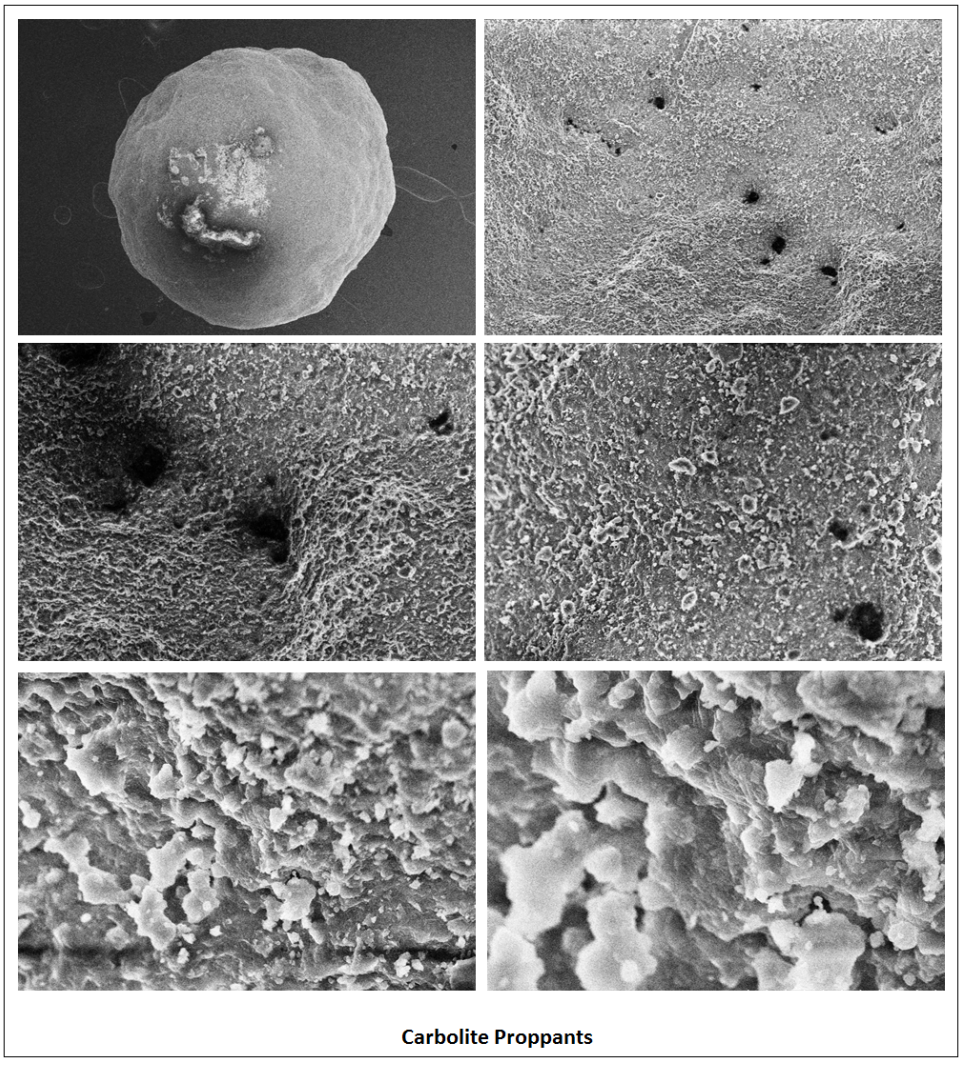

FIGURE B.4: SEM images of gravel proppants particle

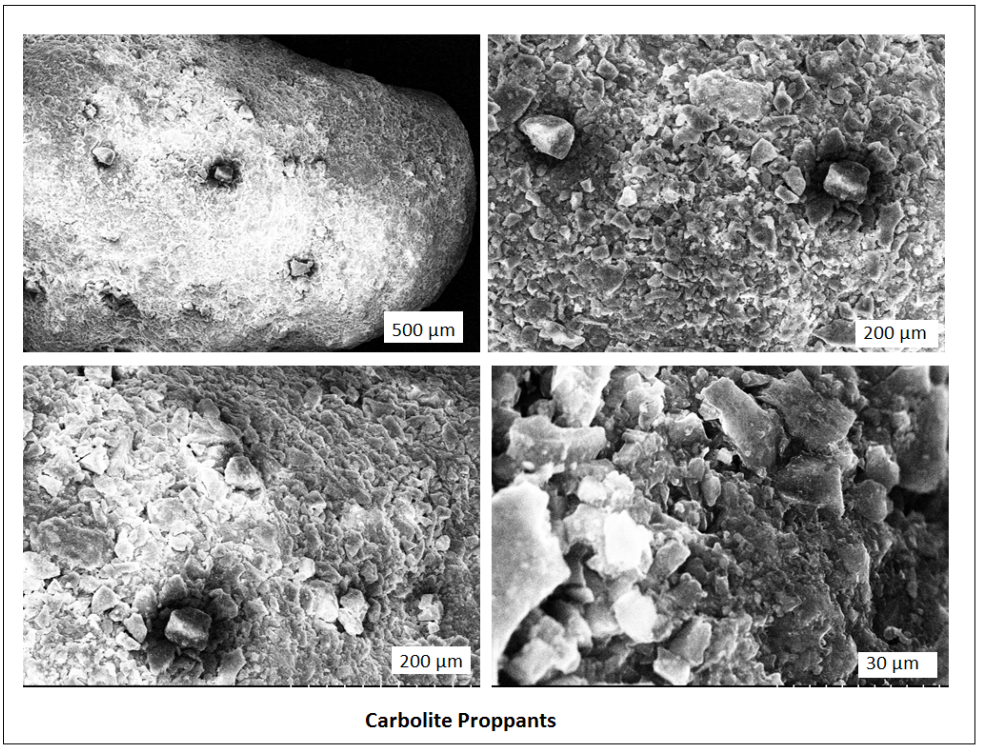

FIGURE B.5: SEM images of CNT on Ni sand for 2hr grwoth time

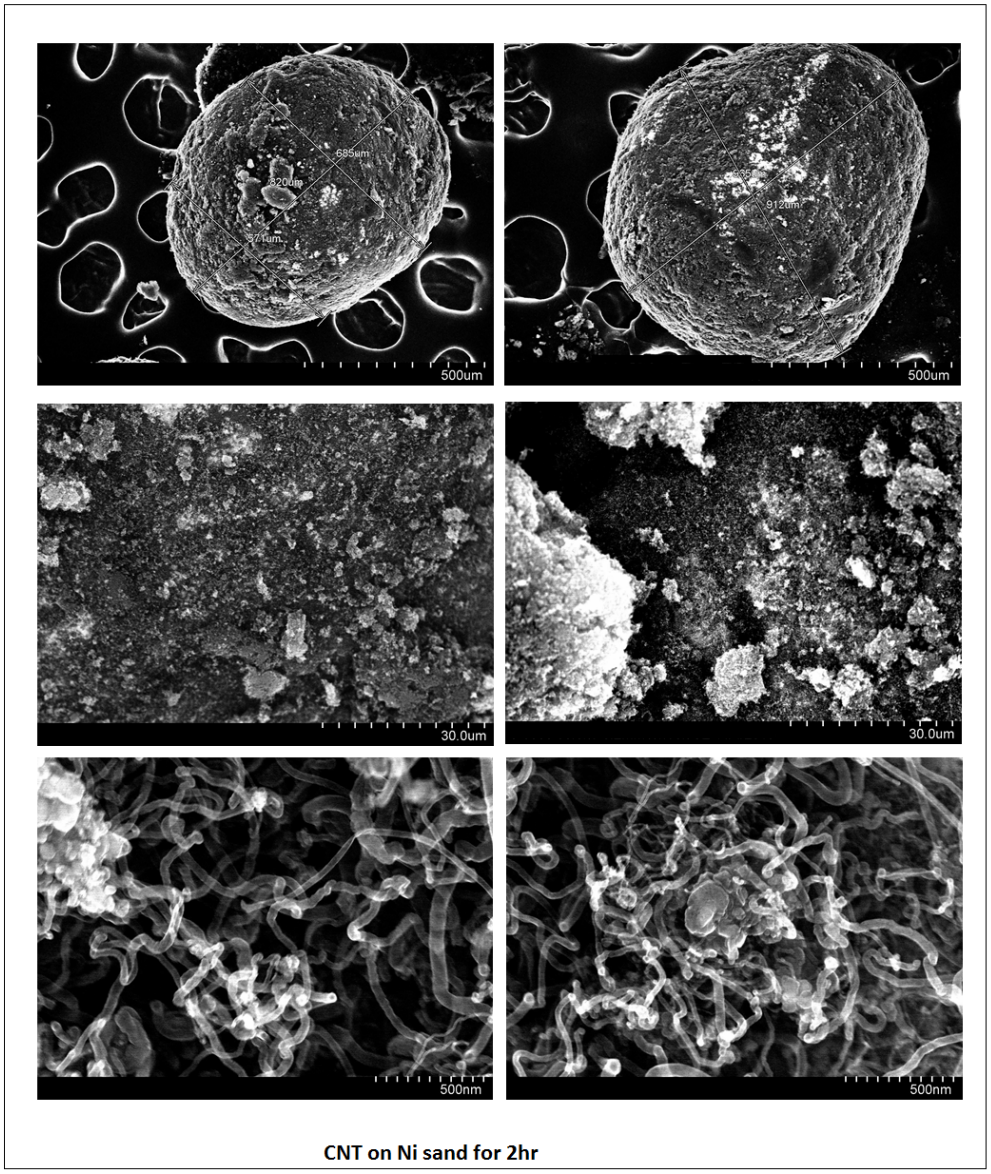

FIGURE B.6: SEM images of CNT on Ni sand for 4hr grwoth time

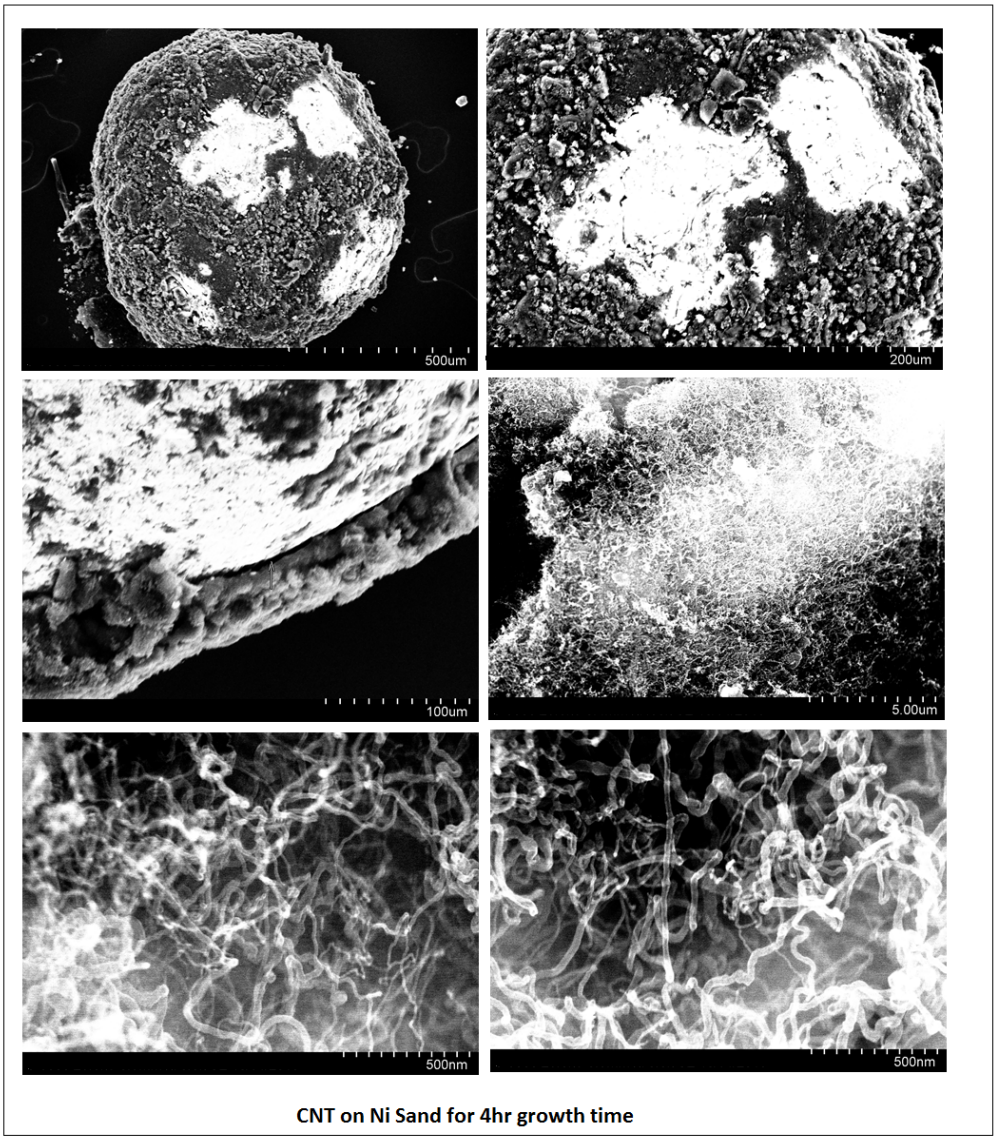

FIGURE B.7: SEM images of CNT on Ni sand for 13hr grwoth time

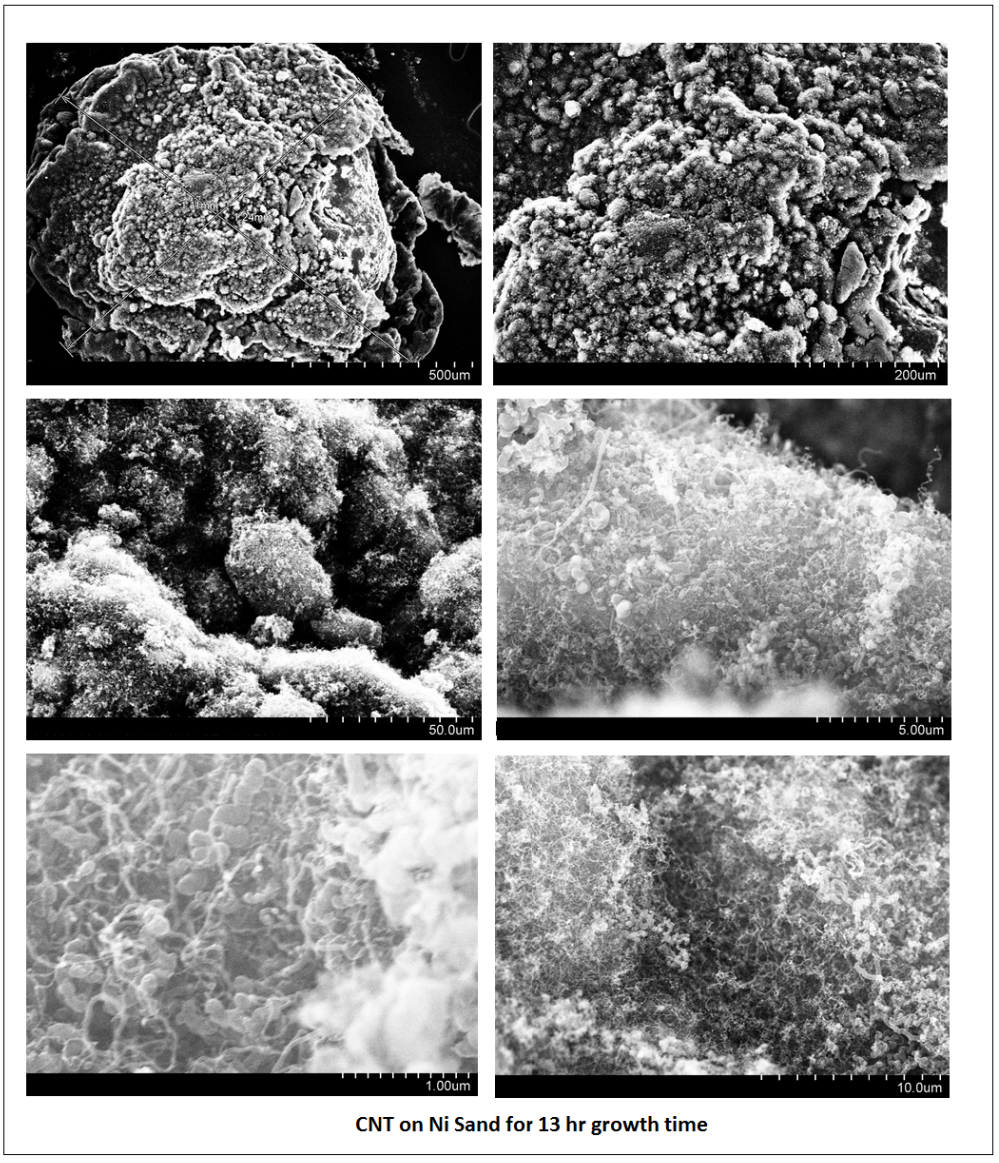

Appendix C

Mechanical Strength Testing

FIGURE C.1: Load deformation curve for sand & cnt sand

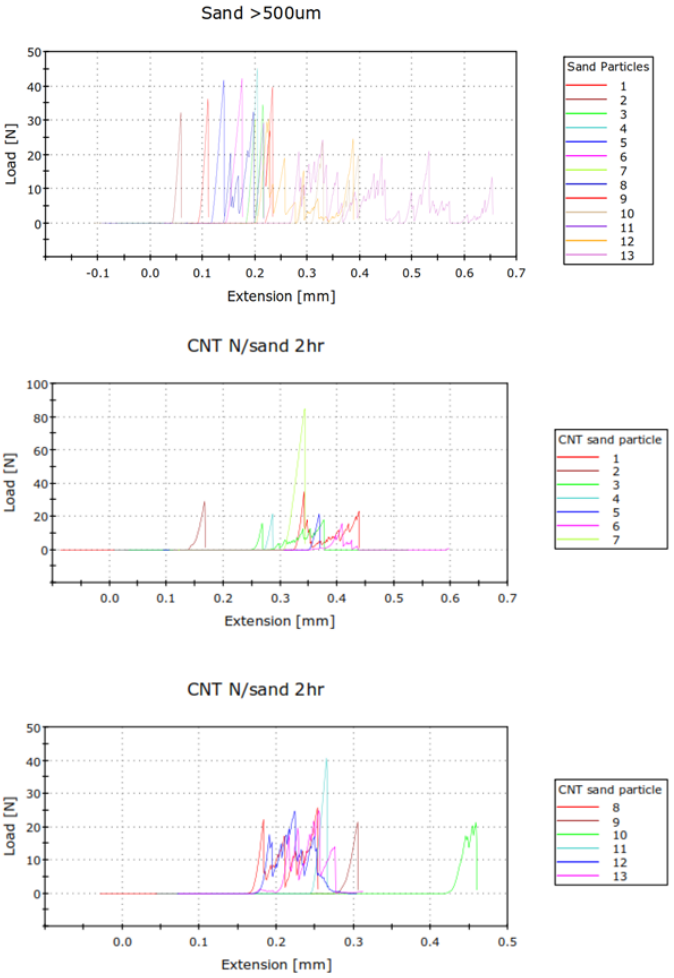

FIGURE C.2: Load deformation curve for ceramics & cnt ceramics

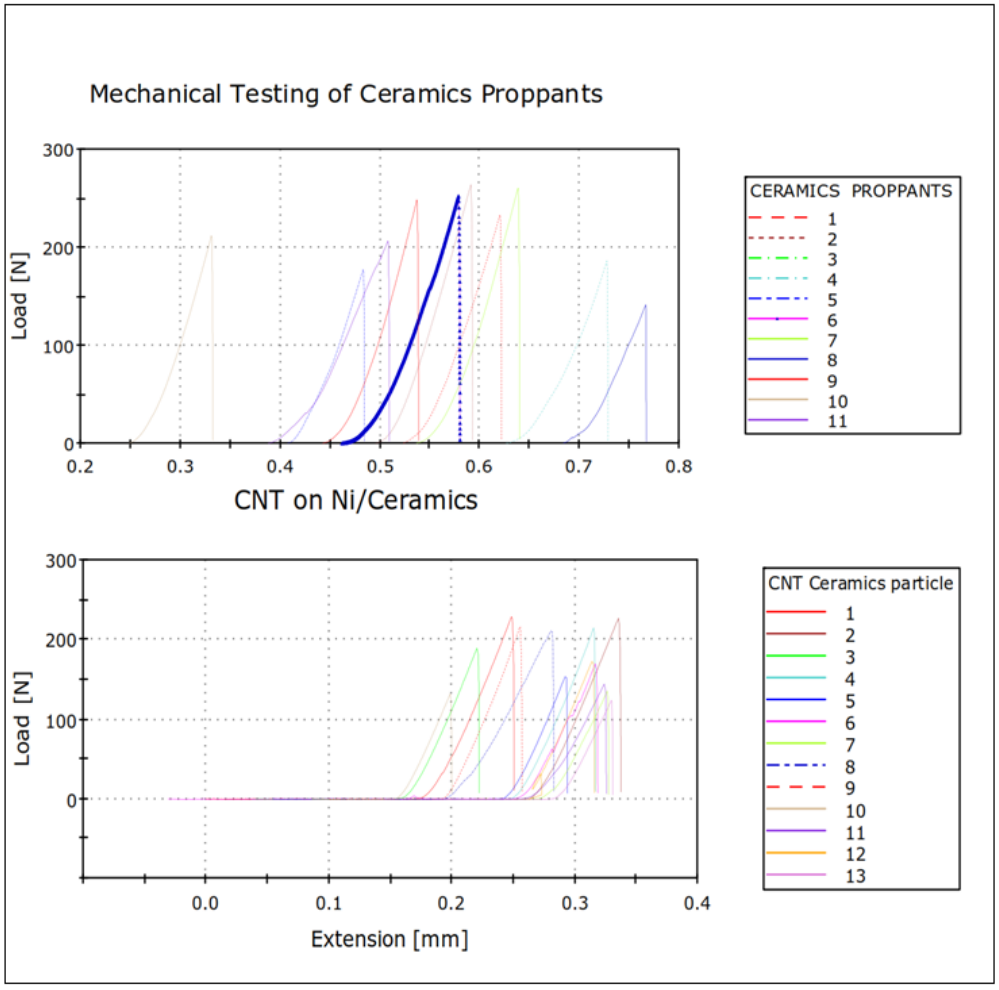

FIGURE C.3: Load deformation curve for carbolite

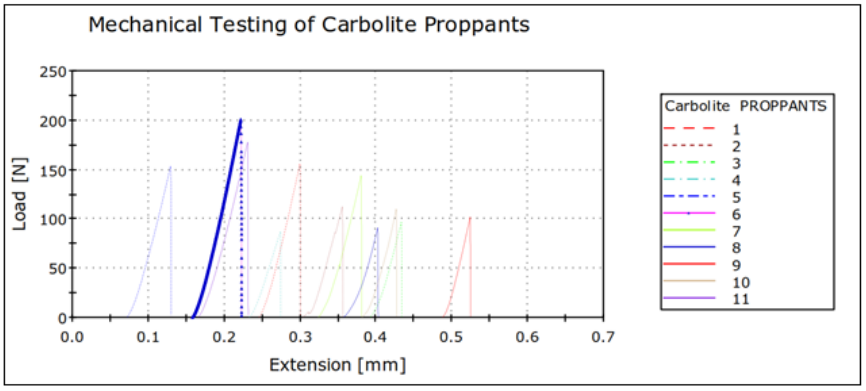

FIGURE C.4: Load deformation curve for alumina

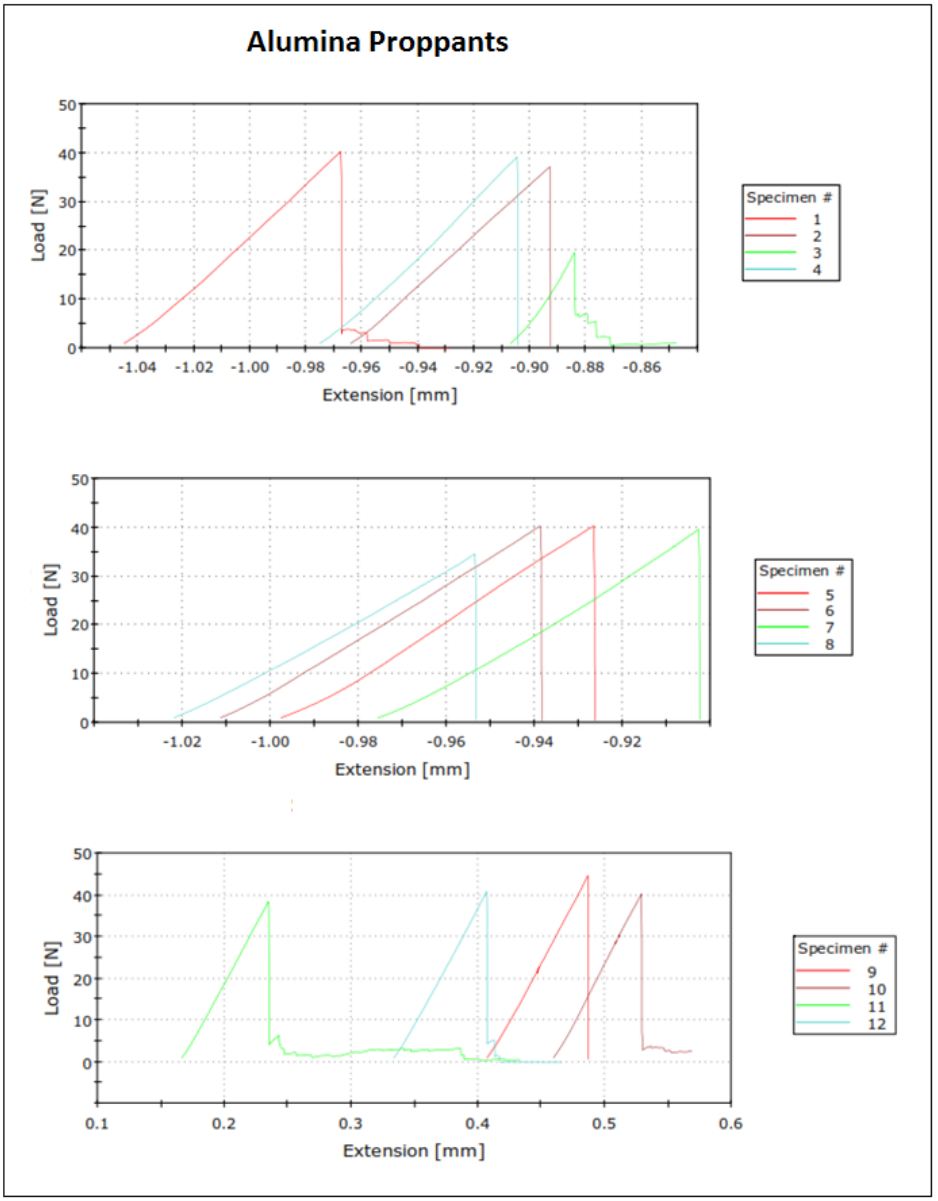

Appendix D

Surface Area Measurement

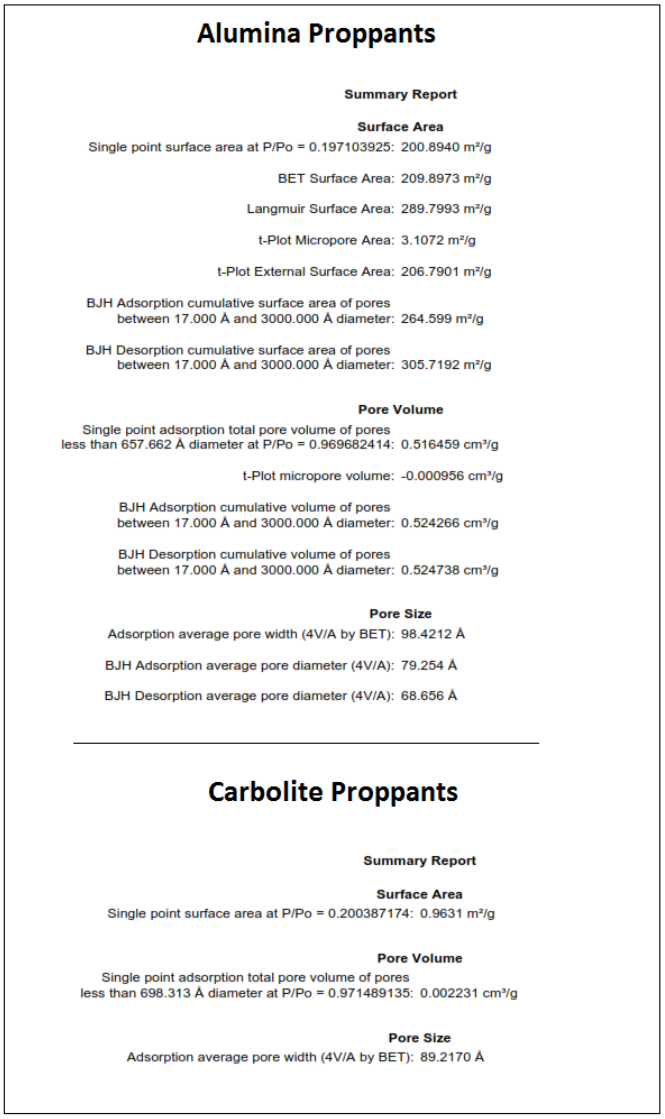

Alumina Proppants

Summary Report

Surface Area

Single point surface area at P/Po = 0.197103925: 200.8940 m²/g

BET Surface Area: 209.8973 m²/g

Langmuir Surface Area: 289.7993 m²/g

t-Plot Micropore Area: 3.1072 m²/g

t-Plot External Surface Area: 206.7901 m²/g

BJH Adsorption cumulative surface area of pores between 17.000 Å and 3000.000 Å diameter: 264.599 m²/g

BJH Desorption cumulative surface area of pores between 17.000 Å and 3000.000 Å diameter: 305.7192 m²/g

Pore Volume

Single point adsorption total pore volume of pores less than 657.662 Å diameter at P/Po = 0.969682414: 0.516459 cm³/g

t-Plot micropore volume: -0.000956 cm³/g

BJH Adsorption cumulative volume of pores between 17.000 Å and 3000.000 Å diameter: 0.524266 cm³/g

BJH Desorption cumulative volume of pores between 17.000 Å and 3000.000 Å diameter: 0.524738 cm³/g

Pore Size

Adsorption average pore width (4V/A by BET): 98.4212 Å

BJH Adsorption average pore diameter (4V/A): 79.254 Å

BJH Desorption average pore diameter (4V/A): 68.656 Å

Carbolite Proppants

Summary Report

Surface Area

Single point surface area at P/Po = 0.200387174: 0.9631 m²/g

Pore Volume

Single point adsorption total pore volume of pores less than 698.313 Å diameter at P/Po = 0.971489135: 0.002231 cm³/g

Pore Size

Adsorption average pore width (4V/A by BET): 89.2170 Å

Sand Proppants

Summary Report

Surface Area

Single point surface area at P/Po = 0.199759319:	0.5472 m²/g
BET Surface Area:	0.5580 m²/g
Langmuir Surface Area:	0.7657 m²/g
t-Plot Micropore Area:	0.1704 m²/g
t-Plot External Surface Area:	0.3876 m²/g
BJH Adsorption cumulative surface area of pores between 17.000 Å and 3000.000 Å diameter:	0.403 m²/g
BJH Desorption cumulative surface area of pores between 17.000 Å and 3000.000 Å diameter:	0.4077 m²/g

Pore Volume

Single point adsorption total pore volume of pores less than 698.631 Å diameter at P/Po = 0.971502441:	0.001164 cm³/g
t-Plot micropore volume:	0.000074 cm³/g
BJH Adsorption cumulative volume of pores between 17.000 Å and 3000.000 Å diameter:	0.001935 cm³/g
BJH Desorption cumulative volume of pores between 17.000 Å and 3000.000 Å diameter:	0.001941 cm³/g

Pore Size

Adsorption average pore width (4V/A by BET):	83.4360 Å
BJH Adsorption average pore diameter (4V/A):	192.278 Å
BJH Desorption average pore diameter (4V/A):	190.430 Å

Ceramics Proppants

Summary Report

Surface Area

Single point surface area at P/Po = 0.200422670:	0.3732 m²/g

Pore Volume

Single point adsorption total pore volume of pores less than 686.830 Å diameter at P/Po = 0.971000821:	0.000936 cm³/g

Pore Size

Adsorption average pore width (4V/A by BET):	87.1856 Å

Appendix E

Density & Acid Solubility Measurement

Bulk density measurement

Bulk Density Measurements

	1st Measurement			2nd Measurement			3rd Measurement			Mean density
Particles	**Volume Cm^3**	**Mass g**	**Density g/cm^3**	**Volume Cm^3**	**Mass g**	**Density g/cm^3**	**Volume Cm^3**	**Mass g**	**Density g/cm^3**	**g/cm^3**
Sand	2	3.392	1.696	4	6.556	1.639	6	9.6755	1.6126	1.649
Ceramics	2	3.3574	1.6787	4	6.1264	1.5316	6	9.15	1.525	1.5784
Limgrus	2	3.21	1.605	4	9.0292	2.257	6	11.87	1.978	1.9468
Alumina	2	1.1501	0.5705	-	-	-	-	-	-	0.5705
Carbolite	2	3.298	1.649	-	-	-	-	-	-	1.649
CNTs/Pure sand	2	2.8175	1.4087	-	-	-	-	-	-	1.4087
CNTs/Ni sand (4.32% yld)	1	1.275	1.275	-	-	-	-	-	-	1.27
CNTs/Ni sand (12% yield)	0.6	0.62521	1.04201	-	-	-	-	-	-	1.04201

Apparent or particle density from fluid displacement methoth

Proppants Particle	Mass (g)	Volume (cm^3)	Density (g/cm^3)
Sand	2.0583	0.8	2.5729
Ceramics	2.0156	0.8	2.5195
Carbolite	2.0315	0.8	2.5394
Alumina	1.2374	0.6	2.0623
Limgrus	1.9896	1	1.9896
Gravel	2.0257	1.2	1.6881
CNT/sand	2.006	1	2.006
CNTs/sand	0.5016	0.26	1.9292

FIGURE E.3: Proppants density & porosity data

Particles	Aparent Density (g/cm^3)	Bulk density (g/cm^3)	Voidage %
sand	2.535875	1.64	0.35328
cnt sand	2.006	1.3085	0.347707
alumina	2.062333	0.5754	0.720996
Ceramics	2.5195	1.5784	0.373526
gravel	1.688083	1.1085	0.343338
carbolite	2.539375	1.649	0.350628
limgrus	1.9896	1.605	0.193305

FIGURE E.4: Acid solubility of proppants

Proppants Particle	Untreated mass m1 (g)	Acid Treated mass m2 (g)	Acid solubility (1-m2/m1)	% Acid solubility
Sand	0.5065	0.5	0.0128	1.28
Ceramics	0.5073	0.507	0.0006	0.06
Carbolite	0.5024	0.4954	0.0139	1.39
Gravel	0.5013	0.4665	0.0694	6.94
Alumina	0.5044	0.1683	0.66	66

FIGURE E.5: Acid solubility of proppants

Proppants Particles	60 min Treatment			90 min Treatment			120 min Treatment		
	Untreated mass (g)	Treated Mass (g)	Acid solubility (%)	Untreated mass (g)	Treated mass (g)	Acid solubility (%)	Untreated mass (g)	Treated mass (mass)	Acid solubility (%)
Sand	0.5012	0.487	2.283	0.5022	0.4861	03.21	0.5013	0.4841	3.43
Ceramics	0.5025	0.5018	0.14	0.5056	0.503	0.5	0.5025	0.5016	0.18

Appendix F

Scale Inhibition

FIGURE F.1: Scale Inhibitor adsorption for cnts on pure sand with less than 1 % yield

Time (days)	Solvent volume (cm^3)	Phosphonates mass (g)	Untreated mass of cnt (g)	Treated mass of cnt (g)	Inhibitor loading (%)
0.4	3	0.05	0.2046	0.2054	0.389
1	3	0.05	0.2048	0.2056	0.389
2	3	0.05	0.204	0.2048	0.391
3	3	0.05	0.199	0.1997	0.35
4	3	0.05			

FIGURE F.2: Scale Inhibitor adsorption for cnts on pure sand with 4 % yield

Time (days)	Solvent volume (cm^3)	Phosphonates mass (g)	Untreated mass of cnt (g)	Treated mass of cnt (g)	Inhibitor loading (%)
1	3	0.05	0.2011	0.2021	0.495
2	3	0.05	0.2039	0.2055	0.779
3	3	0.05	0.2004	0.2016	0.595
5	3	0.05	0.2021	0.2039	0.883

FIGURE F.3: Scale Inhibitor adsorption for cnts on pure sand with 12 % yield

Time (days)	Solvent volume (cm^3)	Phosphonates mass (g)	Untreated mass of cnt (g)	Treated mass of cnt (g)	Inhibitor loading (%)
1	3	0.05	0.1999	0.2016	0.843
2	3	0.05	0.2026	0.2044	0.881
4	3	0.05	0.2066	0.2087	1.006
5	3	0.05	0.2067	0.2096	1.3
7	3	0.05	0.2051	0.2078	1.299

FIGURE F.4: Phosphonates adsorption variation on CNTs with the time

PH	Mass of Phosphonates (g)	Untreated mass of cnt (g)	Treated mass of cnt (g)	Loading (%)
1.1	0.05	0.2021	0.2051	1.462
3	0.05	0.2012	0.2045	1.613
4	0.05	0.202	0.2033	0.63944
5	0.05	0.202	0.2045	1.224
11	0.05	0.2025	0.2049	1.171
12	0.05	0.2008	0.2033	1.229

Appendix G

X-ray Diffraction

G.1 X-ray Diffraction

FIGURE G.1: Xrd analysis for carbolite

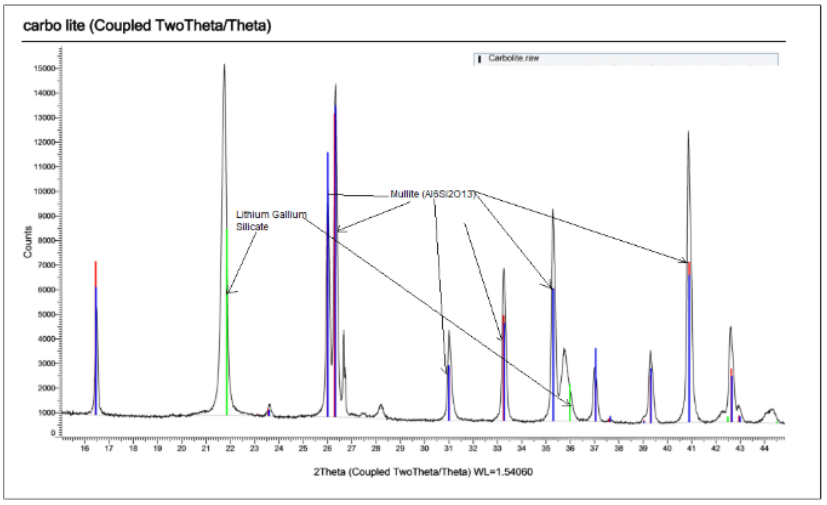

FIGURE G.2: Xrd analysis for ceramics

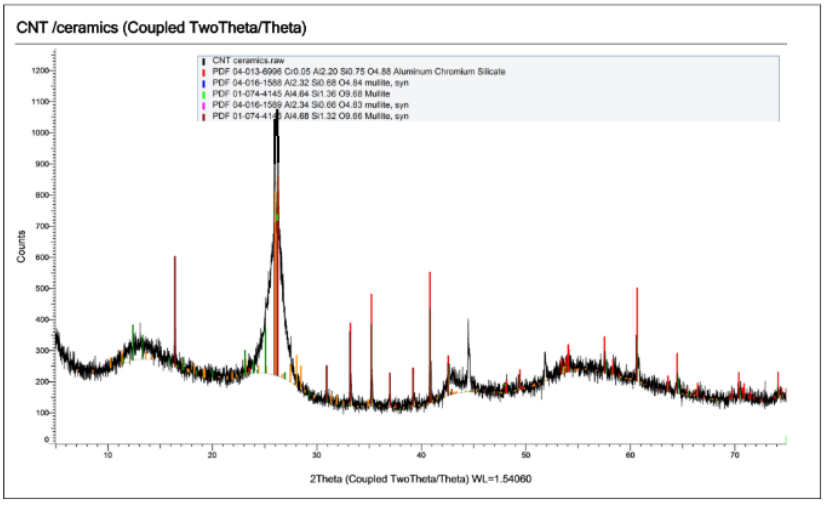

Xrd for Ceramics

FIGURE G.3: Xrd analysis for gravel and limgrus

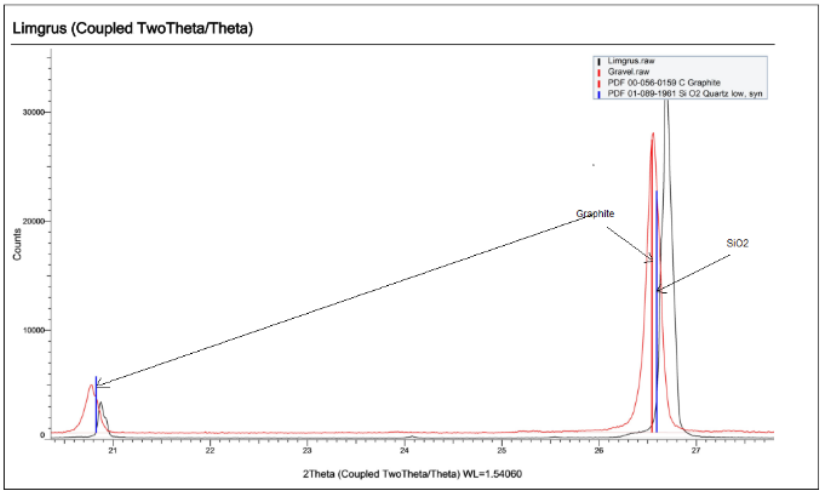

Xrd for Gravel and Ligmurus

FIGURE G.4: Xrd analysis for alumina

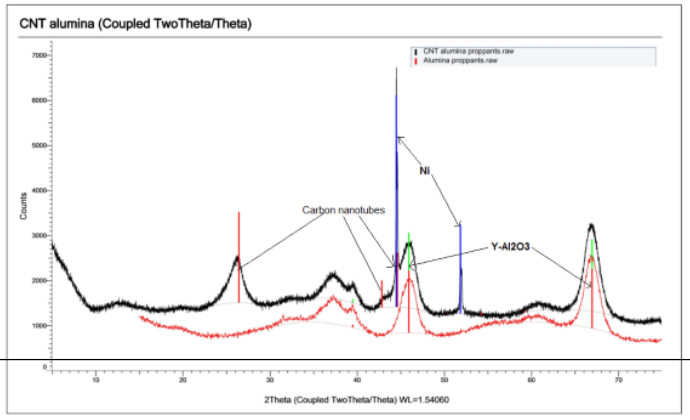

Xrd for Alumina

Appendix H

Sphericity & Roundness

H.1 X-ray Diffraction

FIGURE H.1: Chemsizer analysis for proppants

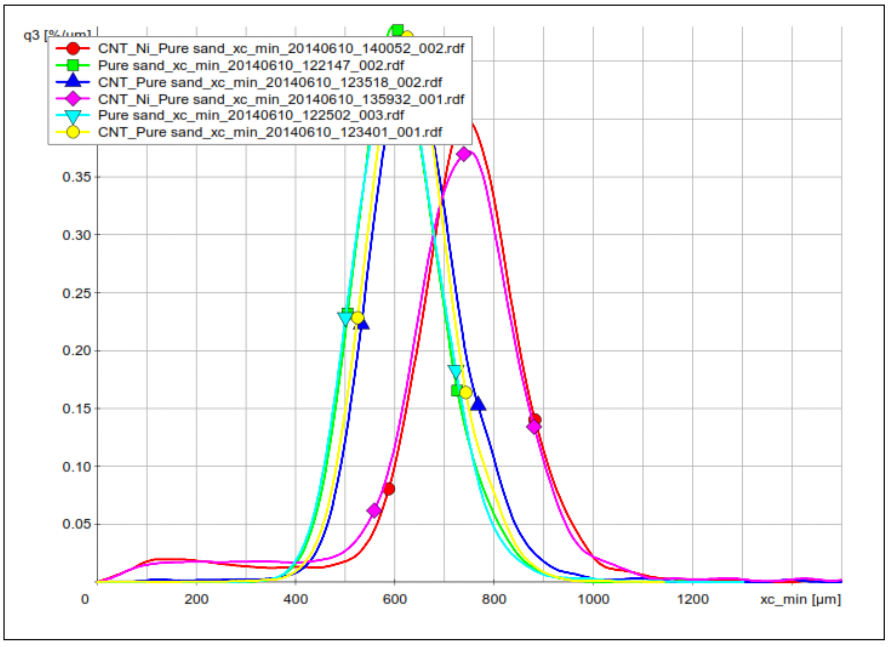

FIGURE H.2: Chemsizer analysis for pure sand

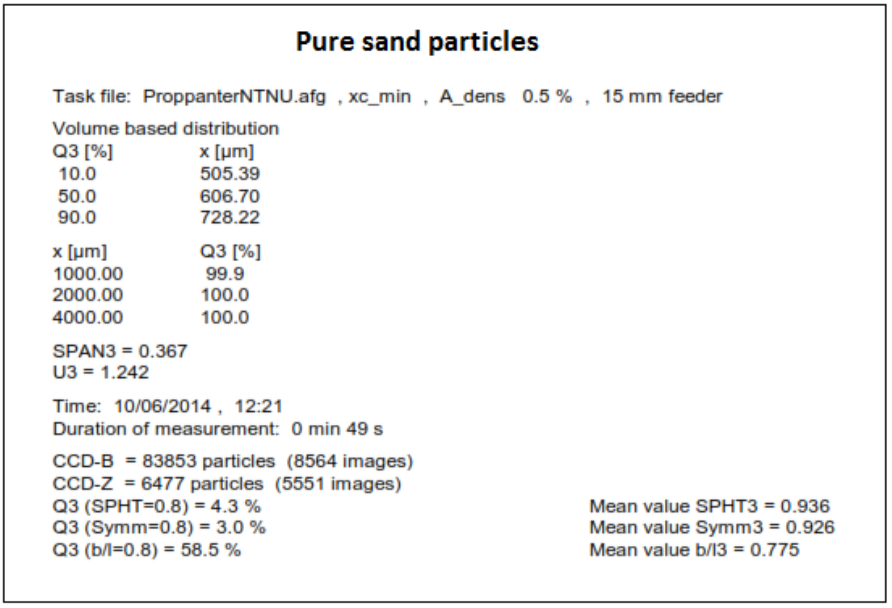

Pure sand particles

Task file: ProppanterNTNU.afg , xc_min , A_dens 0.5 % , 15 mm feeder

Volume based distribution

Q3 [%]	x [µm]
10.0	505.39
50.0	606.70
90.0	728.22

x [µm]	Q3 [%]
1000.00	99.9
2000.00	100.0
4000.00	100.0

SPAN3 = 0.367
U3 = 1.242

Time: 10/06/2014 , 12:21
Duration of measurement: 0 min 49 s

CCD-B = 83853 particles (8564 images)
CCD-Z = 6477 particles (5551 images)
Q3 (SPHT=0.8) = 4.3 %
Q3 (Symm=0.8) = 3.0 %
Q3 (b/l=0.8) = 58.5 %

Mean value SPHT3 = 0.936
Mean value Symm3 = 0.926
Mean value b/l3 = 0.775

FIGURE H.3: Chemsizer analysis for CNTs on pure sand

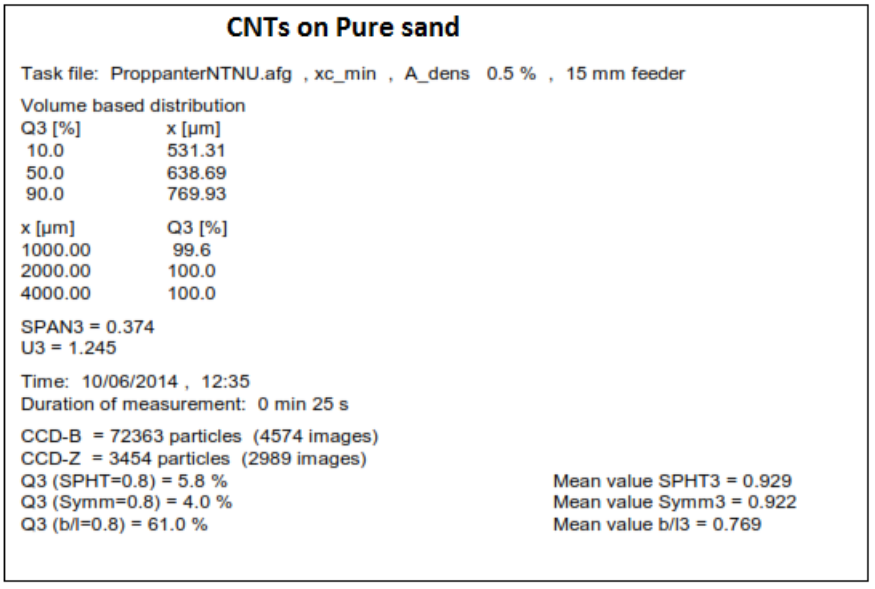

CNTs on Pure sand

Task file: ProppanterNTNU.afg , xc_min , A_dens 0.5 % , 15 mm feeder

Volume based distribution

Q3 [%]	x [µm]
10.0	531.31
50.0	638.69
90.0	769.93

x [µm]	Q3 [%]
1000.00	99.6
2000.00	100.0
4000.00	100.0

SPAN3 = 0.374
U3 = 1.245

Time: 10/06/2014 , 12:35
Duration of measurement: 0 min 25 s

CCD-B = 72363 particles (4574 images)
CCD-Z = 3454 particles (2989 images)
Q3 (SPHT=0.8) = 5.8 %
Q3 (Symm=0.8) = 4.0 %
Q3 (b/l=0.8) = 61.0 %

Mean value SPHT3 = 0.929
Mean value Symm3 = 0.922
Mean value b/l3 = 0.769

FIGURE H.4: Chemsizer analysis for CNTs on Ni sand

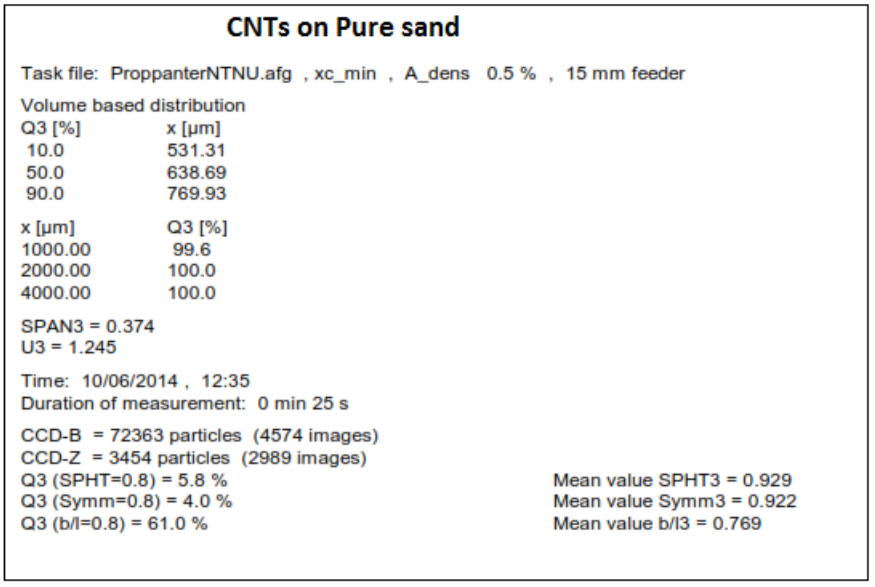

CNTs on Pure sand

Task file: ProppanterNTNU.afg , xc_min , A_dens 0.5 % , 15 mm feeder

Volume based distribution

Q3 [%]	x [µm]
10.0	531.31
50.0	638.69
90.0	769.93

x [µm]	Q3 [%]
1000.00	99.6
2000.00	100.0
4000.00	100.0

SPAN3 = 0.374
U3 = 1.245

Time: 10/06/2014 , 12:35
Duration of measurement: 0 min 25 s

CCD-B = 72363 particles (4574 images)
CCD-Z = 3454 particles (2989 images)
Q3 (SPHT=0.8) = 5.8 %
Q3 (Symm=0.8) = 4.0 %
Q3 (b/l=0.8) = 61.0 %

Mean value SPHT3 = 0.929
Mean value Symm3 = 0.922
Mean value b/l3 = 0.769